ANALYSIS OF LINE WIND POWER PLANT CONCEPT

Lappeenranta–Lahti University of Technology LUT

Master's Programme in Energy Technology, Master's thesis

2023

Nico Passila

Examiners: Docent Aki Grönman

Docent Ahti Jaatinen-Värri

ABSTRACT

Lappeenranta–Lahti University of Technology LUT

School of Energy Systems

Energy Technology

Nico Passila

Analysis of Line Wind Power Plant Concept

Master's thesis

2023

121 pages, 23 figures, 16 tables and 1 appendix

Examiners: Docent Aki Grönman and Docent Ahti Jaatinen-Värri

Keywords: wind energy, concept, analysis, feasibility

The accelerating adoption rate of renewable energy solutions, such as wind energy, provides opportunity for innovations to improve conventional designs or enable new use cases. A Finnish patent describing a line wind power plant (LWPP) concept is said to shore up the downsides of conventional designs and to allow harvesting of previously out of reach wind resources.

The objective of this work is to analyse the LWPP concept's main merits and their feasibility. LWPP is claimed to have improved energy production, energy acreage, buildability, maintainability, and to be more economical compared to conventional wind power plant (WPP) designs. These are to be achieved by building multiple smaller wind turbines on a shared support structure that combines multiple hub heights and turbine sizes to optimize power generation and to reduce loads. Preliminary aerodynamic, structural, cost, and environmental analyses are done on this concept using an example design.

Results of the analyses show that this type of structure has around 5,7 percentage point increased wake loss and quintupled turbulence intensity (TI) compared to conventional WPP. Despite this, energy production, energy acreage and capacity factor increased by 17,1; 107,2; and 13,9 %, respectively. The structure was deemed plausible and estimated costs were close to equivalent conventional wind farm's. LWPP would have greater visual impact, but avian and noise impacts would be on same level as in conventional wind farms.

TIIVISTELMÄ

Lappeenrannan–Lahden teknillinen yliopisto LUT

Energiajärjestelmät

Energiatekniikka

Nico Passila

Linjatuulivoimala konseptin analyysi

Energiatekniikan diplomityö

2023

121 sivua, 23 kuvaa, 16 taulukkoa ja 1 liite

Tarkastajat: Dosentti Aki Grönman ja Dosentti Ahti Jaatinen-Värri

Avainsanat: tuulivoima, konsepti, analyysi, toteutettavuus

Uusiutuvan energian, kuten tuulivoiman, kiihtyvä yleistyminen tuo tilaisuuksia innovaatioille parantaa nykyisiä ratkaisuja ja luoda uusia käyttötapoja. Suomalaisessa patentissa kuvaillun Linjatuulivoimala (LWPP) konseptin on sanottu paikkaavan nykyisten voimaloiden haittapuolia ja mahdollistavan aiemmin saavuttamattomien tuuliresurssien hyödyntämisen.

Tämän työn tarkoitus on analysoida LWPP konseptin suurimpia etuja ja niiden toteutettavuutta. LWPP:lla on väitetty olevan parempi energian tuotanto, energian tuotanto käytettyä maa-alaa kohden, rakennettavuus, huollettavuus, ja olevan taloudellisempi kuin nykyiset tuulivoimalat (WPP). Nämä saavutetaan rakentamalla useampi pienempi turbiini yhteisen tukirakenteen varaan, joka käyttää useita napakorkeuksia ja turbiini kokoja energian tuotannon optimointiin ja rasitteiden vähentämiseen. Konseptille tehdään alustavat aerodynaamiset, rakenteelliset, kululliset, ja ympäristölliset analyysit käyttäen esimerkki voimalaa.

Analyyseista nähdään, että vanavesihäviöt kasvavat suunnilleen 5,7 prosentti yksikköä ja turbulenssin intensiteetti viisinkertaistuu nykyisiin voimaloihin verrattuna. Tästä huolimatta energian tuotanto, energian tuotanto käytettyä maa-alaa kohden, ja kapasiteetti kertoimet ovat kasvaneet kukin 17,1; 107,2; ja 13,9 %. Rakenne todettiin mahdolliseksi ja kulut olivat lähellä vastaavaa nykyistä tuulipuistoa. Linjatuulivoimalalla olisi suurempi näkymällinen vaikutus, mutta linnusto ja ääni vaikutukset olisivat samaa tasoa.

SYMBOLS AND ABBREVIATIONS

Roman characters

A	area	[m^2]
a	shear exponent	[mm]
D	diameter	[m]
d	displacement height	[m]
m	mass	[kg]
M	moment	[Nm]
P	power	[W]
p	pressure	[Pa]
q	specific humidity	[kg_{vapour}/kg_{air}]
R	gas constant	[J/kg K]
r	radial distance	[m]
R	radius	[m]
T	temperature	[ºC, K]
t	thickness	[m]
T_h	thrust force	[N]
u_*	friction velocity	[m/s]
U, u	speed	[m/s]
V	volume	[m^3]
x, y, z	distance	[m]
z	height	[m]
z_0	roughness length	[m]

Greek characters

α	incidence angle	[°]
γ	inverse length scale	[s^{-1}]
ρ	density	[kg/m^3]
σ	stress	[Pa]
σ	wake width	[m]

Constants

g	standard gravity	9,81 m/s^2
R	specific gas constant of air	287,05 J/kgK
κ	von Kármán	0,4

Dimensionless quantities

A	scale parameter
Cp	power coefficient
C_T	thrust coefficient
I, T_i	turbulence intensity
k	shape parameter
k	wake decay constant
δ	correction term for weakened turbulence intensity in lower part of wake flow

Subscripts

a	ambient
ave	average
g	geostrophic
h	hub
r	reference
R	rotor

Abbreviations

ABL	Atmospheric Boundary Layer
AEP	Annual Energy Production
CAPEX	Capital Expenditure
CFD	Computational Fluid Dynamics
DEL	Damage Equivalent Load
DWM	Dynamic Wake Meandering
FLH	Full Load Hour
LCOE	Levelized Cost Of Electricity
LES	Large Eddy Simulation
LWPP	Line Wind Power Plant
MRS	Multi Rotor System
OPEX	Operational Expenditure
PRH	Patentti- ja RekisteriHallitus (Finnish Patents and Registration Office)
RANS	Reynolds Averaged Navier-Stokes
RNA	Rotor Nacelle Assembly

SPL	Sound Pressure Level
TI	Turbulence Intensity
TSR	Tip Speed Ratio
WPP	Wind Power Plant

Table of contents

-

Appendices

Appendix 1. Ishihara & Qian 2018 wake loss model

1 Introduction

Innovations in wind energy technology can enable better energy production. Success of innovations depends on the improvements they proved, their feasibility and how economic they are. This thesis will analyse a line wind power plant (LWPP) concept, an innovative support structure for wind turbines.

1.1 Background

With the growing knowledge and concern over climate change and sustainable future, renewable energy has been on the rise. World is transitioning to energy sources that have low carbon emissions, that will be viable on the long run, and that provide energy security. One of these renewable energy technologies is wind energy. Its share in energy sector has been on rise and it will be an important part of energy transition due to low levelized cost of energy (LCOE), low carbon emissions and plentiful availability.

Statistics show how fast the growth of wind energy has been. Global wind energy generation grew by 70%, from 835 TWh in 2015 to 1420 TWh in 2019. Cost of electricity from wind has dropped by 45% between 2015 and 2020 and has become more economical than fossil fuels in many regions. These rapid developments in wind energy generation have been driven by policy, societal pressure to limit fossil generation, low interest rates, and cost reductions. (Intergovernmental Panel on Climate Change 2022, p. TS-53)

National targets, scenarios and regulations have been and will be important driving factors for up-and-coming energy investments. In addition to policy level, developments and advancements in wind energy technology have improved its efficiency and lowered production costs, which have been major driving factors for the success of wind power. Demand for wind energy is growing and as such it is wise to use wind technologies most suited for each location to maximise energy generation potential.

1.2 Wind turbine design

Currently the most used wind turbine design is a horizontal-axis, three bladed wind turbine – also called a wind power plant (WPP). The WPP term is used in this thesis to refer to a complete wind turbine, while turbine by itself is used to refer to the components on top of wind turbine tower. WPP consists of rotor, nacelle, tower, and a foundation. Rotor assembly has blades, hub, spinner, and blade pitch system. The rotor assembly is connected to the nacelle that houses drive train, gearbox, generator, brake, yawing mechanism, and power electronics. These make up the rotor nacelle assembly (RNA). Tower supports these structures and is itself supported by a concrete foundation. Transformer and controller are usually located at the bottom of a tower in a dedicated transformer space or in the nacelle depending on the turbine model. Multiple wind turbines are connected with cabling to a substation to form an installation known as wind farm. There are other wind turbine designs and ways to classify them.

Wind turbine types are classified based on their axel of rotation to horizontal and vertical axis wind turbines. Newer different concepts have also emerged that are still to reach commercial success. These are airborne wind energy such as kite power, and multirotor designs that have multiple turbines on a single tower. (Roga et. al. 2022, p. 1-2, 5) Multirotor wind turbines are also called multi rotor systems (MRS).

The power that a turbine generates is proportional to turbine swept area and wind speed. This has led to wind turbine towers getting taller since winds are stronger at higher altitudes, and blades getting larger since that increases the covered area from which the turbine can extract the energy from the wind.

For example, in Finland wind turbine hub height has increased from 30 m in 1993 to 150 m in 2021. Similarly average blade height and nominal power have also increased. Currently most onshore wind turbines built in Finland have nominal power of 4,7 MW, rotor diameter of 151 m and hub height of 150 m. Turbines with these specifications constitute 73% of the 141 newly installed turbines in 2021. (Suomen Tuulivoimayhdistys 2021)

Offshore turbines reach even greater heights and powers like one of the largest up-coming ones, the V236-15.0 MW with a hub height of over 200 m and rotor diameter of 236 m. (Electrek, 2021)

Wind turbines used to need the best wind sites to be profitable. This has started to change with technological advancements and development of markets where now sites with even moderate wind conditions are profitable. Currently wind energy has one of the lowest LCOE of energy production systems. Still, conventional designs are constrained in heights they can reach and there are other aspects that could be improved with new innovations.

Some of these challenges are scalability of conventional designs. Larger blades suffer from the mass increase according to cubic-square law. This leads to structural demands outpacing the economic gains from size increase. Larger towers and blades would also be harder to transport and size increase would make erecting the power plant a challenge. (Gasch R. & Twele J. 2012, p. 499)

Wind turbines need to be distanced several rotor diameters (D) apart to reduce energy production losses from inter turbine wake interaction. This leads to wind farms taking up large land areas while having low amount of energy produced per area of land used, or energy acreage. Large wind farms impact the view of the landscape and emit noise. Wind turbines have variation in their energy production which makes production forecasting challenging as well as meeting instantaneous demand.

Since wind energy is on the rise and realising larger turbines using conventional design faces some challenges, it is wise to explore alternate wind energy concepts to gauge whether they might be usable to overcome shortcomings of conventional turbines.

An alternate WPP concept is described in a Finnish patent from 2007 where a WPP uses multiple turbines on a shared support structure. This concept uses smaller turbines situated on taller guy-wired towers that are closer together, with supporting structures between towers providing structural integrity and possible material transport. This concept of a LWPP is claimed to provide improvements to transportability, energy production and density, capacity factor, and to have a low LCOE. (PRH 2010b, p. 1-2)

New innovations in wind technology provide possibilities of improving current practices and used technology which would increase the efficiency and economics of wind power (Jamieson 2018, p. 1). This is the value in examining new novel concepts. Best ways of evaluating new concepts are to compare to a baseline that is current standard, to assess validity of claimed performance and the impact of proposed innovation. (Jamieson 2018, p. 7-8)

1.3 Methods

This thesis analyses the LWPP concept's main features and their merits from aerodynamic, structural, economical, and environmental standpoints, with emphasis on energy production. The concept's main features are defined based on the patent's description. From these the main merits are evaluated and contrasted to conventional WPPs. A literature review on wind resources, turbine aerodynamics, technology, and environmental factors is conducted to assess the validity of the estimated merits.

Calculations and modelling of various aspects of the power plant are conducted. These include simple wake loss, power production, structural loads, costs, and LCOE calculations. 3D models are created to assess and illustrate an example design's visual impact. Results are discussed and compared to conventional WPPs and other multirotor concepts.

Finally, a review and summary of findings is given. Finnish conditions, markets, and regulatory framework are used as the basis for discussion and analysis.

1.4 Structure of the thesis

Second chapter of this thesis describes the concept of a LWPP, as introduced in a patent description. The concept's main benefits are defined, an example design is created, initial comparisons to conventional WPP designs are made and three other multirotor concepts are introduced. In third chapter a literature review on wind resources and aerodynamics is conducted to assess how wind conditions are different for LWPP and what these differences entail. Fourth chapter examines power production and the severity of wake loss in LWPP. Fifth chapter examines the design's structural feasibility using references from literature and simple calculations. Sixth chapter calculates economic factors in this kind of design and how they stand up to competition. Seventh chapter conducts a review of common environmental factors in wind power and how they apply to this concept. Finally, discussion over the various aspects is had and conclusions are made.

2 Line Wind Power Plant concept

Concept of a LWPP originates from a Finnish patent. It includes description of the concept, the main points that make up this alternate type of WPP and what differentiates it from conventional WPPs. The patent introduces some examples of designs using this concept. The overarching points are reviewed at literature level and actual example design is used for closer analyses.

2.1 Origin of the concept

The LWPP concept originates from a Finnish patent with patent number 122078 and application number 20070502. It can be accessed from Finnish Patents and Registration Office's free PatInfo-database. (PRH 2022) Patent was first submitted in 2007 and has had revisions over the years. Most recent descriptions and illustrations are examined in this thesis. The documents of the patent contain a summary of the LWPP concept from November of 2010. This summary includes descriptions for the LWPP, its overall structure and arrangement. The patent also includes descriptions for other innovations, such as a new turbine and blade design, and a floating off-shore wind and ocean current power plant with hovering solar collectors (PRH 2010a). This thesis doesn't focus on these additional innovations for new blade design, nor the floating power plant, but on the concept of the LWPP and its applicability.

The LWPP concept was made over a decade ago and wind power technology has advanced since then, which makes the comparisons made in the patent less relevant nowadays. We'll make reflections onto the comparisons that the author of the patent made for the technologies at the time but also contrast those reflections onto current conventional designs and think of ways that the LWPP concept could be applied with modern technology.

The LWPP concept is realized as a practical design. The patent introduces multiple designs, but they all are centred around the core features that characterize a LWPP. In a description from November 2010 the LWPP is described as consisting of simple modular structures that can be combined to form different sized supporting structures. Structure consists of a central

wireframe or tubular steel tower and possibly additional side towers. The towers are reinforced with guy-wires. Angled support and transport beams are fixed between the central and side towers. These beams can end at towers or continue to the ground. Wind turbines are placed upon poles that are hanged from these angled side beams. Bottoms of the poles are tensioned with guy-wires to the ground. Turbines can yaw on these poles like in conventional wind turbine designs. Alternately the poles can be extended to the ground to act as towers. Angled support side beams provide structural integrity and can be used for transporting parts and for maintenance. Cranes or other lifting devices can be mounted onto the towers or moved alongside the beams on sled like platforms. (PRH 2010b, p. 1, 3) (PRH 2010c) Illustrative figure of a LWPP is shown in Figure 1.

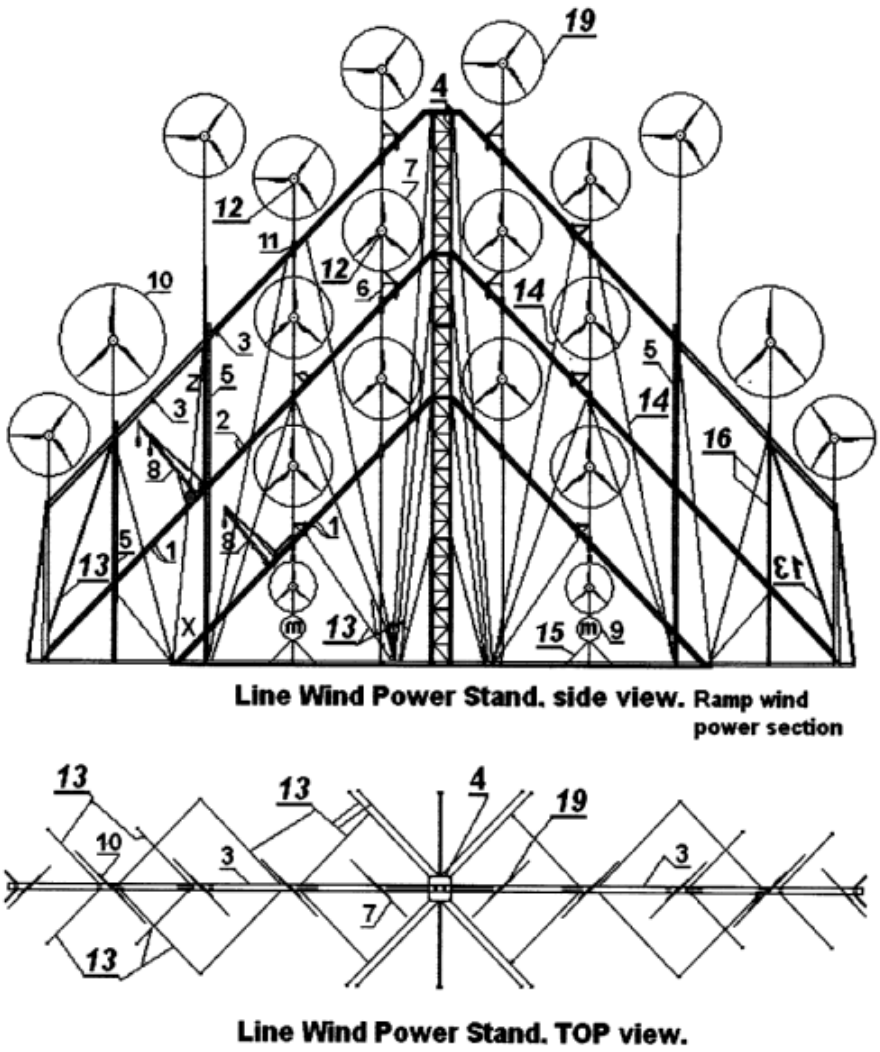

Figure 1. Concept drawing of a LWPP (PRH 2009, p. 1).

Figure 1 shows how the side towers are connected to the central tower by angled support side beams, and the guy-wiring of towers and vertical poles. The figure also demonstrates how wind turbines are arranged onto the shared support structure and how different sized turbines can be used at varying heights.

The LWPP designs uses multiple turbines supported on a shared supporting structure and as such could be considered a multirotor wind turbine design, or MRS. There have so far been no multirotor designs that have reached widespread commercial use, but several multirotor designs have been studied and are being developed.

Another example of a LWPP design from the patent is show in Figure 2. It shows a scale comparison of a conventional WPP next to a LWPP. Height bar shows the scale difference and the aim of LWPP height increase.

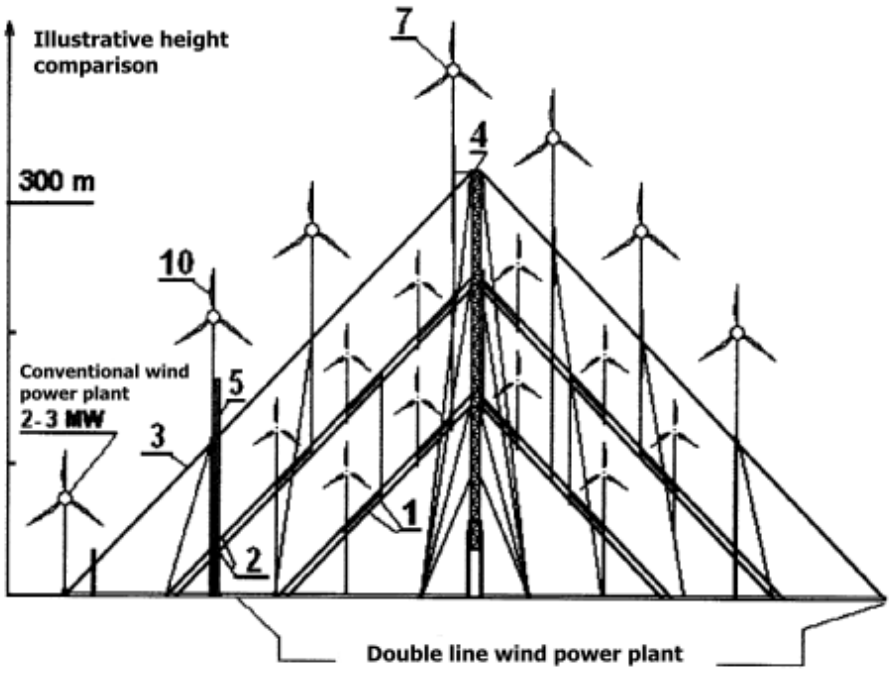

Figure 2. LWPP design with height comparison to traditional WPP. (modified from: PRH 2009, p. 4)

Best available wind turbine technology at the time of patent's creation was 2-3 MW turbines with hub heights of 80 m. Modern conventional wind turbines have grown significantly

during the years and as such comparing the designs as proposed in the patent wouldn't be most fruitful. Therefore, for analysing the LWPP concept, its main benefits are defined. This is to examine how the concept can be adapted to modern technology and compared to current best available technology WPPs and other MRS designs. An updated example design is created to be used in more detailed analysis.

2.2 Challenges of conventional wind turbines

Conventional wind turbines have some downsides that can hinder their adoption and optimal usage. Understanding these downsides helps to assess the merits that a LWPP design might have. Challenges that conventional wind turbines face are explained here.

Possible challenges for conventional WPPs were reviewed in article by McKenna et al. (2016). Main challenges are expected to be societal acceptance, logistics of transport and erection, and the sustainability of political and economic support for wind energy. Logistic, erection and partly societal acceptance challenges are exasperated by the upsizing trend in wind turbine manufacturing.

Increasing blade lengths pose and ever-growing challenge for their transport. Special transport operations are planned and executed to get the blades safely to their destination. Roads usually need to be maintained or even improved to be able to endure these large loads and they need to have sufficient turning radiuses to manoeuvre the blades around. Hoisting areas size of 0,5 ha are needed around the turbines for the lifting equipment to operate. Road turns, slopes, bridge clearances create bottlenecks for accessing some sites. Smaller blades and towers would bypass these bottlenecks more easily. Size of tower parts, nacelle and rotor hub create similar logistical problems. (Gasch R. & Twele J. 2012, p. 499-500)

Blade mass is proportional to the cubic of rotor radius while production is related to square, which makes scaling blades past a certain point unfeasible. This makes multirotor designs a possible solution to keep growing WPP sizes. (Roga et. al. 2022, p. 9) Up-scaling increases in weight tend to outstrip benefits of increase in energy capture. MRSs exploits the weight advantage of smaller rotors. (Jamieson & Branney 2012, p. 52)

Taller towers are also harder to build as they would need to be able to withstand higher loads. This would lead to widening of the tower diameter and increasing plate wall thickness. Manufacturing imposes constraints like weldable wall thicknesses and rollability of steel plates. Wider tower sections face the same 4.3 m diameter limit imposed by overpass heights. Wall thicknesses are limited by rolling equipment and price of steel. (Huang et al. 2022, p. 1)

Size increase of turbine components and towers makes their handling and installation at the site harder. Larger cranes are needed to reach the required hub heights and enough strength to handle the mass of large RNAs. Handling large components is also hard from maintenance point of view as getting larger replacement parts into a nacelle at large height is more difficult. This would increase operation and maintenance (O&M) difficulties.

Wind turbines within a wind farm are usually spaced laterally five rotor diameters apart and seven diameters longitudinally between rows of WPPs. This is done to reduce the losses caused by wake effects that form from interactions between moving blades and flowing wind. (Hau 2013, p. 726) This spacing means that farms require quite a lot of land area to produce energy. A turbine could be assumed to take up a grid of land area the size of lateral and longitudinal distancing. This vast land area requirement for each turbine leads to small energy production per unit of land area used, which is known as energy acreage. Large area need usually leads to large operating costs from land leasing.

In addition to distance between wind turbines, distance to nearby settlements is also required. Countries have different regulations that set the limits on how close to a settlement wind farm can be deployed. These distances are usually one to two kilometres. In Finland there is no set distance, but farms are to be distances as to keep noise levels below determined levels. These regulations limit the areas where wind power can be built, sometimes withholding use of best wind sites.

EU’s wind farms have an average capacity factor of 24% for onshore and 38% for offshore wind farms. Newer farms are expected to reach capacity factors of 30-35% for onshore and 55% offshore. (WindEurope 2020, p. 16) Capacity factor is constantly improving with the growing size of the turbines as they reach more energy rich wind resources. Yet due to the intermittency of wind it can cause fluctuations and deficit in power production. Further

increase in capacity factor would make wind energy more reliable. Capacity factor can also be expressed in full load hours (FLH).

2.3 Merits of a LWPP

Evaluation between new wind turbine innovations is best done by comparing the design's merits, the claimed benefits, to industry standard solutions. These merits need to be realisable and increase production, bring cost savings, enable new markets, or bring some other tangible benefit to be competitive. (Jamieson 2018, p. 7-8) LWPP would need to be to alleviate all or some of the challenges of conventional WPP designs.

Main benefits of the concept are claimed to be reaching stronger wind resources using taller support structures, concentrating more power generating capacity per area of land, easier transportation of the power plant parts, ease of erection and maintenance, and being more economical. Economical improvements are due to reductions in construction and maintenance costs, and improvements in electricity generation. (PRH 2010b, p. 1, 2)

The main design points of a LWPP are condensed into the following table with the claimed benefits for easier reference. These merits are listed in Table 1.

Table 1. LWPP design merits.

Design point	**Effect**	**Benefit**
Height increase	Stronger stabler wind	Increased power generation, higher FLH
Multirotor	Shared structure, multiple smaller turbines	Mass savings, cost savings, mass-to-power efficiency of turbines, energy acreage
Multiple hub heights	Different wind conditions at levels	Optimization
Modular structure	Transportability, erection, configurations	Site accessibility, transportation cost savings, optimization
Support side beams	Rigidity, load bearing, material transport, maintenance access	Maximum height, smaller foundations, thinner towers, O&M cost savings
Guy-wires	Rigidity, load bearing	Maximum height, smaller foundations, thinner towers
Built-in cranes	Maintenance access, erection	Erection cost savings, O&M cost savings

LWPP is meant to harvest higher altitude winds as they contain more kinetic energy. Wind speed slowing effect of ground surface roughness decreases with height which leads to higher wind speeds and greater wind speed distribution. Stronger winds would lead to turbines operating more often at full capacity which improves their capacity factor.

Multirotor designs use multiple smaller turbines on a shared structure. Smaller blades benefit from the cube-square law, which means the mass of turbine blades increases cubically with size while surface area that provides lift increases squarely. This means better performance per mass which increases the number of blades, and thus turbines, that a given structure can hold. Smaller blades are easier to manufacture and transport, which can translate to cost savings. Smaller parts make transport easier, but it also means more parts to transport, which might increase the total number of truckloads needed.

Having multiple turbines packed more densely and with increased wind resources would lead to better energy acreage. This in turn would reduce the required size of a LWPP wind

farm as energy production of an equal WPP wind farm could be achieved with smaller land area. Or same land area could be used to install higher capacity of wind power. Using multiple hub heights, turbine sizes, and having different wind conditions across the structure would enable using turbines with different wind classes to better optimize their performance.

The height increase is meant to be achieved with the novel support structure that is more stable by combining multiple structures together. Main towers can be wireframe or tubular steel type. The shared structure would distribute loads more effectively allowing individual pieces to be smaller and/or thinner. These would reduce the costs of the structural elements.

Angled side beams between the towers would improve structural stiffness and load distribution. They are also meant to be used for transporting parts and equipment. Tops side of the beams has a rail system, either smooth or racked rail, that a sled could move on. A ladder structure could be implemented inside the side beams to help with personnel and material transport. (PRH 2010b, p. 3)

A personnel carriage could be suspended from the support beams. This is to provide easier access for maintenance and inspections, as it would function as a lift to the turbines below support beam rows. (PRH 2010b, p. 3)

Guy-wiring is used to provide additional cheap and easy to implement support for the structure. Main and side towers are wired at two levels. Guy-wiring would be done like in Ramboll's guy-wired wind turbine tower concept, using a connection flange between tower segments for anchoring point (Jespersen & Støttrup-Andersen 2019, p. 783).

2.4 LWPP design

LWPP concept has features that can vary between designs. Number of towers, turbines and support beams and their arrangement can vary. Turbine sizes and heights can also be varied. Horizontal distances between turbines are expected to be small as shown in Figure 2; around 1-2 D. Vertical distances are likewise short to maximise the utilised area between structure elements. These allow creating variants of different of sizes and optimizing individual designs for different wind conditions and sites. Extend to which hub heights and supporting

elements can be altered is examined in structural analysis chapter. An example LWPP design is created to analyse more concretely the properties this concept would have.

The example design uses two turbine models that are based on Vestas turbines as Vestas turbines are most popular in Finland (Suomen Tuulivoimayhdistys 2021). Chosen models are V80-1.8, a 1,8 MW turbine with rotor diameter of 80 m, and V112-3.3, a 3,3 MW turbine with 112 m rotor diameter. Turbines are at three hub heights of 100, 200 and 300 m. Three 3.3 MW turbines are situated on 200 and 300 m hub height rows and four 1.8 MW turbines on the lowest 100 m row. Turbines on lowest row are numbered 1-4, ones on middle row are 5-6 and the top turbine is number 7. Lateral distance from central tower to the next ones are 60, 65 and 75 m. This is to have room for turbines between support beams. This means a spacing of 1,5 and 1,75 D for bottom row and 2,23 D for second row between the turbines. Top support beam extends from the outermost towers down to the ground adding 28 m lateral distance per side, bringing the total width of the structure to 456 m.

This type of design would have combined rated turbine power of 17,1 MW and combined swept are of 49 662 m^2. LWPP would be a bigger structure than conventional WPPs and its power would be that of multiple conventional turbines. Thus, comparing single LWPP to multiple WPPs, or a small wind farm, is fairer. Example LWPP design would equal 3,8 V150-4.5 turbines for rated power or 2,8 turbines for equal swept area. As LWPP operates in different wind conditions due to height increase, a more accurate comparison between LWPP and WPPs could be to compare units on equivalent power production.

If LWPPs were used to create a wind farm they could use similar micro-siting distances as conventional farms, as those distances are based on rotor diameters. The rotor diameter used for distancing is based on the largest rotor assembly size on the structure, which in this design is 112 m. A single 456 m wide LWPP using 5 D lateral and 7 D longitudinal distances would get a grid size of 784 x 960 metres, [long x lat], reserving 0,75 km^2 of land area.

A 3D model of the example LWPP was created to show how it compares to a conventional WPP. The modelling was done using Blender and used Vestas V150-4.5 WPP as reference model for conventional WPP. This turbine has rotor diameter of 150 m. LWPP was created by scaling down the V150 to rotor diameter to 80 m for smaller ones and 112 m for larger ones. Guy-wires were added as well as angled side beams. A modelled Vestas V150-4.5 with 150 m rotor is shown in the figure for scale comparison. Hub height of conventional WPP is

150 m and the LWPP highest hub height is 300 m. Tip height of WPP is 225 m and for LWPP it is 356 m. Resulting render of Blender modelling is shown in Figure 3.

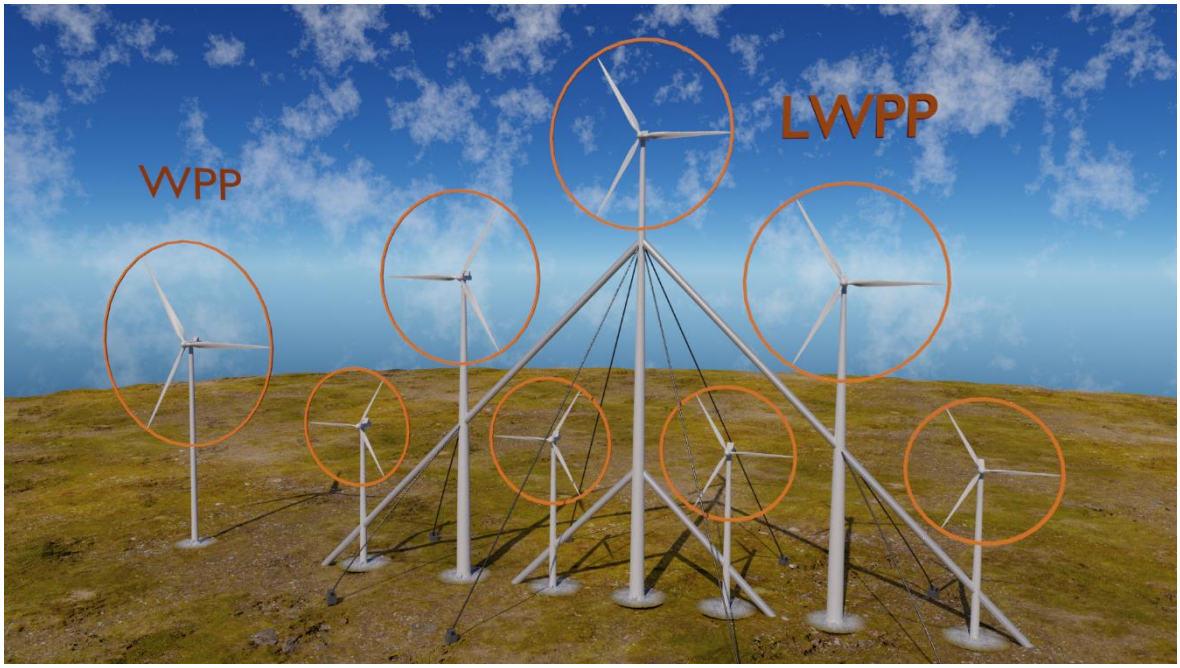

Figure 3. Example illustration of covnentional WPP (left) and LWPP (right) with swept areas indicated by orange circles.

This example design doesn't incorporate the transport rail system on top of side beams nor the inbuilt cranes. Sled-rail system was intended for smaller turbines on hanged pillars as there they could move with little intrusion, but this example design has ground mounted towers for each turbine which would block the sleds. Rail system and inbuilt cranes were omitted to keep the design simple and easier to analyse.

2.5 Other multirotor concepts

Some similar concepts that have multiple turbines located on a shared supporting structure have been made. Comparing LWPP concept to these others allows contrasting the individual merits of each concept. Three different concepts are mentioned here to describe how multirotor designs can vary and to have different points to contrast LWPP concept to.

One of these is Vestas multirotor concept R4-V29 that was tested at Risø Campus of the Technical University of Denmark (Laan et al. 2019a). This design uses four turbines on a single tower, mounted onto offset arms from the tower. Turbines are in two heights as pairs, one on each side of the tower. The rotors are on a same plane. Arms are angled and supported by guy-wires to the tower. The arms are connected at the tower and can pivot around the tower.

Second one is a 20 MW multirotor system concept from the INNWIND project. This design has 45 small 444 kW turbines in a lattice mounted onto a single tower. The lattice structure can rotate on the tower as it is on two bearings. This design takes advantage of turbine mass ratio of smaller turbines. (Jamieson & Branney 2012) This concept leans more heavily to using many smaller turbines to gain mass saving benefits.

Wind Catching Systems is developing a multirotor concept for offshore applications that uses semisubmersible trimaran vessel with off-the-shelf turbines in a linear support structure. The structure can rotate on a turret to face the wind. This concept is claimed to be disruptive technology with extremely efficient use of acreage at five times the power production per acreage compared to conventional off-shore turbines, easy operation and maintenance with inbuilt elevator system. The design uses 117 1 MW turbines mounted onto 300 m high and 350 m wide sail structure. (Fearnleysecurities 2021, 3:10:00 onwards) This concept utilizes a similar linear design to a LWPP, but it can rotate the whole structure on a point avoiding wake losses from within the structure.

3 Wind resources and aerodynamics

Wind resources - wind speed, wind direction and ambient turbulence - are important factors for WPPs. One of the fundamental goals of the LWPP concept is to harvest the higher energy winds that are available at higher elevations. It is therefore essential to understand the atmospheric features and phenomena to better assess how they would improve the power generation, and the magnitude and differences in structural loads that the power plant would need to endure.

A dive into physics and equations behind wind meteorology is done to find the determining factors that would affect LWPP energy power production and that can be applied in vast conditions. From these main factors of suitable accuracy are used to do example calculations for LWPP using data gathered from Finnish wind atlas. Main aspects that are considered are changing atmospheric variables with height and turbine interactions trough wake loss. These are atmospheric stratification, air density, vertical wind profiles, thermal gradients, surface roughness, turbulence, and wind direction.

Characteristics of wind turbines affect their ability to extract energy from the wind. Wind turbines are classified based on the wind speeds and turbulence intensities (TI) that they are suited for. LWPP offers optimization possibilities for using turbines of different classes, which is why turbine characteristics are examined.

Due to linear design and small distances between rotors, wake loss is expected to be more important for LWPP than for WPP. Wake loss can reduce energy production of conventional wind farm by 10-20 % (Cao et al. 2022, p. 1). LWPP has turbines in closer proximity than conventional wind farms, which makes these losses assumedly greater, and that is why they deserve greater inspection.

3.1 Atmospheric features and phenomena

Wind energy forms from, and is continuously replenished by, solar energy. Wind energy is available nearly all over the world. Tropical belt gets the main input of solar energy while higher latitudes lose energy through thermal radiation. This heating difference causes global

atmospheric circulation, with features such as large circulations cells of Hadley, Ferrel and polar cells. Hadley and polar cells have direct thermal circulation while Ferrel cells are thermally indirect. These systems cause the meridional winds, and with Coriolis force they produce the trade winds. (Emeis 2018, p. 5, 11-12)

A basic explanation of winds includes horizontal heat gradients. Sun heats surface, heat gets transported upwards through heat fluxes, and this forms horizontal temperature gradients. Air density depends on air temperature, and warmer air is less dense and has a larger vertical distance between two given pressure surfaces. Air pressure is closely related to air density, and it decreases with height. Pressure difference of air masses creates compensating pressure driven winds that move these gradients. (Emeis 2018, p. 13)

Frictional forces slow down the wind, but above the atmospheric boundary layer in free troposphere their effect on wind speeds is negligible. Geostrophic wind is determined by large-scale horizontal pressure gradient and latitude-dependent Coriolis parameter. This wind blows parallel to the isobars of pressure field on constant height surfaces. In northern hemisphere these winds blow counterclockwise around low-pressure systems and other way in high pressure ones. The situation is reversed in southern hemisphere. (Emeis 2018, p. 16-17)

Another factor for large-scale forcing of near-surface winds is thermal wind which is the difference in wind vector of geostrophic wind at two heights. This is caused by atmospheric large-scale horizontal temperature gradient that make horizontal pressure gradient height dependent. (Emeis 2018, p. 18)

The wind speed in atmospheric boundary layer (ABL) decreases to zero towards the surface. This is due to surface friction. Surface layer, also known as Prandtl layer, can be up to 100 m deep and the forces in it are dominated by turbulent viscosity of air. Wind speed increases strongly with height in this layer. There is usually an equilibrium of pressure and frictional forces. Above this layer is the Ekman layer which makes up around 90% of the boundary layer. There Coriolis force is important and causes a turning of wind direction with height. There is usually an equilibrium of pressure, frictional and Coriolis forces. The depth boundary layer varies vastly from 0,1 to 3 km with windiness and solar irradiance. (Emeis 2018, p.19)

3.1.1 Thermal stratification

Thermal stratification describes the vertical temperature gradient in the atmosphere. Stability can be divided to neutrally, stably, and unstably stratified atmosphere. Wind speeds, TI and atmospheric stability are usually correlated. Unstable atmosphere happens when cooler air flows over warmer surfaces and stable on the opposite. Unstable conditions are usual with low wind speeds while stable stratification favours higher wind speeds. Vertical motions lead to higher TIs in unstable atmosphere, and these motions mix the air reducing vertical gradients. Turbulence is smaller in stable atmosphere as are vertical gradients. Impact of thermal stratification is largest for small wind speeds while less so for higher speeds. (Emeis 2018, p. 23-25)

Temperature changes differently depending on the prevalent stratification. Temperature changes most in unstable and least with stable stratification. The temperature difference at one kilometre of elevation can be 30 % between these. Change in air temperature over elevation is characterized by lapse rate or adiabatic vertical temperature gradient. Stratification is important for vertical profiles of atmospheric variables which makes it impactful for larger wind turbines. (Emeis 2018, p. 24-25)

Wind speed profile laws in ABL can be used to interpolate and/or extrapolate profiles from measurements or model layer heights. These laws apply only to the surface layer. Conventional wind turbines usually also reach into the Ekman layer, which is why their planning requires knowledge of wind conditions at both layers. (Emeis 2018, p. 31)

ABL stratification depends on surface properties such as shape, roughness, albedo, moisture content, heat emissivity, and heat capacity. This is due to affecting the momentum and energy exchange between the surface and the atmosphere. ABL is unstable when heat input from below dominates. When atmosphere cooled from below, we get stable. When heat flux at lower surface is vanishing and dynamic shear forces dominate, we get neutral or dynamic boundary layer. (Emeis 2018, p. 32)

Since LWPP design aims to reach greater heights than normal designs, understanding of the ABL vertical structure is needed to assess the wind profiles at those heights. Stratification affects LWPP more than WPPs due to turbine elevation. This could lead top turbine to experience more variation in wind conditions as atmospheric stability changes.

3.1.2 Air density

Air density affects the kinetic energy of wind linearly. Humid air is less dense than dry air. Air density decreases with height due to pressure decrease, and it also decreases as temperature increases. The difference in air pressure can be up to 20 % between cold high-pressure air and warm low-pressure air. Determining air density requires knowing air temperature, pressure, and humidity. (Emeis 2018, p. 21-22)

The effect of humidity on air density can be calculated using virtual temperature. It represents the temperature that dry air would have to have to match the density of humid air. It is defined as:

$$T_v = T(1 + 0.609q) \tag{1}$$

Where T_v is virtual temperature [K], T is temperature of humid air [K] and q is specific humidity of air mass [kg_{vapour}/kg_{air}].

Air density can be calculated with:

$$\rho(z) = \frac{p_r}{R\bar{T}} exp\left(\frac{-g(z - z_r)}{R\bar{T}}\right) \tag{2}$$

Where ρ is air density [kg/m^3], p_r is the air pressure at reference level [Pa], z_r is the height at reference level [m], R is the specific gas constant of air [J/kgK], $\bar{T}$ is the vertical mean temperature of the calculated layer [K], and g is standard gravity [m/s^2].

It should be noted that the vertical mean temperature is accurate only over small vertical intervals as temperature decreases with height (Emeis 2018, p. 23). Equation (1) can be used with equation (2) to calculate the vertical mean temperature for humid air masses. Air density change will differ depending on prevailing stratification, as that affects the temperature profile (Emeis, 2018. p. 25).

As most of atmospheric parameters apply both to conventional WPPs and the LWPP, the main difference will be the height component. The change in air density over the example LWPP's elevation increase of 200 m between top and bottom turbines is around 0,03 kg/m3, or 2 %. Stratification can increase or decrease this change, but total effect on air density is expected to be minor.

3.1.3 Wind speed

Wind speed is a central variable in wind energy power generation. It's dependent on many atmospheric variables and it behaves differently in different parts of the ABL. Differences between ABL's lower part or Prandtl and higher Ekman layer are discussed first.

Wind speed profile in Prandtl layer

Wind speed increase with height is an important factor for upscaling wind turbines. This is described by the laws of vertical wind profile. Two methods are used: logarithmic wind profile and power law. Logarithmic wind profile has equations for three atmosphere stabilities. (Emeis 2018, p. 35, 38) The equation for neutral stratification is as follows:

$$u(z) = \frac{u_*}{\kappa} \ln \frac{z - d}{z_0} \tag{3}$$

Where u is wind speed [m/s], z is height [m], u_* is friction velocity [m/s], κ is von Kármán constant (κ = 0,4) [-], z_r is reference height [m], d is displacement height [m], and z_0 is roughness length [m].

Displacement height is the height above the ground where zero wind speed is achieved for the flow regime over areas which are densely covered with obstacles. In less dense areas this can be omitted. (Emeis 2018, p. 35)

The equation (3) can be used to calculate wind speed at a wanted height using a known reference wind speed at reference height. Combining two of the equations for different heights together and rearranging them so that friction speed and von Kármán constant cancel out results in following equation:

$$\frac{u(z)}{u(z_r)} = \frac{\ln\left(\frac{z}{z_0}\right)}{\ln\left(\frac{z_r}{z_0}\right)} \quad (1)$$

Where u is wind speed [m/s], z is height [m], z_r is reference height [m], and z_0 is roughness length [m].

The equation of power law used to describe vertical wind profile is:

$$u(z) = u(z_r)\left(\frac{z}{z_r}\right)^a \quad (2)$$

Where u is wind speed [m/s], z is height [m], z_r is reference height [m], and a is shear exponent [mm]. (Emeis 2018, p. 40)

Shear exponent a is dependent on surface roughness and thermal stability of Prandtl layer. This means that it will vary with height and change more strongly with height when surface roughness is greater. In neutral stratification shear exponent is equal to TI and can be expressed as:

$$a = ln^{-1}\left(\frac{z}{z_0}\right) \quad (3)$$

Where a is shear exponent [mm], z is height [m], and z_0 is surface roughness [m]. (Emeis 2018, p. 40)

In neutral stratification logarithmic wind profile and exponent law give similar results. In other stratification the shear exponent differs from TI as it varies with height. Power law is better used for smooth surfaces while logarithmic profile is better for more complex terrain. In Emeis' demonstration case of three computed wind profiles using different height-to-roughness ratios of z/z_0, logarithmic and power law wind velocity curve values differed by 0,3-1,3 % at 100 m and 2-11,2 % at 10 m of height. (Emeis 2018, p. 42-44)

Wind speed profile in Ekman layer

In Ekman layer equilibrium of forces is different than in Prandtl layer as there Coriolis force gets stronger and turns wind direction more as height increases. Coriolis force is estimated with Coriolis parameter that is latitude dependent. Geostrophic wind speed is determined by Coriolis parameter and large-scale horizontal pressure gradient. This can be used to calculate the wind speed in Ekman layer with:

$$u(z) = \sqrt{{u_g}^2(1 - 2e^{-\gamma z}\cos(\gamma z) + e^{-2\gamma z})} \qquad (5)$$

Where u_g is geostrophic wind speed [m/s], γ is inverse length scale [s^{-1}], and z is height [m]. (Emeis 2018, p. 51)

Above equations (3) and (6) describe wind speed in their layer. A unified method is used when turbine acts simultaneously in both of those layers. This would be usually the case for LWPP as it has turbines on multiple levels, so it is more likely to have turbines operating in Prandtl and Ekman layers, or the mixture of them.

Weibull distribution is used to describe the low-frequency end of wind speed spectrum as a probability distribution of wind speed. It is defined by scale parameter A and shape parameter k. Scale parameter expresses the mean wind speed of the whole time series and it typically increases with elevation. Shape parameter expresses the shape of the distribution, and it decreases with elevation due to rising wind speed variability. Weibull distribution can be calculated using: (Emeis 2018, p. 215)

$$f(u) = \frac{k}{A}\left(\frac{u}{A}\right)^{k-1} exp\left(-\left(\frac{u}{A}\right)^{k}\right) \qquad (4)$$

Where u is wind speed [m/s], A is scale parameter [m/s], and k is shape parameter [-].

3.1.4 Turbulence

Turbulence plays a major part in assessing structural load calculations of wind turbines. Parameters for it are TI, high-frequency wind speed variances, turbulence length scale and inclination angles, and the wind speed variation with time during typical gust events. (Emeis 2018, p. 135-136)

TI depends on roughness length and is created by shear or thermal instability. It increases both mechanical loads and power output of turbines. Onshore roughness length is dependent on surface characteristics, but offshore it is also affected by wind speed. This is due to wind speed affecting ocean wave formation, which in turn changes ocean surface roughness. (Emeis 2018, p. 136-137)

TI increases with surface roughness and in a neutral atmosphere it decreases with height. In unstable atmosphere TI also increases with instability. TI is much lower in stable conditions. (Emeis 2018, p. 36, 38)

Example plot of TI profiles by Emeis showed that the TI decreased by 25 % over height of 100-150 m for stable, by 11 % for neutral, and by 5 % for unstable conditions. (Emeis 2018, p. 40) The decrease in intensity was strongest near the ground and less so at higher elevation. This would lead to top turbines in a LWPP experiencing higher TI than lower ones.

Onshore longitudinal, transverse, and vertical wind components are independent of wind speeds but offshore they aren't. There is more variance at lower wind speeds for both cases, but offshore the variance reduction is greater at high wind speeds. (Emeis 2018, p. 141-142)

Turbulence elements that are similar in size to turbine rotor often hit it only partially. This unevenness causes differential loads on the rotor. Turbulence elements are usually inclined forwards which makes them impact upper tip of rotor slightly earlier than the lower tip, which causes differential loads on rotor. This inclination increases with wind speed. (Emeis 2018, p. 143) Therefore LWPP top turbines could face more differential loads that would increase torsional forces on blades and tower.

In a typical gust event wind speed decreases before experiencing a large increase and finally decreasing before returning to undisturbed wind speed. Extreme operating gust is an event with a duration of 10,5 s. Gusts can happen on single height, not registering on others.

(Emeis 2018, p. 144-146) This increases the chance of LWPP experiencing uneven wind loads in a gust event.

Sea surfaces are smoother than land surfaces which leads to higher wind speeds, smaller TIs. These vary with wind speed due to it affecting wave heights and thus surface roughness. Low levels of turbulence reduce structural loads on single turbines but reduces the vertical turbulent fluxes that provide kinetic energy to wind farms. (Emeis 2018, p. 114, 152) This means that if LWPP was used off-shore it would lessen loads due to lower turbulence, but the lower turbulence would also lead to longer wakes.

3.1.5 Wind direction

Wind direction is dominantly from seas to inland as that is where high pressure gradients form. Uneven warming of surfaces, movement of pressure gradient zones, and concentrating effect from land topology affect the directionality of wind.

Real terrain is inhomogeneous and complex. Topography is used to address the variation in surface properties and elevations while orography addresses especially the heights. Topography affects wind speeds by changing surface roughness and creating accelerating narrowing for it. Orographic features create a channelling effect that alters wind directions. (Emeis 2018, p. 90-92)

As wind flows over hills, mountain chains, summits, or crest lines it speeds up. This speed up is marginal and largest near the surface of the hill. ABL after the hill has less wind shear at the hub heights of conventional turbines compared to ones over flat terrain. These factors would lead to only relatively low gain in power yield of higher towered turbines in hilly terrain. (Emeis 2018, p. 107, 109)

Local frequency of wind directions is indicated by wind roses. These show the direction of the wind with the frequency in a radar plot. They can be found at global level in Global Wind Atlas or at national level for example from tuuliatlas for Finland. Wind roses are used for wind farm micro-siting and estimating production. Especially wake loss analyses need them.

Wake loss is expected to be more prominent in LWPP which makes wind directionality major component for energy production. Wind sites with high directionality would be

optimal for them. These would be areas with orographic features such as mountains and valleys, that concentrate the wind directions along one major axis.

3.2 Wind turbine properties

Properties of wind turbine affect how they can tap into wind resources. Main properties of wind turbines are tip speed, rotor power coefficient and power curve. There are different kind of turbines that are suited for different conditions. LWPP is designed to use multiple turbine types with different properties, such as wind class or drive train configuration. This is so their potential can be optimized based on the wind conditions at each elevation level and placement on the support structure.

Tips speed ratio (TSR), usually denoted by λ, is the ratio of circumferential speed at the blade tip to the wind speed. It is a significant parameter in aerodynamic design of rotor blades. Wind turbine with low tip speed ratio provides high torque while running at a low rotor speed and vice versa. Conventional turbines operate at higher tip speed ratios of 5-8 and use variable-speed to keep tip speed ratio at the designed value while operating at a large wind speed range. Favourable tip speed is maintained by pitch control. (Gasch R. & Twele J. 2012, p. 49, 51-52)

Turbine thrust coefficient describes the force exerted by the turbine onto the incoming flow. It is usually higher at low wind speeds, decreases with increasing wind speed and reaches a low value near cut-out wind speed. (Stoevesandt et al. 2022, p. 158) Example of thrust coefficient values is from V80 at Horns Rev offshore wind farm were they were 0.1-0.8 with highest values between 4-9 m/s (Bhattacharya 2019, p. 72). Turbines are typically pitch controlled so their TSR stays optimal, so 0.84 can be assumed for calculations. (Gasch R. & Twele J. 2012, p. 211)

Power curve is used to show how much energy turbine is expected to produce at certain wind speed. These are usually shown in a plot of power over wind speed. The curve includes cut-in speed where a turbine can produce more power than what is lost due to low loads. Turbine is stopped when wind speed reaches cut-out speed to protect the turbine from damage due to excessive loading. Rated power is achieved after transition region that is typically around 11-12 m/s. (Jamieson 2018, p. 216)

Turbines are planned to reach rated power at medium wind speeds as that is close to the average speed of a typical wind speed distribution. Turbines could be designed to reach rated power at higher wind speeds, in principle nine times increase in power for 25 m/s wind speeds, but that would entail larger drive drains to handle those forces. Due to low occurrence of higher speed winds, it wouldn't be economically feasible. (Jamieson 2018, p. 217) Higher wind speed distribution would allow a turbine to operate more often at rated power, which would increase its capacity factor.

Power curves are used to assess the example LWPP design's power production. Power curves of the V80-1.8 and V112-3.3 turbines used in this work are from Wind-Turbine-Models. They are shown in Figure 4 and Figure 5.

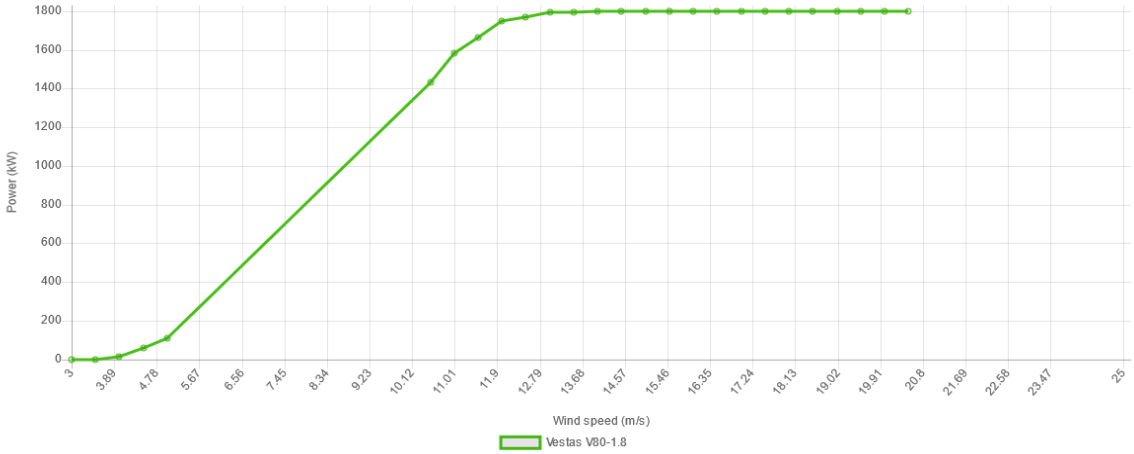

Figure 4. Power curve of V80-1.8. (Wind-Turbine-Models, 2022)

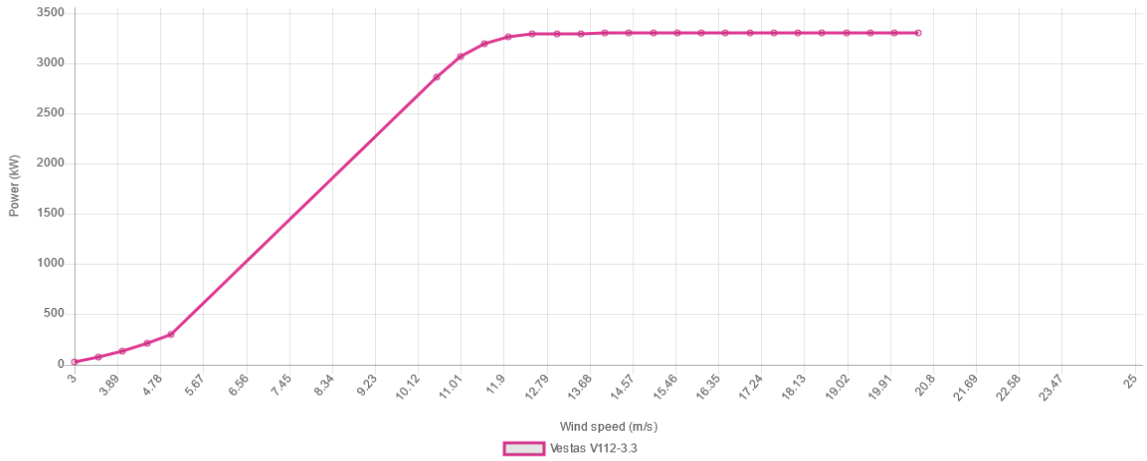

Figure 5. Power curve of V112-3.3. (Wind-Turbine-Models, 2022)

Figures show that both turbines have cut-in speed at three m/s and cut-out at 20.5 m/s. Turbines at hub heights of over 100 m rarely experience less than 3 m/s wind speeds, which leads to less zero production time for them. Cut-out speed will be more important for top turbines as at those heights the wind distribution is more skewed towards higher speeds. Still the probability of wind speed exceeding this limit is small.

Turbines are classified according to IEC 61400-1 standard to four wind classes based on environmental conditions. Design parameters are expected extreme 50-years gust u_r, annual average wind speed u_{ave}, and characteristic turbulence intensity I_r. (Gasch R. & Twele J. 2012, p. 310) Wind turbine classes are shown in Table 2.

Table 2. Wind turbine classes. (Rao K, 2019, p. 182-183)

Wind turbine class		**I**	**II**	**III**	**S**
u_r	[m/s]	50	42.5	37.5	Values specified by the designer
u_{ave}	[m/s]	10	8.5	7.5	
A	I_r [-]	0.16			
B	I_r [-]	0.14			
C	I_r [-]	0.12			

This means that turbines are optimised for different wind speeds and turbulences. As LWPP uses multiple levels of height for turbines, their classes can be picked based on the typical wind speeds and shear forces for each level.

Previous chapters on wind resources have discussed that wind speeds and turbulences are typically higher at greater elevations. This would make it that the turbines on the top level of LWPP should be of higher wind speed and turbulence class. At middle and lower levels wind conditions might be reduced by an amount that would make those turbines better suited to be of lower class.

3.3 Turbine wakes

Turbines cause wakes when they operate, and these wakes affect the wind conditions for turbines downstream. Wakes are distinguished to near and far wakes. Near wakes are the area just behind the rotor and they are affected by rotor characteristics. Near wakes reach approximately up to three rotor diameters downstream. Far wake is the area beyond the near wake, and it can reach 4-20 D downstream. (Emeis 2018, p. 157-158) (Kaldellis 2021, p. 2) Near wake can further be divided to near wake and very near wake. In very near wake the tip spirals are dominant. (Stoevesandt et al. 2022, p. 917)

Wake development is based on many parameters such as turbine generated TI, ambient TI, inter-array distance and the blade pitch angle, wind speed and wind direction, tip speed ratio of upstream turbine, ABL, and surface roughness. (Kaldellis 2021, p. 2)

The LWPP design has multiple turbines on varying heights in close proximity, which increases the importance of near wake effects compared to conventional wind parks where turbines mainly experience far wakes due to longer spacings.

Near wakes are formed from the rotation of the turbine blades, and they form tip and root vortices. Tip vortices are shed into the wake in a continuous fashion and emanate from a radius slightly smaller than the radius of blade tips. Root vortices form closer together and are destroyed quicker, making the near wake dominated by tip vortices. Tip vortices destabilize and break down into turbulence, where turbulent mixing finally results into what is called the far wakes. (Stoevesandt et al. 2022, p. 916, 919) Tips vortices have random

fluctuations called vortex jittering, and it increases with vortex age and incoming TI Turbulent inflow reduces vortex lifetime significantly. (Porté-Agel et al. 2020, p. 7) Vortex generation is increased with dynamic stalling of the blades that results from aerofoil pitching. (Stoevesandt et al. 2022, p. 778) Example of wake flow complexity is in Figure 6.

Figure 6. Example of wake showing iso-surface of vorticity in the flow field from LES. (Stoevesandt et al. 2022, p. 916)

A rough and ready equation for assessing near wake length has been developed by Sørensen (2011) expressed as:

$$\left(\frac{1}{R}\right)_{nwl} = -\left(\left(\frac{16u_c^3}{N_b\lambda C_T}\right)\ln(C_1T_i) + C_2\ln(T_i)\right) \quad (5)$$

Where R is rotor radius [m], u_c is convective propagation velocity of the wake system [m/s], N_b number of blades [-], λ is tip speed ratio [-], C_T is thrust coefficient [-], T_i is turbulence intensity [-], and C_1 and C_2 are constants with values $C_1 = 0.3$ and $C_2 = 5.5$. (Stoevesandt et al. 2022, p. 924)

This equation shows how length of near wakes is mostly dependent on blade characteristics and turbulence levels, which is significantly affected by atmospheric conditions. An example case by Stoevesandt et al. (2022) showed that the modelled near wake reached 12 D at 2% T_i and 6D at 15 % T_i. Very near wakes were around 15 % the distance of near wake. (Stoevesandt et al. 2022, p. 924-925)

Distances between turbines in a LWPP design are less than 12 D which makes every turbine be in near wake during certain wind directions. Lengths of the near wakes will vary for each turbine in LWPP as turbulence levels will increase for turbines downstream. Even shortest wakes are expected to reach across the whole structure. Note that these wake lengths are based on an example case and their real lengths will vary in different conditions, but they offer good approximation for initial LWPP considerations.

Far wakes have more universal characteristics. Wake grows in lateral and horizontal directions downstream due to entrainment of outer flow. LES, wind-tunnel, and field studies have shown wake width σ to increase linearly with downstream distance. Wake speed increases until it recovers far downstream. Streamwise velocity profiles have an axisymmetric Gaussian distribution. (Porté-Agel et al. 2020, p. 8-9)

Wakes cause a flow speed deficit and adds TI. Rate of wake weakening is done by downwind decay coefficient k, that describes the rate of wake refilling due to atmospheric turbulence. Empirical evidence has showed that it is about half of TI, with typical value for onshore being 0,075. Speed deficit and added TI are determined by turbine's thrust coefficient and the ambient atmospheric turbulence, that is often characterized by TI parameter. (Emeis 2018, p. 158-159) Relative velocity deficit in far wake is calculated with:

$$\frac{\Delta u}{u_h} = \frac{u_{h0} - u_h}{u_h} = A\left(\frac{D}{s}\right)^n \tag{6}$$

Where u_h is the wind speed in the wake at hub height [m/s], u_{h0} is the undisturbed wind speed at hub height [m/s], D is rotor diameter [m], s is the distance from turbine [m], and A and n are constants [-]. A is 1-3 and n is 0,75-1,25, and they depend on ambient TI. (Emeis 2018, p. 158)

The speed deficit of multiple wakes add sup together in quadratic manner. The quadratic superposition of single wakes in a wind farm is formulated as:

$$U_i = U_\infty - \sum_k (U_k - U_{ki}) \quad (7)$$

Where U_i is velocity at turbine *i*, U_∞ is the undisturbed velocity [m/s], U_{ki} is the wake velocity of the turbine *k* at turbine *i* considering only those turbines whose wake interact with turbine *i* [m/s]. (Niayifar & Porté-Agel 2016, p. 5)

This is for far wakes and might not be suitable for LWPP estimations, as there wake summation is most likely happens at near wakes.

Wakes also increase mechanical fatigue of downstream turbines, which in turn increases the wear and tear of mechanical components. This can lead to increased failure rates and reduced availability. (Kaldellis et al. 2021, p. 3) Fatigue is induced by high TI and the fatigue increase from wakes can be 5-15 % in large offshore wind farms. (Cao et al. 2022, p. 3)

Wind tunnel experiments have shown that TI profiles at hub height present a dual peak and approximately asymmetric distribution. Highest turbulence occurs in the near wake near tip-side positions. Nacelle and tower generate considerable turbulence, but it vanishes in the near wake region. (Ishihara & Qian 2018, p. 281-282)

Frandsen et al. (2006) created a model complex that links small-scale and large-scale flow features in wind farms. The model was developed for offshore wind farms of any size, with array geometry of straight rows of wind turbines with equidistant spacing between turbines in a row and equidistant space between rows of wind turbines. An example implementation of the model was done using Bonus 500 kW wind turbine thrust curve, hub height of 38 m, rotor diameter of 35 m, free stream speed of 10 m/s, wind farm of 10 rows and along-row spacing of 300 m. (Frandsen et al. 2006, p. 39-40, 50-52) Resulting wake behaviour is illustrated in Figure 7.

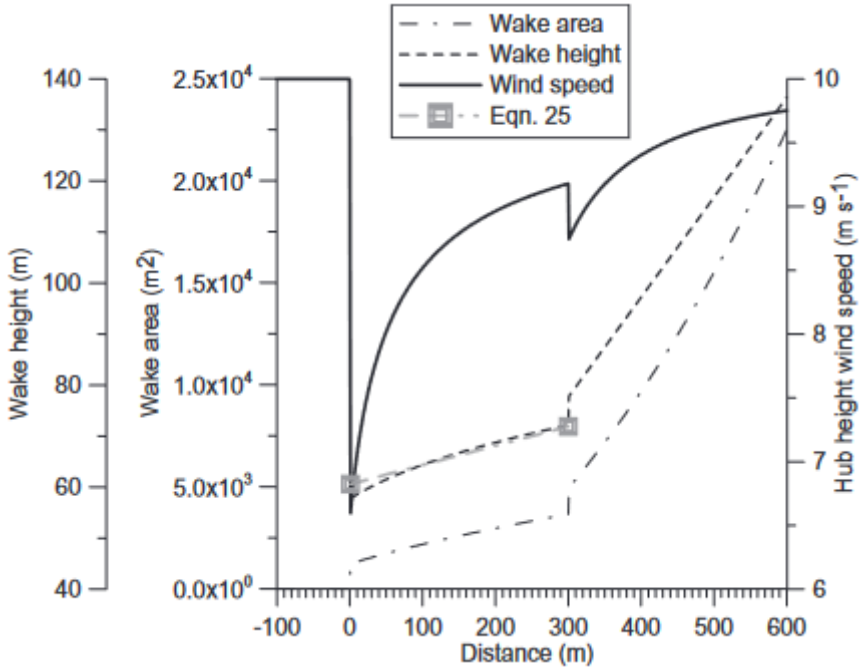

Figure 7. Model operationalized for a wind farm with 10 rows. The wake height, wake area and wind speed are shown for the turbine in the centre row. (Frandsen et al. 2006, p. 52)

An example of wake speed deficit and wake area growth can be seen in Figure 7. Wake speed can be seen to recover before experiencing another drop from a second turbine. Sharp increase in wake area after second turbine is due to wake front from first row coalescing and not from individual wakes multiplying. In LWPP these behaviours would be similar, only less recovery due to short turbine spacings and no spike in area due to single wakes. LWPPs in a wind farm configuration might face similar strong wake front addition.

3.3.1 Wake models

Wake models are used to estimate the wind speed deficit and the wind speed field downstream of an examined wind turbine's hub. These can be analytical, empirical or simulation based. Models can be further divided to near and far wake models. Different models are better suited for different situations. Most use upstream wind speed, rotor radius, and downstream distance as parameters, but some of the models require additional input

parameters. (Kaldellis et al. 2021, p. 4) This is why several models need to be considered to find the optimal one for LWPP wake analysis.

Analytical wake models, also known as kinetic models, provide a simple and computationally cheap prediction for average velocity deficit in wind turbine wakes. They are less accurate than numerical simulations. They are derived from basic physical equations relating to mass, momentum, and energy balances. (Porté-Agel et al. 2020, p. 3) These are typically top-hat models where wake width is assumed to expand constantly and wind deficit inside wake is laterally uniform. Other model type is gaussian distribution for velocity profile. (Stoevesandt et al. 2022, p. 930, 933) An additional turbulence model is usually needed to get a full picture of wake flow field. (Kaldellis et al. 2021, p. 5)

Example of a wake behind a turbine calculated by analytical Jensen, Larsen and Frandsen models is shown in Figure 8. It was calculated for a GE 1.5sl wind turbine with wind speed U_∞ = 10 m/s, wake decay constant k = 0,075 for Jense, ambient turbulence intensity I_a = 0,1 for Larsen, and shape parameter k = 2 and expansion constant α = 0,7 for Frandsen. (Renkema 2007, p. 8)

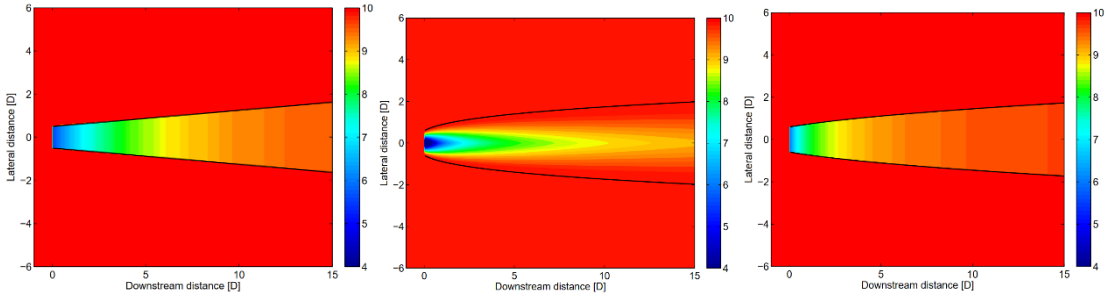

(a) (b) (c)

Figure 8. Wake behind GE 1.5sl using (a) Jensen, (b) Larsen, and (c) Frandsen models. (Renkema, 2007. p. 6, 8-9)

Jensen and Frandsen use constant wake expansion which leads to iconic top-hat shape for wake expansion. Larsen model uses approximation of Prandtl turbulent boundary layer equations to solve the rotor wake radius (Renkema 2007, p. 7). Larsen model has radial velocity deficit variance while others use constants deficit only based on downstream

distance. A model with radial variance would be more accurate for estimating LWPP wakes as there turbine are more likely to be partially in wakes.

Empirical models are like analytical ones as they are simple, but they are solely based on fitting experimental or numerical data. They generally assume power-law relationship with velocity deficit and downstream distance and use equation (6). Additional coefficient *A* and *n* are derived from experimental and analytical data. (Porté-Agel et al. 2020, p. 13)

Semi-empirical near-wake models are blade element method, actuator disc and vortex wake models, and they mainly calculate the flow induced forces acting on the rotor. Due to this focus, they are unable to reveal flow features. (Sedaghatizadeh et al. 2018, p. 1167) These would need knowledge of blade properties and that is too precise for LWPP preliminary analysis.

Most widely used computational fluid dynamic (CFD) wake models are uniformly loaded actuator disc model, an advanced actuator disc model, and actuator line model (Stoevesandt et al. 2022, p. 1002). They are usually applied in Reynolds averaged Navier-Stokes simulations (RANS) or large-eddy simulations (LES). These simulations are computationally expensive and thus too cumbersome for preliminary analysis.

Another method for analysing wind turbine wakes is dynamic wake meandering (DWM) model. This method ranks between CFD simulations and simple analytical engineering models as it is less computationally demanding than full CFD, and closer to physics than purely analytical models. DWM models use small scale turbulence, quasi-steady deficit, and meandering to calculate the wind field with wake. (Reinwardt et al. 2018, p. 1-3)

The article by Reinwardt et al. (2018) compared different analytical and DWM wind wake models and concluded that out of the analytical models Larsen model provided best match for experiment data, but the results were still conservative. Meanwhile more demanding DMW models provided more accurate results, but those models tended to overestimate the results. (Reinwardt et al. 2018, p. 9)

They also simulated damage equivalent loads (DEL) with different DMWs and found that both Larsen and DWM-Keck models overestimated the results when compared to measured ones. (Reinwardt et al. 2018, p. 6)

The problem with choosing an appropriate wake model for LWPP analysis is that most models are created for analysing wake behaviour in the far wake area, whilst LWPP would need accurate data on near wake region. Wakes are more likely to combine in LWPP which makes it also a requirement for wake models. Kaldellis et al. (2021) analysed nine well know analytical semi-empirical wake models and compared them to experimental and simulated data.

> "Under the present work, emphasis has been put mainly on the far-wake area, as the near-wake area is characterized by intense airflow swirl, strong vortex structures and significant wind energy deficit. Moreover, the majority of analytical wake models are unable to generate reliable outcome concerning the wake development in the near-wake area." (Kaldellis et al. 2021, p. 2)

Out of the models, Ishihara & Qian 2018 provided excellent results (Kaldellis et al. 2021, p. 2). Their model is also applicable in near wake region (Ishihara & Qian 2018, p. 283). This is essential for LWPP wake performance evaluation which is why it is used to model wake behaviour in this thesis.

Ishihara & Qian model is a semi-empirical wake model. It assumes an axisymmetric velocity deficit in respect to turbine rotation axis and self-similar distribution in the wake cross-section. Velocity deficit is a product of streamwise function and a self-similar shape function. Velocity deficit is normalised by mean wind speed. Wake deficit can be calculated at a point in wake at *x* downstream, *y* spanwise distance from rotor centre and *z* height-wise distance from ground. Various variables have been empirically fitted to previous LES data to infer their form. (Ishihara & Quan 2018, p. 282-283)

Wake deficit is calculated with:

$$\frac{\Delta U(x,y,z)}{U_h} = \frac{1}{\left(a + \frac{bx}{D} + c(1+x/D)^{-2} + p\right)^2} \exp\left(-\frac{r^2}{2\sigma^2}\right) \qquad (8)$$

Where x is streamwise, y is spanwise, z is heightwise distance [m], D is rotor diameter [m], r is radial distance from wake centre [m], σ is the wake width at a downstream distance [m], ΔU is velocity deficit [m/s], U_h is free velocity at hub height [m/s], variables *a*, *b*, *c*, and *p* are functions of C_t and I_a. More details of equations are in Appendix 1.

The model uses gaussian distribution for velocity deficit. This is illustrated in Figure 9.

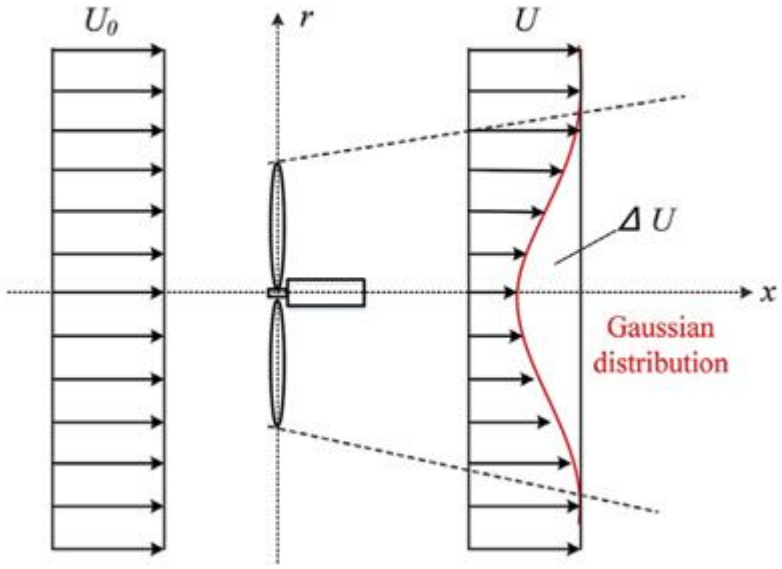

Figure 9. Schematic of gaussian distribution for velocity deficit used in Ishihara & Qian model. (Ishihara & Qian 2018, p. 283)

TI uses double peak gaussian distribution with peaks at edges of wake width. TI is calculated by:

$$\Delta I_1(x,y,z) = \frac{1}{d + e\frac{x}{D} + f(1+x/D)^{-2} + q}\left(k_1 \exp\left(-\frac{\left(r-\frac{D}{2}\right)^2}{2\sigma^2}\right) + k_2 exp\left(-\frac{\left(r/\frac{D}{2}\right)^2}{2\sigma^2}\right)\right) - \delta(z) \quad (9)$$

Where δ is correction term for weakened turbulence intensity in lower part of wake flow [-], variables *d*, *e*, *f*, and *q* are functions of C_t and I_a. More details of equations are in Appendix 1.

This model is based on numerical simulations, wind tunnel experiments, field tests on utility scale wind turbine, and LES studies. It has been validated on wind tunnel experiments, LES

studies and other analytical wake models. Used variables were fitted based on numerous LES studies. (Ishihara & Quan 2018, p. 275-276)

3.3.2 Effect of wind direction on wake loss

Due to the linear design of a LWPP, when wind direction is from close to parallel to the LWPP line, turbines start to experience wake losses from other turbines on the same and possibly from nearby elevation levels. These wakes will be near wakes due to the short vertical and horizonal distances between the turbines.

For wake loss calculations the incoming wind directions that cause turbines to be in each other's wakes needs to be solved. This is done by assuming no wake expansion and calculating the angle below which turbines overlap each other. These are calculated from simple geometry with following equation:

$$\alpha = \cos^{-1}\left(\frac{D}{x}\right) \tag{10}$$

Where α is angle between turbine normal and LWPP line normal [˚], D is turbine diameter [m], and x is distance between turbines [m].

Illustration of the situation is here in Figure 10:

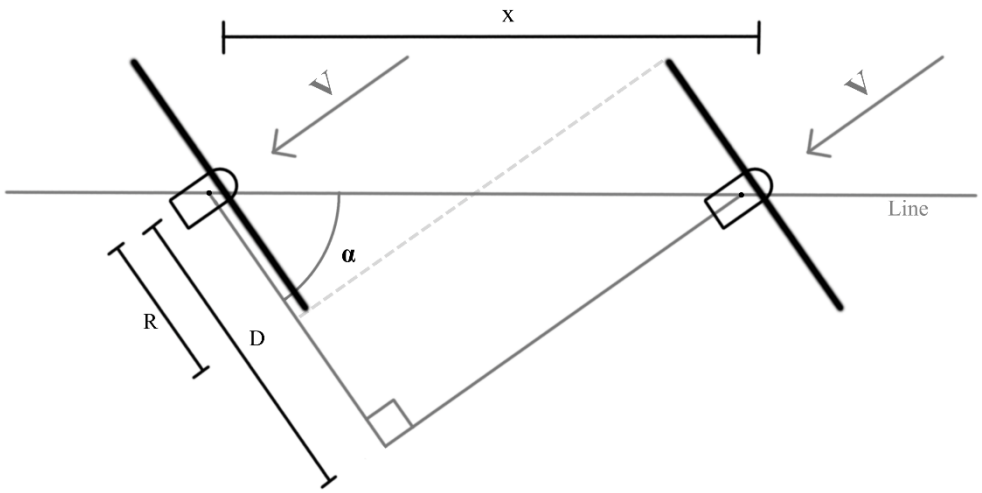

Figure 10. Angle limits for turbines in line. α is the angle above which this turbine pair's downstream turbine experiences wake effects.

Distances between lowest turbines 1-4 are 140, 260 and 400 m. Distances between middle turbines is 250 m. From these we get angle limits that are shown in Table 3. Same limits apply for pairs when wind comes from the opposite direction.

Table 3. Angle limits for inflow between turbine pairs, below which the second turbine will experience wake loss from the first in pair.

Turbine pair	**Angle limit α [˚]**
T1-2	55.2
T1-3	72.1
T1-4	78.5
T2-3	48.2
T2-4	72.1
T3-4	55.2
T5-6	63.4

From Table 3 it can be seen how the number of turbines in each other's wake increases when wind direction approaches parallel to the LWPP line. This causes the wakes to sum up and their effect on turbine power production and wind loads to stack up. This effect would also

be noticeable when using multiple LWPP as a wind farm where the combination of wakes is more likely to reach downstream systems during certain wind directions. This would add to the complexity of LWPP micro-siting.

4 Power production analysis

Wake loss is expected to be a major part of LWPP design's power production due to the proximity of turbines. This would be most prominent in lower levels where most turbines would be due to pyramidal structure of the concept. Previous chapters looked at the range of wind conditions that a LWPP would face, how wakes are formed and how they affect LWPP operation. In this chapter we examine and apply those to the example LWPP design to estimate power production and losses that wakes impose on it.

4.1 Wind sites

Estimation of LWPP production including wake losses is done by examining four wind sites around Finland and simulating operation based on publicly available wind data. Sites provide varied wind conditions for analysing performance. Wind data is from Finnish tuuliatlas. Locations are picked to be Tahkoluoto, Kalajoki, Sodankylä and Joensuu. Tahkoluoto is chosen for considering off-shore applicability and comparison to those conditions. Kalajoki is chosen as that is the prime spot for wind projects due to excellent wind conditions. Sodankylä is chosen for more northern location where icing and cold provide different conditions and thus an additional interesting aspect for analysis. Joensuu is chosen for deep inland conditions and eastern location for novelty as there is only a little wind power in eastern Finland.

Tuuliatlas data is based on dynamic weather prediction models. It provides wind data on 2,5 km^2 resolution size for whole Finland and some location with more accurate data in 250 m^2 resolution. Weather model uses real life measurements from 72 months chosen to present 50 years' timeline. (Ilmatieteen laitos 2010, p. 7) Locations of tuuliatlas data sites are shown in Figure 11.

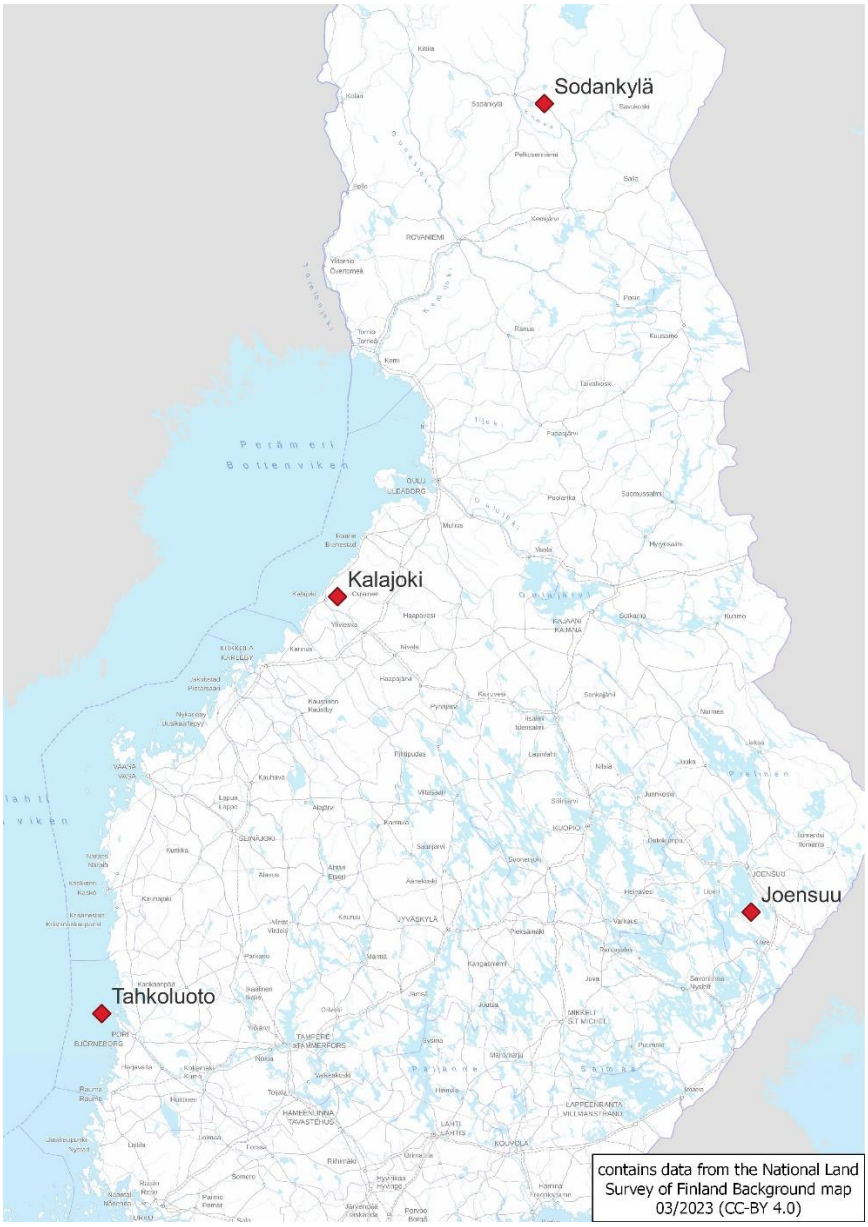

Figure 11. Sites of tuuliatlas data.

From tuuliatlas data we get the wind data for each site. Wind speeds are estimated at heights of 50, 75, 100, 125, 150, 200, 300 and 400 meters. Wind direction is given as frequency between 12 sectors each consisting of 30 degrees segment of a circle. Weibull shape parameter k and scale parameter λ were given for each height and atmospheric stability state. The data also contains turbulency and gust factors, and estimations for wind power production on turbine sizes of 1, 3, and 5 MW. From the data's Weibull parameters, we get following wind speed distributions at various heights for each site show in Figure 12.

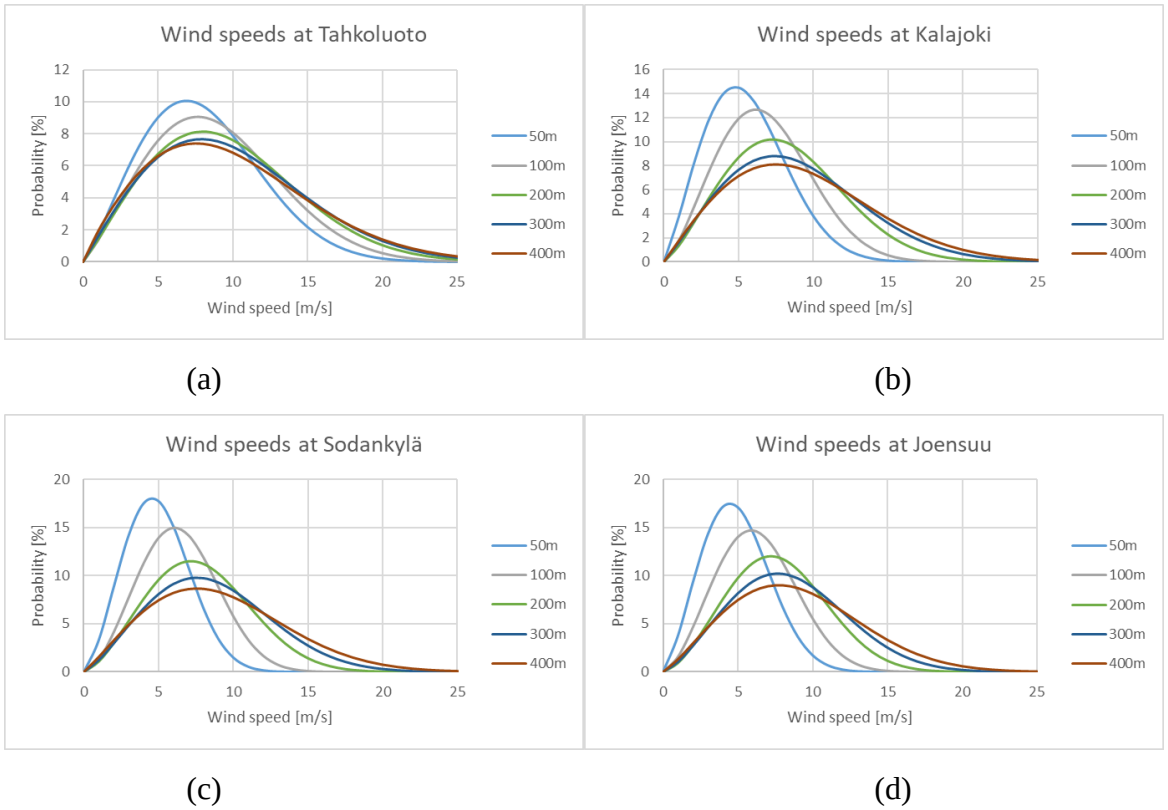

Figure 12. Weibull probability density distributions for various heights at the sites as function of wind speed. Figure (a) Tahkoluoto, (b) Kalajoki, (c) Sodankylä and (d) Joensuu.

These figures in Figure 12 show how the wind speeds and the frequency of their occurrence changes as height increases and how they differ between locations. The wind speeds at deep inland locations of Joensuu and Sodankylä have similar distributions. Kalajoki is only ten kilometres inland while Tahkoluoto is six kilometres offshore. Both of these near shore locations have wider wind distributions that are slanted towards higher speeds. These figures show how much surface roughness of land masses slows down wind speeds. This is more prevalent at lower heights and at 400 m the distributions are very similar between sites despite location differences.

Figures show that probability of high wind speeds increases with height but so does the wind speed variance. Change in probability is more prominent in inland sites than for near shore sites. This lends credence to the idea of LWPP benefitting from increased wind speed due to top turbines reaching higher hub heights. Wind speed increase and variance increase also means that turbines up higher require different turbine classes for optimal performance.

An Excel calculation tool was created for estimating the power production of a LWPP. The tool uses tuuliatlas data, wind power curves, dimensions of the example design, and the wake loss model by Ishihara and Quan. The Excel tool version of wake loss model was validated by replicating example calculations done by Ishihara & Quan (2018) and comparing the resulting plots visually to figures provided by them.

As the LWPP design has turbines in a line, wake effect losses need to be calculated at different wind speed directions. Tuuliatlas wind frequency and speed data is visualized in Figure 13, Figure 14, and Figure 15 where 0 degrees means north. Tuuliatlas data was given per sector, but his was spread out to be per degree. Figures include the chosen orientation of LWPP line at each site. LWPP line orientation was calculated by multiplying wind speed and frequency at 200 m for each direction and finding the average direction from these.

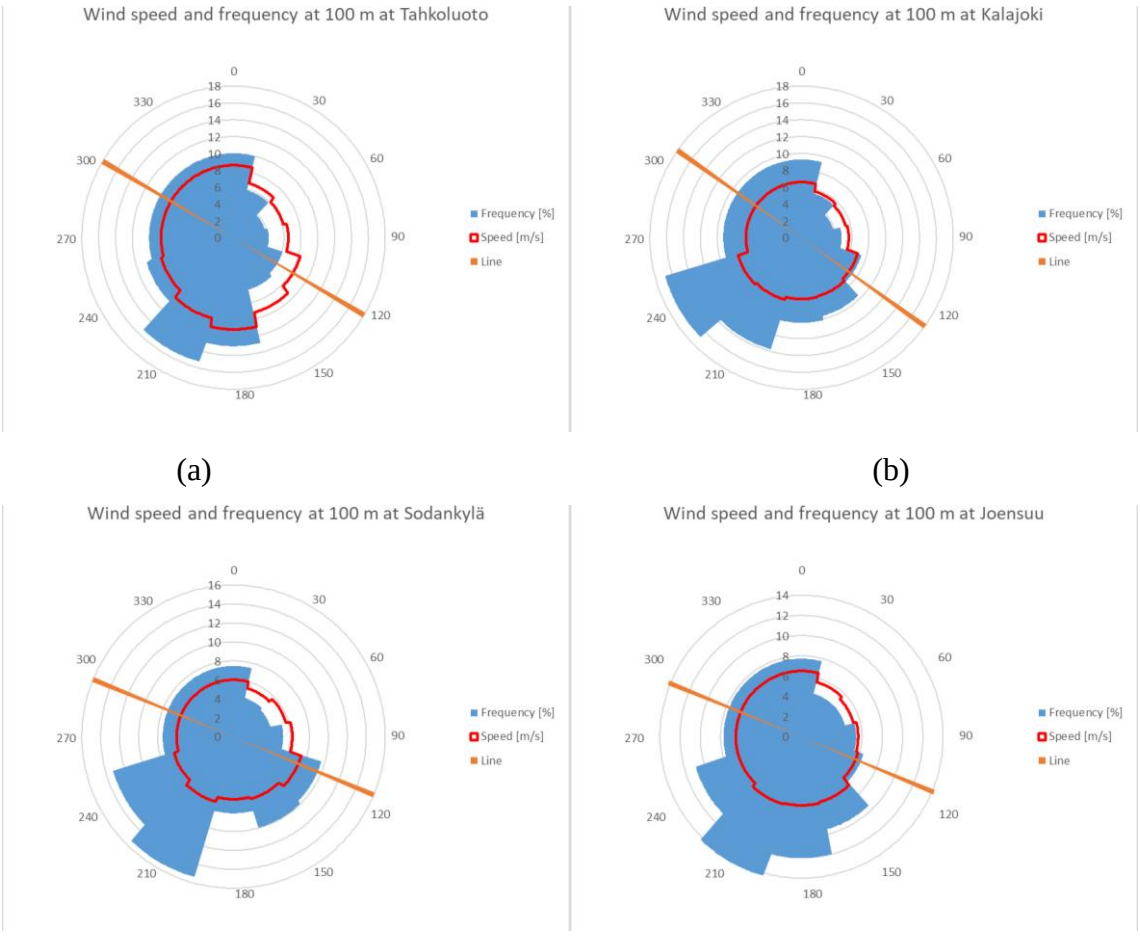

Figure 13. Wind speed and frequency at 100 m height for each site as a radar plot. Figure (a) Tahkoluoto, (b) Kalajoki, (c) Sodankylä and (d) Joensuu.

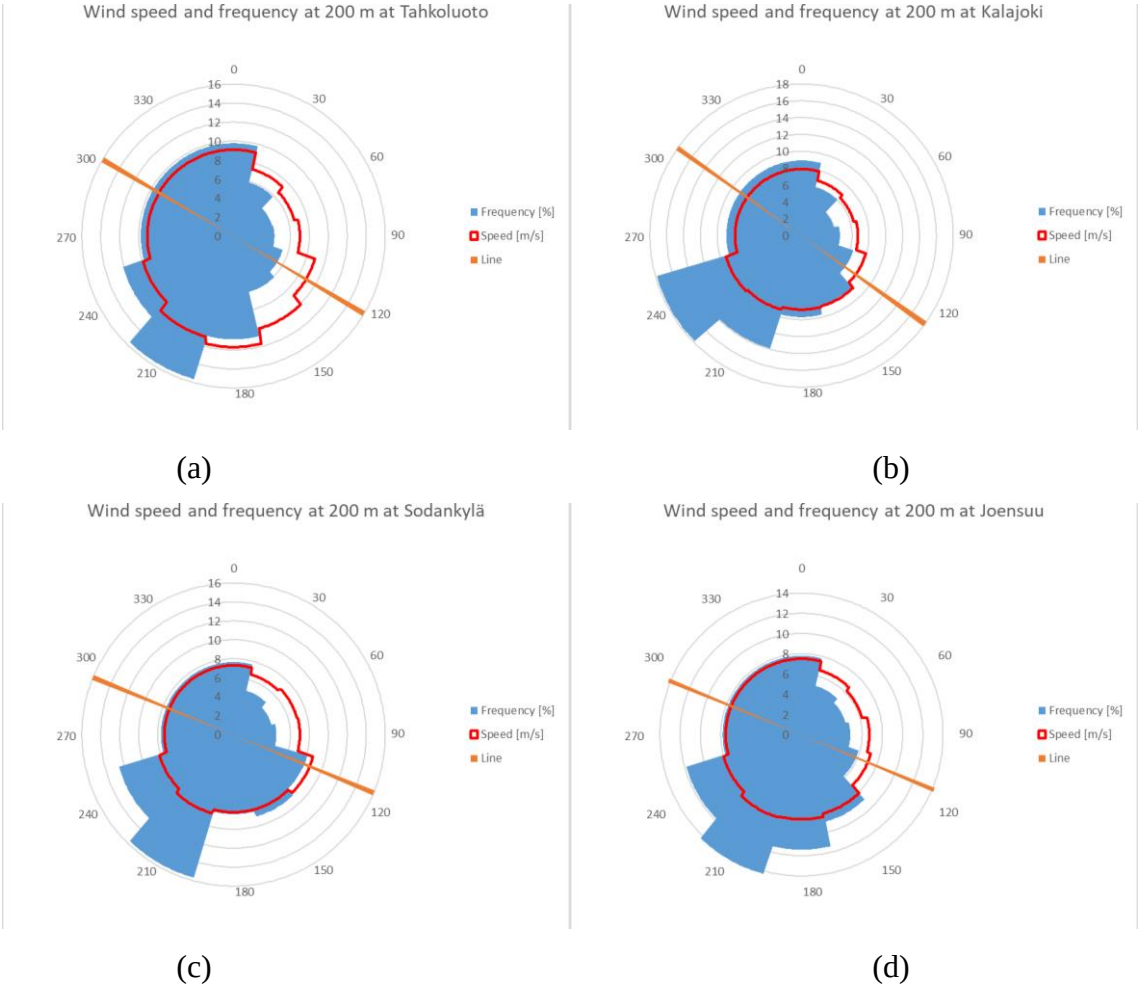

Figure 14. Wind speed and frequency at 200 m height for each site as a radar plot. Figure (a) Tahkoluoto, (b) Kalajoki, (c) Sodankylä and (d) Joensuu.

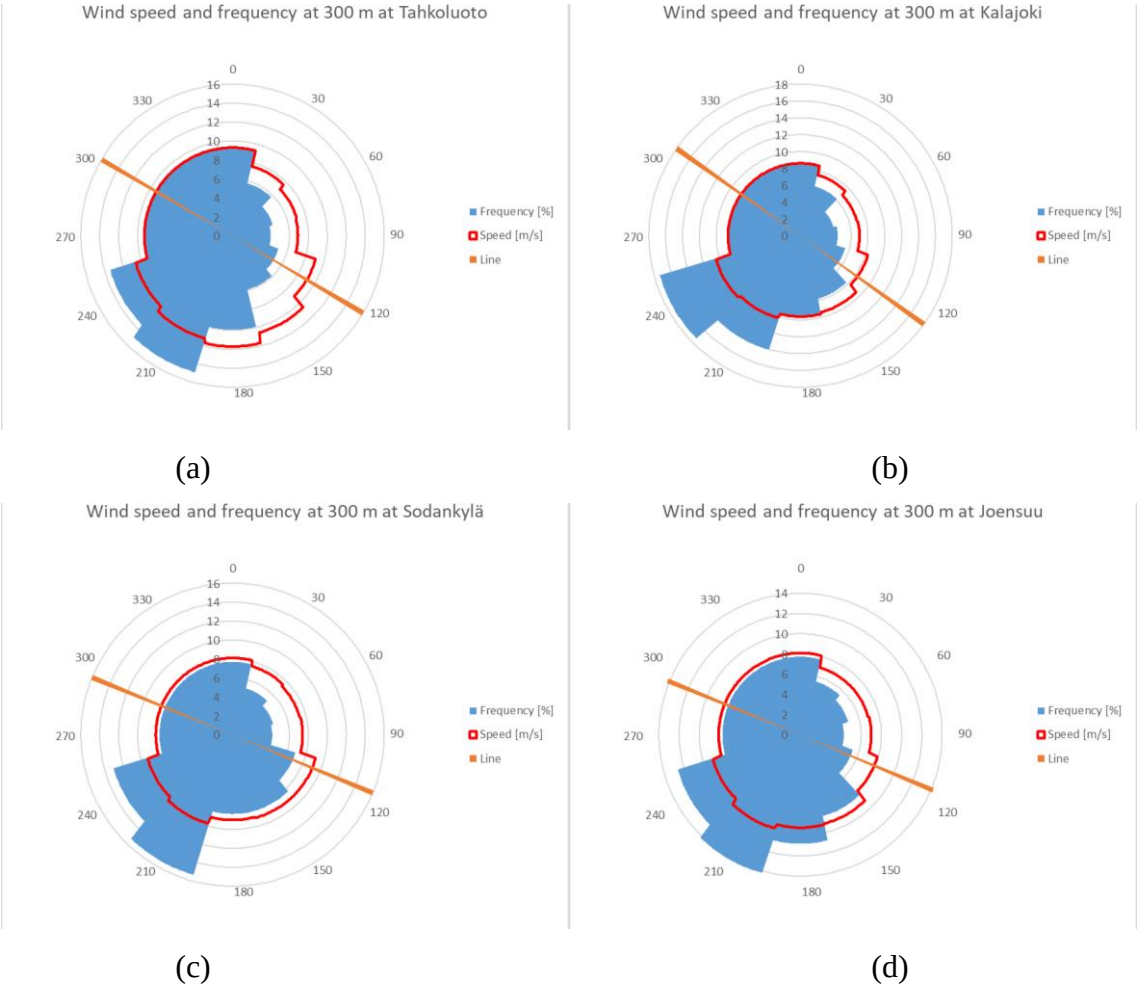

Figure 15. Wind speed and frequency at 300 m height for each site as a radar plot. Figure (a) Tahkoluoto, (b) Kalajoki, (c) Sodankylä and (d) Joensuu.

These figures show how the directionality of wind flow remains same with height increase. Speeds increase with height, but proportionality remains with directionality.

4.2 Wake loss analysis

Wake loss was calculated using Ishihara & Quan wake loss model for each degree of incoming wind flow direction. Input values were turbine thrust coefficient and ambient turbulence. Thrust coefficient was assumed to be 0,81 as that is typical operating value near design speeds and it was used by Ishihara & Quan (2018, p. 280). Wake loss includes both wind speed deficit and added TI calculations.

4.2.1 Wind speed deficit

Wind speed deficits for each turbine were calculated using analytical wake loss formula (8). Limit angles were calculated in chapter 3.3.2 and are used to apply the velocity deficit formula at appropriate wind directions. Velocity deficit was calculated for each turbine pair and resulting wind speeds with deficit were used as inflow values for turbines downstream. Multiple wakes were combined using equation (7). Calculations used T1 as the first flow wise turbine which is why deficits for turbines 1 and 5 are zero. In real life case the flow wise turbines would experience less wake loss and first ones more than shown in these calculations.

A more detailed graph of resulting wind speeds after deficit is shown in Figure 16. This is shown only of one location to illustrate how the deficit changes between turbines over the incoming wind flow directions. Calculations for this figure used correct flow wise directionality for turbines, which is why T1 is shown to experience wake loss.

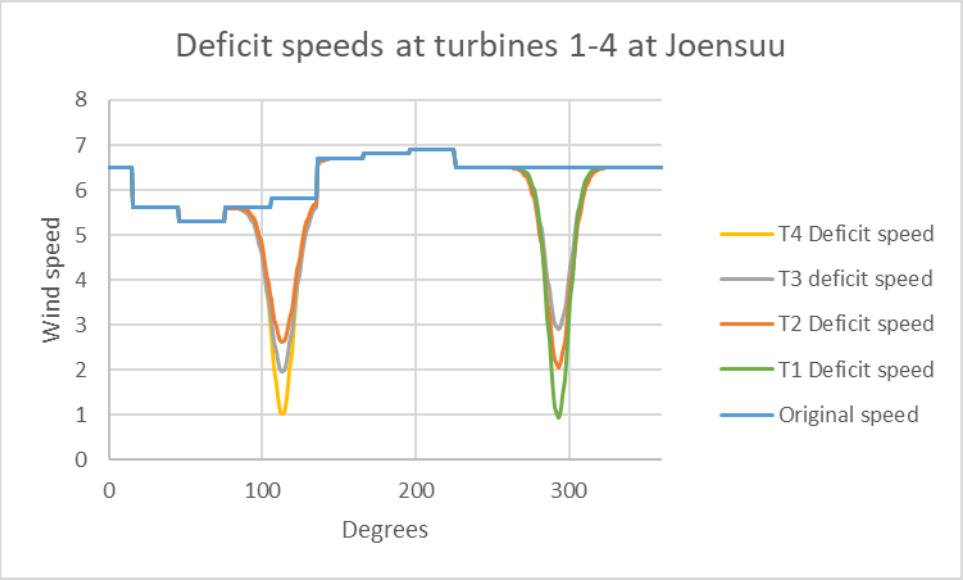

Figure 16. Deficit speeds of turbines 1-4 per wind direction relative to LWPP line normal at Joensuu.

The cumulative nature of wake loss and the effect of wake angle limits can be seen Figure 16. Turbines experience the wakes at different incoming wind directions. The wake reduces the inflow wind speed for turbines. Wind speed deficits over the inflow directions are

averaged and adjusted by inflow direction frequencies to represent average annual wind speed deficit for each turbine. Calculations resulted in reductions in wind speed as per following Table 4.

Table 4. Annual average wind speed deficit from wake loss per turbine for each site.

	Average wind speed deficit [m/s]			
Turbine	**Tahkoluoto**	**Kalajoki**	**Sodankylä**	**Joensuu**
T1	0	0	0	0
T2	0,4	0,43	0,42	0,38
T3	0,56	0,53	0,52	0,48
T4	0,65	0,58	0,57	0,52
T5	0	0	0	0
T6	0,35	0,39	0,4	0,35

Turbine seven is the only one at 300 m and doesn’t experience wake from other turbines, so wake deficit wasn’t calculated for that height. Graphs of average wind speed deficit across hub heights per wind direction for each site are shown in Figure 17 and Figure 18.

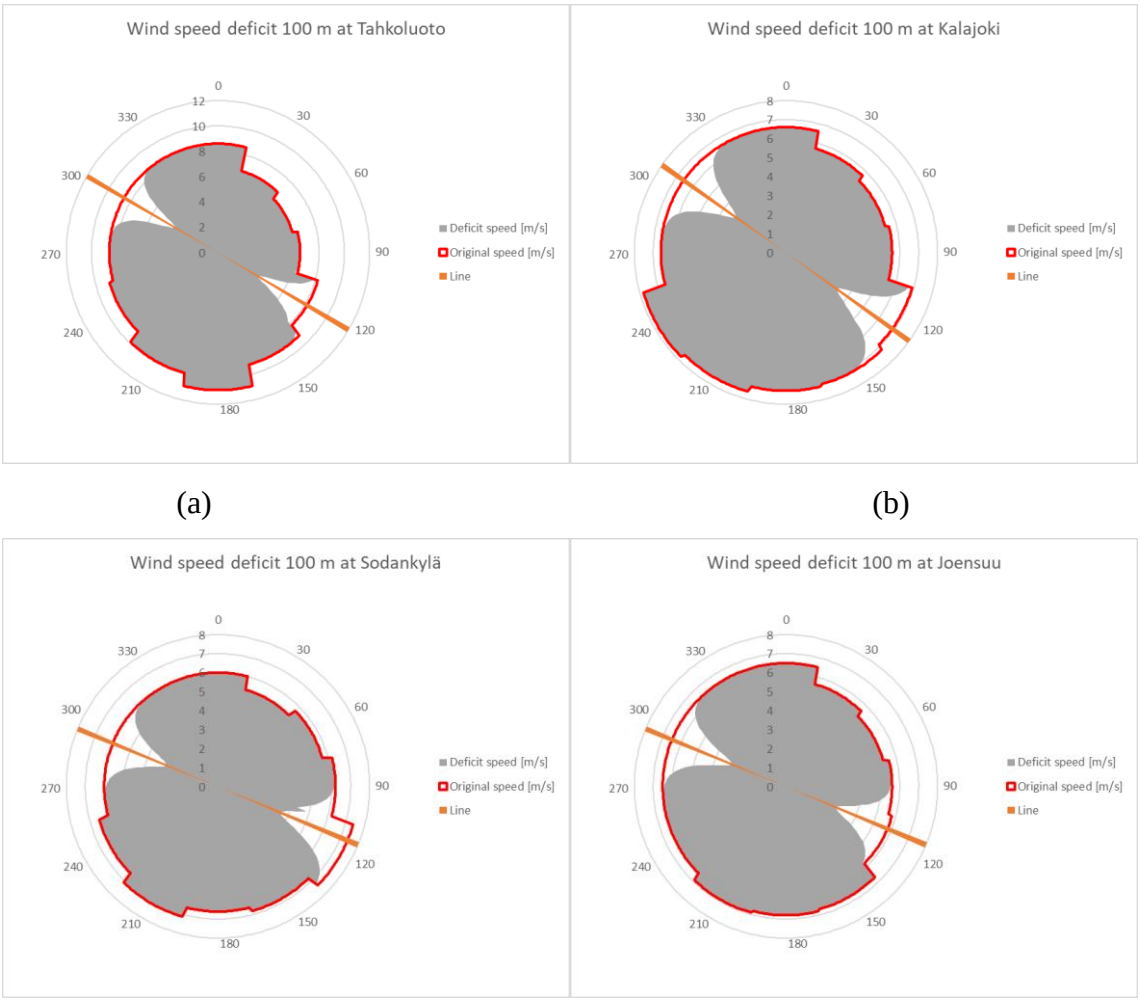

Figure 17. Wind speed after wake deficit, and original speed at 100 m for each site as a radar plot. Figure (a) Tahkoluoto, (b) Kalajoki, (c) Sodankylä and (d) Joensuu.

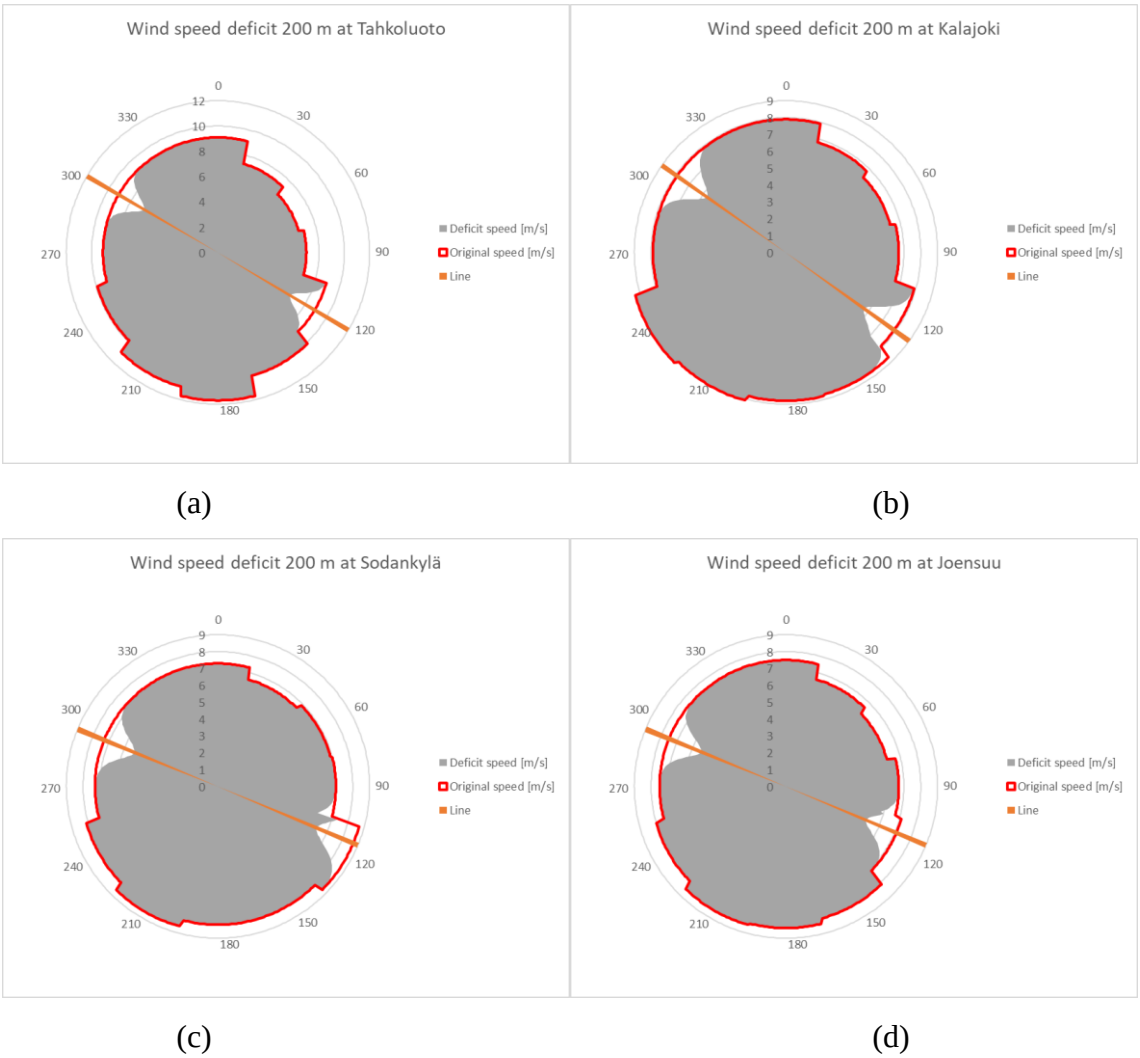

Figure 18. Wind speed after wake deficit, and original speed at 200 m for each site as a radar plot. Figure (a) Tahkoluoto, (b) Kalajoki, (c) Sodankylä and (d) Joensuu.

These calculations don't account for the wind speed deficit caused by blockage from structures like towers, support beams or guy-wires. These would obstruct the flow and change the three-dimensional wind flow field.

A wind tunnel investigation by Pierella and Sætran (2017) found that a tower of conventional wind turbine causes a tower wake that combines with turbine wake to form mean wake. Tower wake increased the horizontal expansion of the mean wake and made the centre of mean wake travel more downward. This was due to differences in bottom-tip and top-tip blade momentum transfers that were induced by the tower. In two tower tandem setup the downwind turbine's wake recovered faster due to increased turbulence in the inflow. Tower

wake effect was done at 3 D distance downstream. (Pierella & Sætran 2017. p. 1753, 1767-1768)

LWPP has more structure elements that can generate wakes like the towers. This would mean that the wakes in LWPP would be wider and thus start to interact with turbines at lower wind direction deviations from the line normal. Faster wake recovery would be beneficial, but the distances between closest turbines is less than 3 D, making the increase in wake recovery not take full effect.

4.2.2 Turbulence intensity

Excel tool is used to calculate TI increase from the wakes using equation (9). Values were calculated at a point where wake edge hits the rotor as there intensity is greatest and represents maximum load increase that would hit turbine blade. Inflow TI also affects wake recovery which in turn decreases wake speed deficit. TI increase was calculated only from T1 turbine, as that is seen sufficient for preliminary examinations. TI contributions would add up quadratically (Stoevesandt 2022, p. 948). Intensity increase is also less dependent on ambient TI at inflow, as tested increase of inflow intensity from 0,07 to 0,5 only increased added turbulence from 0,17 to 0,20 at 120 m distance downstream, where the increase is greatest.

Amount of turbulence increase from T1 wake and the resulting wake speed deficit changes are shown in Table 5.

Table 5. Wake turbulence increase and effect on wake speed deficit experienced per turbine at Joensuu.

Turbine	Max turbulence increase	Min turbulence increase	Max speed deficit decrease [m/s]	Max speed deficit increase [m/s]	Average speed deficit increase [%]
T1	-	-	-	-	-
T2	0,18	0,09	0,53	0,40	0
T3	0,19	0,09	0	1,27	3
T4	0,19	0,09	0	1,81	4

Speed deficit calculated with wake TI was larger than with ambient. Interesting find was that for pair T1-2 speed deficit also had a small decrease. This was due to the valley of dual peak shape of TI profile coinciding with the peak of velocity deficit at parallel wind direction lessening the wake deficit from improved wake recovery from increased inflow TI.

TIs for turbines with increase from wake are shown in Figure 19.

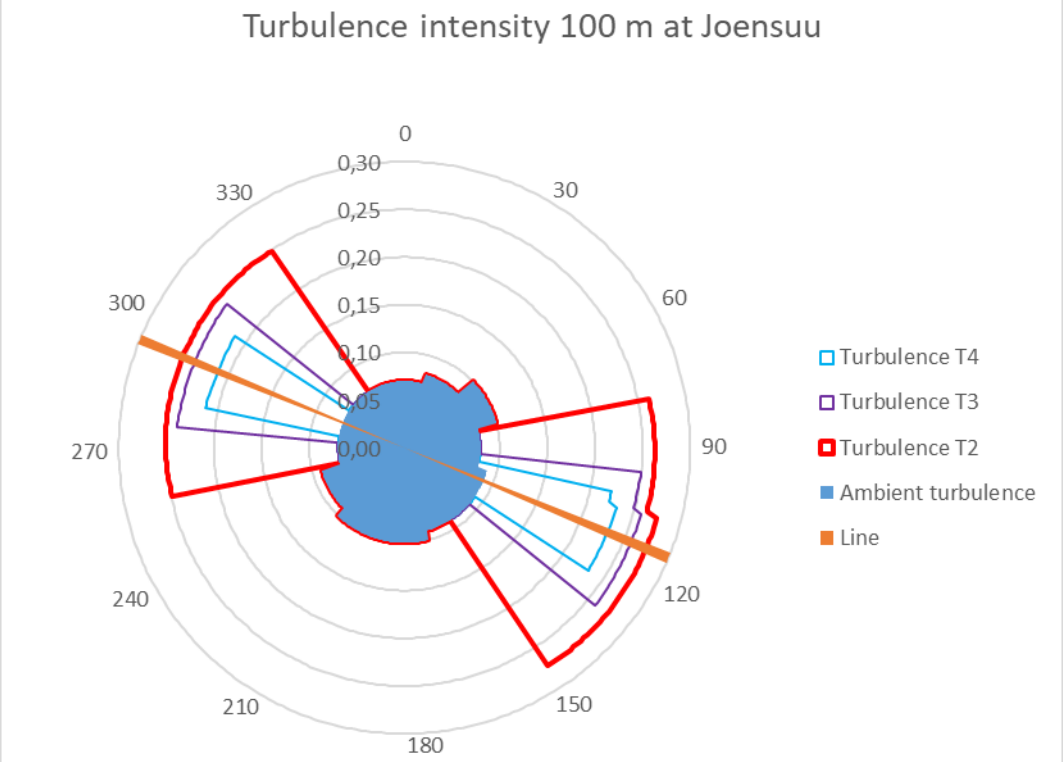

Figure 19. TI at each turbine from wake of T1 at Joensuu.

Changes in TI for downstream turbines had mixed results. TI increase varied from 0,09 to 0,19. Increase was strongest when wind direction was parallel to the LWPP line and weakest 15 degrees before and after this for T2. For other turbines this double peak was less pronounced, didn't result in decrease, and happened closer to parallel inflow direction.

Wind speed deficit was different when calculated with wake added TI when compared to deficit speed calculated by ambient turbulence. Difference between these was between -6 % to 9 %. On the average the deficit speed difference for turbines T2-4 were -0,02; 0,17; and 0,16 m/s, respectively. It should be noted that for T2 the inflow wind speed increased due to reduced wind speed deficit calculated using wake added TI than with only using ambient TI. This averaged speed deficit is added to power production calculations to inflow speeds for corresponding turbines in addition to the previously calculated wind speed deficit using only ambient TI.

These increased TIs are above normal values defined by wind turbine classes, which sets additional requirements for turbine choices. Special turbines might be required to withstand these turbulences.

4.3 Power production

Wind turbine annual energy production (AEP) can be calculated using wind speed distribution and the power curve. This is usually done in sectors to account for shading effect of other turbines. (Gasch R. & Twele J. 2012, p. 143)

LWPP AEP was calculated for each site and each turbine with wind speed distributions from Figure 7 and digitized power curves from Figure 4 and Figure 5. Effect of wake loss on power production was estimated by simplifying and averaging the velocity deficit that a turbine experiences over to a whole year. Velocity deficit used averaged This averaged loss was then subtracted from the wind speed distribution individually for each turbine. A yearly 3 % downtime for maintenance was assumed and reduced from annual operating time as that is a typical value estimated by turbine manufacturers (Vestas 2022, p. 13).

Calculations gave following results in Table 6.

Table 6. LWPP energy production per turbine at the sites.

		Annual lossless production [GWh]	**Annual wake loss [GWh]**	**Annual net production [GWh]**	**Change [%]**
Tahkoluoto	T1	8,07	-	8,07	-
	T2	8,07	0,29	7,78	3,5
	T3	8,07	0,82	7,24	10,2
	T4	8,07	0,93	7,14	11,5
	T5	16,37	-	16,37	-
	T6	16,37	0,24	16,13	1,5
	T7	16,31	-	16,31	-
	Total	81,33	2,75	78,58	3,4
Kalajoki	T1	5,28	-	5,28	-
	T2	5,28	0,59	4,70	11,1
	T3	5,28	0,97	4,32	18,3
	T4	5,28	1,02	4,27	19,2
	T5	14,25	-	14,25	-
	T6	14,25	0,87	13,38	56,1
	T7	15,30	-	15,30	-
	Total	64,93	4,71	60,22	7,3
Sodankylä	T1	4,50	-	4,50	-
	T2	4,50	0,60	3,90	13,3
	T3	4,50	0,97	3,53	21,6
	T4	4,50	1,02	3,48	22,7
	T5	13,36	-	13,36	-
	T6	13,36	1,00	12,36	7,5
	T7	15,03	0	15,03	-
	Total	59,76	5,04	54,71	8,4
Joensuu	T1	4,37	-	4,37	-
	T2	4,37	0,52	3,85	11,9
	T3	4,37	0,89	3,48	20,4

	T4	4,37	0,94	3,44	21,5
	T5	13,19	-	13,19	-
	T6	13,19	0,92	12,28	7,0
	T7	15,00	-	15,00	-
	Total	60,08	4,60	54,28	7,8

These results show that LWPP would have major production losses on lowest turbines, around 11,5 % of AEP. Production losses are less for middle turbines at 2,8 % and due to assumptions, no losses for top one. The total wake losses amount to 6,7 % of AEP.

These calculations have some inaccurate due to trying to match power productions calculated by velocity distributions to power productions from average wind speeds. Losses are expected to be slightly larger due to velocity deficits increasing probability of turbines experiencing wind speeds below cut-in speed.

Capacity factors for power production can be calculated from the production amounts. These are shown for each turbine in Table 7.

Table 7. LWPP capacity factors per turbine at the sites.

		Lossless capacity factor [%]	**Capacity factor with wake loss [%]**	**Change [%]**
Tahkoluoto	T1-4	51,2	47,7	6,7
	T5-6	56,6	55,5	2,0
	T7	56,4	56,4	-
	Total	54,3	52,2	3,9
Kalajoki	T1-4	33,5	30,0	10,5
	T5-6	49,3	47,7	3,2
	T7	52,9	52,9	-
	Total	43,3	41,0	5,4
Sodankylä	T1-4	28,5	25,0	12,3
	T5-6	46,2	44,5	3,8
	T7	52,0	52,0	-
	Total	39,9	37,4	6,1
Joensuu	T1-4	27,7	24,0	13,4
	T5-6	45,6	44,1	3,5
	T7	51,9	51,9	-
	Total	39,3	36,2	7,8

This analysis only looked at one unit of example design LWPP. If multiple such LWPPs were installed into a wind farm, the losses would increase, and capacity factors decrease. Typical wake losses in wind farm are around 15 %. (Cao et al. 2022, p. 1). These come from arrangement of turbines constantly casting wakes to some turbines and would apply the same to LWPP wind park.

The unimpeded capacity factors are similar to current Finnish wind farms that had capacity factor of 33 % in 2019 with best farm being 47 % (Suomen Tuulivoimayhdistys 2022b). Turbines T5-7 even surpassed these values across sites. But after factoring in the wake losses, the capacity factors fell. Largest changes were at T1-4 where losses were greatest, averaging 10,7 % reduction from unimpeded capacity factor.

An interesting finding was that at Tahkoluoto, T7 didn't outperform turbines 5-6. Although T7 had stronger winds, it couldn't fully use these due to turbine power curve coinciding less with wind distribution at 300 m. than at 200 m, as can be seen from Figure 5 and Figure 12. This could be improved on by using another turbine model more suited for higher speeds at the top row. Turbine optimisation could use offshore turbines on top row, as there wind conditions resemble offshore speeds and turbulences.

Total energy production can be used to estimate energy acreage of the example LWPP. LWPP is 400 m wide between the outermost turbines and if we add to this 4 D lateral spacing to each side and 7 D longitudinal distancing, using V112 turbines for diameter, we get a grid size of 1,02 km^2. This would mean that the energy acreage for the sites would be 81 to 110,3 with average being 89,8 GWh/km^2, or 16,8 MW/km^2 as per installed capacity. These are shown in Table 8.

Table 8. LWPP energy acreages for the sites.

Site	**Energy acreage [GWh/km^2]**
Tahkoluoto	104,4
Kalajoki	80,0
Sodankylä	72,7
Joensuu	72,1
Average	82,3

Turbine distribution to multiple heights and their optimisation averages out the local temporal wind speed variance which reduces the short time scale variability of LWPP energy production. This is only inferred but would be beneficial from grid operation standpoint.

4.4 Comparison to other concepts

Resulting LWPP power production is compared to equivalent conventional WPP wind farm to estimate merits. Other MRS concepts are commented on.

Tuuliatlas data includes estimates for a 1, 3 and 5 MW WPP's annual power productions at the chosen sites. Estimations were made using power curves of WinWinD 1 MW with 56 m rotor diameter, WinWinD 3 MW turbine with 90 m rotor diameter, and Repower 5 MW turbine with 126 m rotor diameter. Estimation used wind distributions based on tuuliatlas weather model. (Tuuliatlas 2022, p. 29) These results are shown in Table 9.

Table 9. Tuuliatlas data for WPP AEP predictions per turbine for the sites.

Site	**Production [MWh]**		
	1 MW	**3 MW**	**5 MW**
Tahkoluoto	4 260	12 971	21 263
Kalajoki	2 478	8 330	14 601
Sodankylä	2 034	7 100	12 680
Joensuu	2 001	6 888	12 072

AEPs of the WPPs were also estimated using the calculation Excel. An unspecified 3 MW turbine with 125 m hub height was used for them. The power curve was approximated by downscaling known V112-3.3 power curve by a factor of 0,91, the difference between turbine nominal powers. The calculations used a small wind farm of 4 WPPs in a line formation with 5 D lateral spacing. The AEP calculations resulted in values shown in Table 10.

Table 10. Excel results for WPP AEP predictions per turbine for the sites.

Site	**Production [MWh]**
	3 MW
Tahkoluoto	14 315
Kalajoki	10 463
Sodankylä	9 308
Joensuu	9 094

These values calculated with the Excel tool are 9,4-24,3 % higher than the estimations from tuuliatlas data's 3 MW turbine AEPs. The difference between these can partially be explained with different turbine model used for modelling and additional wake losses that a larger wind farm would have. Still the discrepancy implies that the tuuliatlas data uses some constraints that the Excel tool lacks. This leads to Excel tool calculations overestimating energy production. This is accounted for by increasing the tuuliatlas data values by forementioned differences for energy acreage calculations and other comparisons.

From the adjusted tuuliatlas AEP predictions we see that conventional WPPs yield 2 486 to 4 730 MWh per MW of rated capacity with average of 3 400 MWh/MW. LWPP yields on average 3 873 MWh per MW of rated capacity. This implies that LWPP would generate more energy per installed capacity. The AEP was on average 17,1 % higher in LWPP and capacity factor 13,9 % than in equivalent conventional wind farms using adjusted tuuliatlas data Excel tool calculations.

For energy acreage of conventional WPPs, their land usage per turbine and energy production need to be known. Using common wind farm distancing of 5 D laterally and 7 D longitudinally we get a grid sizes of 350x250, 840x600, and 1155x825 metres for 1 MW, 3 MW, and 5 MW turbines, respectively. Dividing total energy produced per grid size gives the energy acreage. The resulting WPP energy acreages are in Table 11.

Table 11. Energy acreage of WPPs using adjusted tuuliatlas data for the sites.

Site	**Energy acreage [GWh/km^2]**		
	1 MW	**3 MW**	**5 MW**
Tahkoluoto	42,5	50,0	41,9
Kalajoki	27,2	35,4	31,6
Sodankylä	22,9	31,0	28,2
Joensuu	22,7	30,2	27,0

These values are nearly half of the respective LWPP values. This shows that LWPP has considerably higher energy acreage, 1,9-2,3 times greater between the sites.

LWPP's wake loss was compared to the example WPP wind farm's wake loss at Joensuu. Calculations with the Excel tool resulted in speed deficit at narrower angle and to a smaller degree than in LWPP bottom or middle rows. Speed deficits for the WPP turbines were on average 0,14 m/s or 2,1 % deficit from the original speed. This wind speed reduction was less than in LWPP bottom row where the deficit was 6,4-7,9 %, and middle row where the deficit was 3,8-5,2 %. The WPP speed deficit was smaller even though there were 4 turbines in the WPP example compared to 2 turbines in LWPP middle row. This shows how much greater the wake loss in in LWPP, around 3,7 times more based on calculations at Joensuu site. Graph of average inflow wind speeds for the WPP wind farm is in Figure 20.

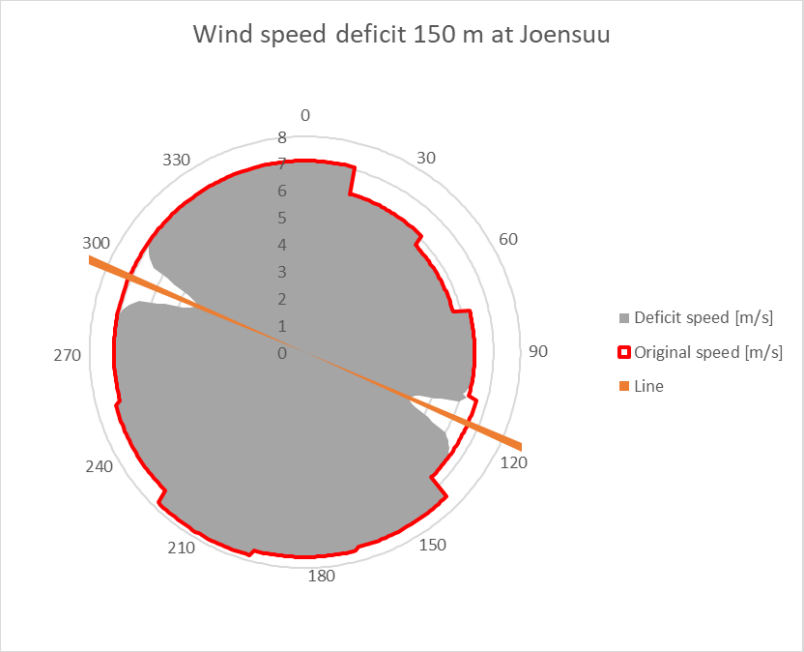

Figure 20. Wind speed after wake deficit, and original speed at 150 m for the WPP wind farm at Joensuu.

Power production of other multirotor concepts has been researched to a degree. Initial reports show power production increases of few percent for concepts that have turbines close to each other side by side on the same plane (Laan et al. 2019b, p. 1). This isn't present in LWPP as it has turbines yawing on separate pivot points which breaks the unified plane. In addition to slight production increases, the other MRS concepts also avoid the self-wake losses that LWPP has by having turbines rotate on a shared axel which lets them rotate without wake

shadowing the other turbines on the same system. This seems give them similar benefits as LWPP but without the increased wake losses.

5 Structural analysis

A LWPP differs from conventional wind turbines in its structure. Pros and cons of this new supporting structure need to be analysed as its feasibility is a major criterion for the success of the concept.

Conventional WPP consists of a foundation, tower, nacelle, and the rotor assembly. The LWPP concept combines multiple of these and adds guy-wires to support the towers in horizontal directions and angled support beams to support lateral and vertical loads. Aim of this supporting structure is to enable higher hub heights and denser arrangement for turbines. Other design points like included cranes, transportation sleds are covered briefly.

LWPP is expected to experience different static and dynamic loads due to its design. Higher wind speeds at higher elevations increase loads to turbines and supporting structure. Added TI from wakes increases blade and structural fatigue. Taller towers increase bending moments at the base of the structure. Guy-wiring and side beams alleviate these loads, but to which extent, needs to be analysed.

Structural analysis is conducted by quantifying the difference in forces acting on a LWPP. From these, structural elements are sized according to similarity laws to establish proximate functional dimensions for them. Guy-wiring and side beams are examined based on literature. Maintainability of the system is commented on. The size and complexity of LWPP inherits certain risks that are examined.

5.1 Forces acting on the structure

Main forces that act on the LWPP structure are gravity, thrust force and bending moment. These are examined using theory of similarity and simplified assumptions to scale known forces on a reference WPP to match the dimensions of LWPP. Theory of similarity is explained by Gasch R. & Twele J. and its limits are maintaining TSR, blade profile, number of blades, materials and making proportional adjustments to all dimensions between scaled turbines (Gasch R. & Twele J. 2012, p. 257). Scaling with geometric similarity works mainly from stress point of view, but self-weight loads can become driving factor for large wind

turbines (Jamieson 2018, p. 106). Turbines in example LWPP aren't all identical, but they are assumed to be similar enough to use theory of similarity on for structural analysis. This means that they would operate at same TSR. Size of LWPP could make self-weight loads important.

5.1.1 Forces with scaling laws

Gravity pulls all the parts of the structure downwards. Structures need to be able to support their own weight and the weight of components on top of them. RNA mass is on top of tower, and it scales with rotor diameter. Jamieson (2018) has given a diameter to RNA mass graph fit that is based on commercial data. There is variability, especially for larger turbines, but this graph is used for estimating RNA masses. A V150-4.5 MW RNA weighs 400 t based on the graph. For V112-3.3 and V80-1.8 these are 200 t according to Jamieson and 104 t according to Wind-turbine-models, respectively (Jamieson 2018, p. 114) (Wind-Turbine-Models, 2022). This would mean that LWPP towers would need to support 46,4 and 73,9 % smaller turbine top masses compared to reference V150-4.5 tower top mass. Gravitational loads caused by tower top mass scales linearly with mass increase reducing these loads by forementioned amounts.

Loads caused by component self-weights scale with volumetric increase. The vertical load on foundation is calculated with $F = mg$ (Bhattacharya 2019, p. 81). In LWPP this needs to consider masses of all the structural elements such as RNAs, towers, side beams and guy-wiring. These weights are roughly estimated here based on scaling of components and reference models. Especially side beam self-weights need to be examined as they have a risk of bending and even buckling due to it and possible additional loads moving on them.

Tower scaling cannot be done with scaling laws, as LWPP towers increase in height more than in horizontal plane, making their scaling geometrically not self-similar. V80-1.8 tower is around 203 t for 78 m hub height (Wind-Turbine-Models, 2022). This means around 2,6 t/m of height. Taller tower requires a diameter increase to bear the increased stresses. Diameter increase is assumed to be 0,013 m per m of elevation, and tower diameter to be 3 m at the top of tower, like in Ishihara & Qian MWT-92/4.2 turbine (2018, p. 278). Using these we get LWPP tower diameters at the base to be 4,3; 5,6; and 6,9 m for 100, 200, and

300 m towers, respectively. Tower wall thickness is assumed to be 1/250 of tower diameter (Störtenbecker et al. 2020, p. 1124). Using this thickness, we get 42,6 % increase in cross sectional area from tower top to tower bottom for the model tower used in Ishihara and Qian (2018). These are 41, 83, and 126 % increases for LWPP tower cross sectional areas from top to bottom. Using estimated mass per tower height with diameter scale increase for LWPP towers we get 278, 723, and 1337 t for 100, 200 and 300 m towers, respectively.

Side beams are assumed to be structurally similar to towers, a hollow cylindrical steel tube. The top side beam can be divided to sections between the towers and the lengths of these sections are 170, 110 and 40 m. If the previous tower mass per height was used for top side beams, then the sections would weigh 442, 286, and 104 t. These sum up to 833 t total weight for top beams. Bottom beams are around 170 m long making their weight 442 t. Side beams could use smaller thicknesses to reduce weight, as the loads they face are smaller than in main towers, which would make these weight estimations highly overestimating.

The decrease in tower top mass and increase in tower and side beam masses shifts the overall centre of mass of the structure closer to the middle. In a WPP it is more concentrated to the top. This shift shortens the bending moment arm. But on the other hand, the tallest hub height of 300 m in the example LWPP is twice the height of V150-4.5 WPP hub height. This would double the moment arm as it scales linearly with length. Towers at 200 m would be 33 % increase and towers at 100 m would have 33 % decrease in the moment. Combining the two factors for bending moment arm length and force acting on the arm results in larger moments compared to reference V150-4.5.

Bending moment depends in addition to the length of the bending arm, on the force applied to it. Part of the kinetic energy in the wind is converted to rotation energy of the turbine blades, but this isn't 100% efficient. Part of that energy is applied as thrust force onto the blades an also on the supporting structures. This thrust force increases with wind speed and rotor swept area. Thrust force on a wind turbine rotor can be estimated with:

$$Th = \frac{1}{2}\rho_a A_R C_T u^2 \tag{11}$$

Where *Th* is thrust force [N], ρ_a is air density [kg/m^3], A_R is rotor swept area [m^2], C_T is rotor thrust coefficient [-], and *u* is wind speed [m/s] (Bhattacharya 2019, p. 70).

Average wind speed at 150 m over the examined sites is 7,8 m/s. Speeds at 100, 200, and 300 m are 7,1; 8,3; and 9 m/s, respectively. Scaling laws assume turbine thrust coefficient to remain the same between scaled turbines. Thrust force increases with square of change in velocity (Gasch R. & Twele J. 2012, p. 260). The difference in wind speed leads to 82, 114, and 133 % multipliers for thrust forces when compared to 150 m wind speeds.

Rotor swept areas of the V80-1.8 and V112-3.3 turbine models used in LWPP are 5 027 and 9 852 m^2, respectively, while V150-4.5 has swept area of 17 671 m^2. Thrust force increases with square of change in rotor diameter (Gasch R. & Twele J. 2012, p. 260). This leads to 72 and 44 % percent reductions to drag forces for V80 and V112 turbines, respectively. Stresses to the blades from aerodynamic forces remain constant as they scale uniformly.

Liu et al. (2020) did a numerical simulation of fatigue loads on wind turbines operating in wakes which included calculations in the near wake region. Blade and tower bending moments were found to be on average smaller at 2 D distance due to velocity deficit from upstream turbine, but the moment fluctuation was greater due to strong wind shear and large turbulence. Time histories of bending moments showed periodic fluctuation between 100-0 % of free flow bending moment strengths. Moment fluctuations weakened for positions further downstream. Blade bending moments were more sensitive to wake-induced flow field than the tower base. Equivalent fatigue loads were 10 times larger at 2 D distance when compared to free flow loads. At typical wind farm distance of 6 D the equivalent fatigue loads were only 2 times as large. (Liu et al. 2020, p. 1307-1310) This indicates that the turbines in LWPP would experience increased fatigue.

Weight of the guy-wiring depends on cable diameter, length, and material. Cable weights, diameters and tensile strengths could be modified with material choices. Basic steel with yield strength of 250 MPa and density of 7,8 g/cm^3 is used for example calculations. Length of top cables on centre tower is 250 m and bottom ones on side towers are 130 m long. Top ones are at 25-degree angle vertically and bottom ones are at 35-degrees. Cable diameter is chosen according to thrust loads. Extreme case of 20 m/s winds would cause 1 222 kN thrust force, using equation (11) with 1,25 kg/m^2 air density, V112-1.8 turbine diameter and C_T of 0,5. Using a right side triangle, the angle of the cables reduces the horizontal component of

the loads to 42 % of total force, while vertical component is 90 %. Smaller diameter cables are easier to handle and are cheaper, which is why two cables are used for each tether. Guy-wiring is dimensioned to support over half of the horizontal thrust force resulting in 700 kN of maximum tension load. Cable cross sectional area that corresponds to this requirement is 28 cm^2 which is 5,9 cm in diameter. This would lead to cable masses of 10,9 t for each top cable pair and 5,6 t for bottom pairs.

Total weight increase from side beams is 2 551 t and from guy-wires is 66,3 t, which comes to total of 2 617 t from new structures. The mass of LWPP towers comes to 3 894 t. Combined they give total mass of 9 117 t for example LWPP design. For comparison an equivalent WPP wind farm of four V150-4.5 turbines would be 3 864 t, using scaled RNA mass, and the height and diameter scaling for tower mass. This indicates that LWPP would be more massive structure, but these mass calculations have yet to consider load distribution of the shared support structure and weight savings that it could bring. Side beams where also assumed to bear large forces which led them to be massive.

5.1.2 Force distribution in support structure

The combined support structure would be able to dampen and distribute the loads from turbines onto the towers. A force diagram for the LWPP structure is formed to better understand the fundamental forces acting on it. Hinged connections are assumed between towers and side beams. Guy-wiring uses cables made from small steel wires. Diagrams are made for frontal and side views showing dimensions and the forces acting on the structure, and they are in shown Figure 21.

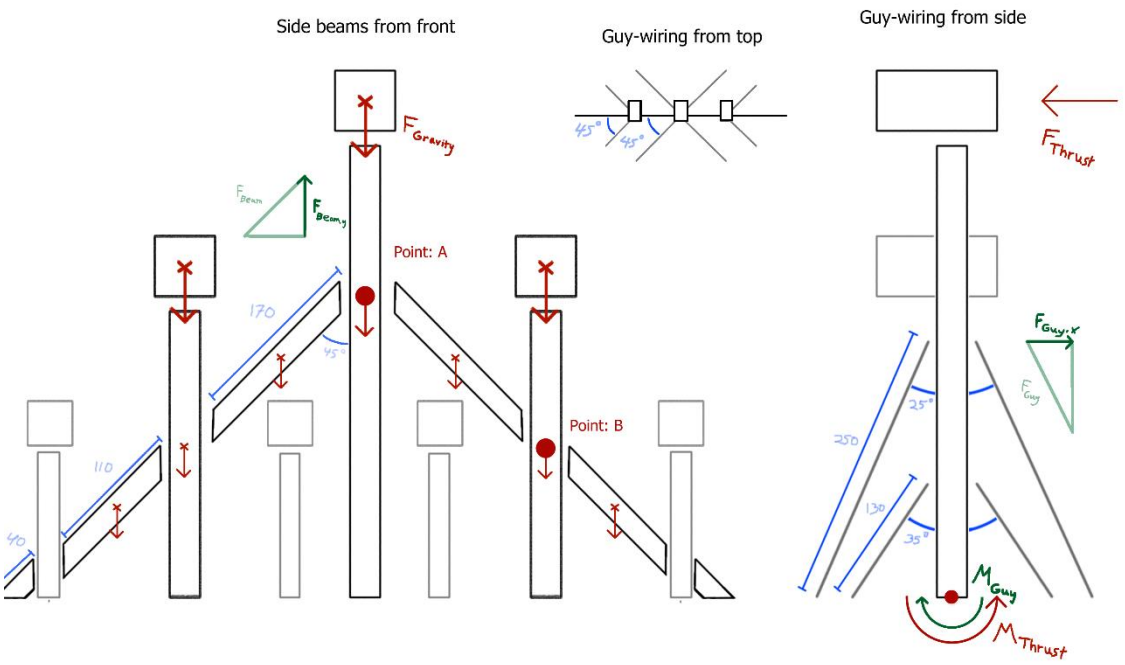

Figure 21. Schematic of forces on example LWPP structure from front and side views. A and B mark points of interest.

Side beams support vertical and lateral loads but provide only little support to longitudinal forces. Guy-wires are more spread out and provide tensioning to both directions. Largest aerodynamic loads come from normal direction as that is where the strongest winds most often come, due to positioning of the LWPP line. Side beams therefore don't contribute much versus these strongest loads but help against smaller loads when wind direction is away from normal of LWPP line.

If loads were assumed to be distributed evenly among the structural elements based on right triangle angles, and structures were weightless, then the tower at point A would experience 42 % of the load when compared to a tower without side beam support. Each top section side beam would in this case bear 29 % of the vertical load. Forces transmitted through the top section side beams need to be supported at point B in addition to the force from second row turbine top mass. This is an 29 % addition to the vertical load, but the middle section support beam would compensate for most of the additional load. Forces on the 200 m tower would increase by 9 % compared to tower with only tower top mass to support. This scenario

would be the maximum load reduction for the towers as it is more feasible to have smaller side beams that aren’t dimensioned to bear the maximal loads.

Guy-wiring connects to the 300 m tower at 226 m height and to the 200 m tower at 100 m. Yield strength of the cables at their angle allows them to bear 590-834 kN horizontal loads depending on if the load is distributed to single cable pair or evenly between two pairs of them. With 226 m moment arm this would equal 133 MNm of moment at tower base. Without guy wiring the calculated thrust force from 300 m turbine would cause 366 MNm of moment at tower base. This would mean that guy-wiring would be able to reduce the bending moment at the base by 72,8 %. For comparison a Siemens SWT-3.6-107 turbine with 83,5 hub height at Walney 1 wind farm experienced 28 MNm dynamic and 81 MNm static fore-aft bending moment loads from 20 m/s wind speed (Bhattacharya, 2018, p. 292, 297). These show that bending moments in LWPP would be greater, but they can be reduced with the guy-wiring.

These calculations ignored the bottom side beam and guy-wiring on 200 m towers, as the largest contributions come from the examined top beam and top guy-wirings, and they illustrate their effect on force distribution.

Summary of force scaling is in Table 12.

Table 12. Force modifiers of example LWPP scaled to V150-4.5 ones, and support effect from shared structure.

Forces [%]	**Source**	**Turbine tower**		
		100 m	**200 m**	**300 m**
Gravitational load	RNA mass	26	54	54
	Tower mass	49	128	236
	Side beam support	ignored	108	42
	Total	12,7	74,6	53,5
Bending moment	Wind speed	82	114	133
	Rotor area	28	66	66
	Moment arm	67	133	200
	Guy-wiring support	-	67	64
	Total	15,4	67	112,4

These considerations show that total gravitational loads on towers from common elements would be smaller than in a V150-4.5. Table 12 doesn't include gravitational load increases from guy-wiring or side beams, as weight of guy-wires is less than 10 % of reference tower weight, and the weight of side beams is overestimated in previous section where they would add up to 80 % of tower mass to be supported by the towers. Bending moments are smaller except for the 300 m tower where bending moment increased by 12,4 %. These reductions in loads would allow towers to be thinner, which in turn reduces the loads further. Reduced loads allow thinner side beams, but the gravitational load they cause would counteract some of the load reductions.

5.2 Considerations for structural elements

Additional considerations need to be given to certain structural elements based on the preliminary calculations. More detailed design for new support structures of guy-wiring and side beams is given. Tower vibration behaviour and comments on transportation and mass

differences are done. Validity of tower preliminary dimensioning calculation is checked by comparison to literature reference. The increase in tower and support structure masses increases loads on foundations, which are estimated roughly. Additional requirements for turbine blades are given.

5.2.1 Guy-wires

Guy-wires comprise of many single streel wires in parallel or spirally wound configuration. They are commonly used for radio masts, small scale wind turbines, and they are starting to gain attention in utility scale wind energy too.

Some of the tallest wind turbines built in Finland use guy-wiring (Suomen Tuulivoimayhdistys 2022b). Guy-wiring in conventional WPPs is connected to the tower below bottom of rotor swept area, which amounts to around midpoint of tower (Jespersen & Støttrup-Andersen 2019, p. 780). In LWPP rotor swept areas are smaller and this allows guy-wires to connect closer to RNAs on the tower. This decreases the distance between connection point and RNA that aerodynamic forces act on, but also increases the distance between guy-wire connection point and tower base. LWPP concepts could use multiple sets of guy-wires on different levels per tower for increased and vertically more evenly distributed support.

Length of these guy-wires for conventional WPPs is around 60 m if they are at midpoint of 150 m tower and at 35˚ angle. Diameter of guy-wires can be 15 cm (Iin kunta 2020, p. 2). This would make them weigh 8,5 t using same values as in LWPP guy-wiring dimensioning.

Longest guy-wires in LWPP are expected to be several times this length. In example design they are 4 times longer. Preliminary calculations estimated guy-wire diameters to be 5,9 cm which is considerably less than in conventional cases, but weight of top guy-wires is 2,4 t more than in conventional cases. This means that LWPP guy-wires would be less stiff and have lower tensile strength.

Guy-wires are pretensioned to 20-45 % of their minimum breaking load to reduce sagging and increase their stiffness (Jespersen & Støttrup-Andersen 2019, p. 780). This tensioning would apply a force on tower pulling it downwards. This would slightly increase tower

vertical loads, by around half of applied pretensioning, due to angle between guys and the tower. Horizontal loads from pretensioning are cancelled out by symmetry of guy-wiring.

Angle between tower and guy-wire alters the load distribution. Larger angle increases the horizontal load bearing capability but requires further distance from tower. This would increase length and need for clearing vegetation from around the guy-wire.

Connection between guy-wires and the tower can be made with a plate insert guy attachment -piece that has been developed by Ramboll. It is a flat steel plate with bent to align with guy-rope inserts. It is inserted between flanges of a tubular tower. (Jespersen & Støttrup-Andersen 2019, p. 782-783)

Suzuki et al. (2020) studied a very-light offshore wind turbine with guy-wired support tower. Using scaled down model and numerical analysis to analyse motion results in waves, they found that guy-wiring enabled cost-effective load bearing. The pretensioned guy-wires experienced no slacking with measured tension always remaining positive. Bending moment at tower base using guy-wires reduced to less than half during most loads, and down to quarter at times, when compared to simulation without guy-wiring. (Suzuki et al. 2020, p. 1, 13, 16) These results aren't directly comparable to LWPP as their study used a very-light offshore wind turbine, where main examined forces came from wave movement. Heavier structures of LWPP have higher inertia which requires stronger guy-wires. Larger forces acting on LWPP structure which increases loads on guy-wires, but the structure is less reliant directly on guy-wiring, more so using them as additional load bearing than main force mitigation method.

Several foundation techniques for guy-wire anchoring have been made. These include standard soil, concrete-steel hybrid, pile, inclined injected ground anchor, and rock anchor foundations (Jespersen & Støttrup-Andersen 2019, p. 781-782). These foundations are ideally suited for tension loads. Best technique to use for LWPP can be chosen based on site soil properties. Size of the foundation varies, but they are small compared to typical WPP foundations.

5.2.2 Angled side beams

The angled side beams are connected between the towers. In example design they are on two levels in sections with top ones spanning between 300 m, 200 m towers and ground, and lower side beams between 300 m, 100 m towers and ground. Side beams provide structural integrity and are also supposed to act as rail mounts for moving material onto the structure by transport sleds. This makes their function and design resemble bridges, which is why some basic bridge design is applied to them here.

Side beams would need to be able to bear similar loads to bridges and use same design elements. Side beam design most closely resembles that of a flyover bridge as they are suspended in air between piers, or in case of LWPP, the towers. (Weiwei & Teruhiko 2017, p. 1)

In bridge building, superstructure is the portion of a bridge that is above bearings and includes deck, girder, truss etc. Superstructure bears the loads passing over it and transmits them to substructures. (Weiwei & Teruhiko 2017, p. 3) In LWPP the side beams would act as the superstructure. In bridges the loads on superstructure are mostly vertical while in LWPP they would be also in beam wise direction. This would make a tilted bridge a better analogy.

Bridge bearing is a component that transmits loads from deck onto the substructure. These allow controlled movements for temperature variation or seismic activity to reduce stresses. (Weiwei & Teruhiko 2017, p. 3) In LWPP this would be the cross-section between towers and the support beams. These bearings would channel the forces from tower movements onto the side beams in a flexible way without damaging them. Type of connection is to be decided upon in more detailed design work.

Bridges are classified by their span lengths, which is the distance between centres of two bearings. According to a typical classification, medium-span bridge has approximately 38 to 125 m long span. (Weiwei & Teruhiko, 2017. p. 6) The example LWPP design's lateral tower distances are 60-75 m. Support beams between neighbouring towers would be similar to medium-span bridges, but the top support beams cross one tower over making them cross 125 m lateral distance. The beams are also angled which increases their spans. Spans on the

lower beam are 82 and 36 m long, and on the top one they are 173, 110 and 40 m long. This shows that side beams aren't abnormally long from bridge design standpoint.

LWPP side beams are meant to be able to handle the loads from transporting whole RNAs along the side beams. For side beams to be able to use sled type configuration for transporting they would need to be designed to support their dead weight and the additional point load from sled with RNA. This type of load would be similar to live load on bridges from a moving vehicle, except the force would be larger. European bridge standard uses axial load of 40 t for largest vehicles (Weiwei & Teruhiko 2017, p. 77). This is little over third of smallest RNA mass in LWPP. The load from moving material on sleds would be concentrated on small area, the size of the sled, of the side beam at a time. This would increase the load bearing capacity need for side beams compared to typical bridges.

Side beams are meant to be hollow to enable personnel and light material to move through them. This sets a minimum hollow space requirement for them. Hollow space would reduce the cross-sectional area which in turn reduces structural stiffness and strength.

Preliminary calculations assumed the side beams to resemble turbine towers in their shape and dimensions. The loads on side beams are mostly beam wise made of vertical (z) gravitational load and horizontal (y) thrust force that is transmitted to them through tower coupling. Tangential (x) forces are rarer on them which makes the load distribution focus on z-y plane. Turbine towers are tubular as they are designed to handle forces from all directions. A more elliptical shape for side beams would increase vertical stiffness while reducing lateral one.

Another potential shape would be to have hollow tube shape with I-beam like flanges on top and bottom, as I-beams provide great second moment area in vertical and horizontal directions with minimal material use.

5.2.1 Tower

Feasibility of tall LWPP towers is an important consideration as they are essential for the concept. Wind turbine towers make up significant portion of turbine initial costs, approximately 15 to 20 %, and costs for transport and erection (Gasch R. & Twele J. 2012,

p. 95). This makes them a major part of costs and affect economy of the concept. Height of the tower determines the wind speeds that turbine can reach, which affects power production. Manufacturers usually offer turbines with choice of tower sizes (Gasch R. & Twele J. 2012, p. 95). Some of LWPP towers can be of commercially available types, like towers for lowest turbine row, but some need to be specially crafted and optimized for LWPP.

Tower design must achieve prescribed modal behaviour, avoid risk of instabilities or resonance, meet strength and deflection limits, while having economically optimized load distribution and material utilization. Manufacturing constraints like weldable wall thicknesses and rollability of plates can limit maximum tower size. (Ng & Ran, 2016, p. 264)

Tower design needs to account for gravitational forces and dynamic states of tower which are caused by vibrations. Typical vibrations come from 1P and *n*P loads, where *n* is the number of blades in a turbine.

1P load is caused by the vibration at the hub level due to the mass and aerodynamic imbalances of the rotor. Frequency of this load comes from rotational frequency of the rotor, and it is a frequency band as rotational frequency changes during turbine operation. (Bhattacharya 2019, p. 52) This load and its frequency are expected to be same for LWPP as support structure doesn't affect turbine rotational frequency.

Blade-passing load loss, known as 3P, comes from blade passing through the tower and reducing load from wind onto the tower by shadowing. This is similarly a frequency band, and its frequency is third of rotor rotational frequency for three bladed rotors. (Bhattacharya 2019, p. 52)

Tower natural bending frequency needs to fall outside the frequency interval denied by 1P and 3P frequencies. Tolerances of -15 % and +10 % are generally used for estimating this. Example of admissible frequency ranges for turbine sizes close to LWPP ones are 0,343-0,795 Hz and 0,253-0,587 Hz. (Rebelo et al. 2014, p. 286) These types of values need to be satisfied by tower design in more detailed design and there are different methods to achieve them.

Wind turbine towers are made of hollow steel tubes. Steel grades S235 and S355 are typically used (Baniotopoulos et al. 2011, p. 211). Towers are wider at the bottom and taper upwards. Thickness likewise decreases with height. Typical tower diameters can be around 2-5 metres

and thicknesses 1-3 cm (Baniotopoulos et al. 2011, p. 256). Largest LWPP tower dimensions are expected to be larger than these, based on the preliminary calculations.

Tower stiffness affects their natural bending frequency. Towers are generally divided to soft or stiff types. Stiff towers have a first natural bending frequency that is above the exciting rotor speed. In soft towers the first natural bending frequency is below rotational frequency of the rated speed. Soft towers require frequency control during start-up to prevent resonation. (Gasch R. & Twele J. 2012, p. 96) Taller towers have greater height to diameter ratio which makes them less stiff. Soft towers are more popular as they need less material due to lower tower diameter.

Some tower solutions for taller towers have been analysed. These are concrete tower with pretensioned steel tendons, hybrid tower with lower concrete and upper steel shell parts, and lattice tower. Concrete towers can absorb large moments economically. Concrete parts can be prefabricated and transported in sections, or they be manufactured on site which reduces transporting bottlenecks from large tower sections.

Lattice towers were the original tower type choice for LWPP concept according to the patent. They have low weight and cost, but amount of bolt connections and their checking need, and the hard to control dynamic properties make this tower type disadvantageous. (ELFORSK 2010, Summary) Lattice tower reaching 300 m height would be very costly to set up, and the steel profiles would need to be scaled up to handle the loads. Lattice would be easier to transport and to manufacture, and it would be easier to make modular as per one of the LWPP concept goals.

Another way to control tower frequency response is with tuned mass or active mass damping. This could be used to guarantee sufficient damping, but these increase costs. (Ng & Ran, 2016, p. 292)

Towers in LWPP are connected with side beams which limits their freedom of movement. Tower movement would transfer to neighbouring towers trough these causing tensile and compressive loads on side beams. The beams would dampen this movement, but they would also propagate those movements throughout the structure, further dampening them. Guy-wiring also was estimated to reduce these loads.

Taller towers face challenges in their erection. Swedish study by ELFORSK in 2010 examined possible methods for tower height increase and found that crane technologies limit

maximum tower heights. Above 120-150 m hubs specialized lifting cranes are required. Increase to 300 m would require new lifting solutions to be developed especially for LWPPs.

Tower wall thickness was assumed constant for all tower sizes, but this might need to increase for larger towers. This would increase tower mass considerably depending on the required thickness increase. Continuation of the preliminary calculations shows that Ishihara & Qian model tower would be under 8,73 MPa stress at the tower top and 17,11 MPa stress at tower bottom. Tower top stress is from RNA weight and tower bottom includes RNA and tower weight. For LWPP the 300 m tower would be under 16,80 MPa at top and 40,97 MPa at the bottom. To reach similar bottom stress the tower diameter would need to be increased to 11 m when using constant wall thickness of 1/250 t/D ratio, or tower wall thickness would need to be increased to 1/71 t/D meaning 6,2 cm if the tower diameter was limited to 4,5 m. These don't account for support effect from side beams, which could reduce the required diameter, but these calculations also do not account for the additional mass from side beams. The effects from side beams on 300 m tower are therefore assumed to cancel out and result in no improvement for tower diameter or thickness.

Dykes K. et al. analysed taller towers for wind applications and made weight estimations between tall soft and stiff towers based on design constrains. The examined tower cases were based on relaxed constraints of transportability, maximum tower base diameter, and on-site manufactured tower with no diameter limit. Transportable case had diameter limited to 4.3 m and wall thickness was increased for taller towers. Out of these tower cases transportable was heaviest, maximum the second, and on-site the lightest. Tower masses were plotted against hub height of 80-180 m. Tallest stiff towers of examined cases had 7,7; 3,8; and 1,6 times more mass than soft types. (Dykes K. et al. 2018, p. 1-4)

Extrapolating tower mass plots from Dykes K. et al. (2018) study to maximum LWPP hub height of 300 m gives mass range of 12 000 – 1 150 000 t for stiff towers and 4 200 – 12 000 t for soft towers, between the cases. Conventional towers would be between transportable and maximum diameter cases. This shows that LWPP tower mass increase would be more severe than anticipated in preliminary calculations. Mass increase wouldn't be to the extent of these estimations as in LWPP the loads from RNAs are smaller and supporting structure reduces loads on towers. Still, tower masses might need to be around double from preliminary calculations, resulting in 1 446, and 2 674 t for 200 and 300 m towers. These would be 256 and 472 % increase to tower mass compared to reference V150-4.5.

5.2.2 Foundation

Wind turbines are usually built upon steel reinforced concrete blocks that act as gravity foundations. They are dimensioned to bear the vertical and eccentric loading from the turbine tower, and to resist sliding. Soil needs to be able to support them, which why they have shallow and wide footprint. Minimum width of shallow ones is dictated by foundation stiffness or maximum allowable edge pressure (Sørensen J. 2011, p. 34). Pile type foundations are also used, and they are embedded into bedrock. These principals give insight to main factors determining foundation size and whether LWPP concepts would see size and costs savings for them.

Different soil types have different load bearing capabilities. They can affect the size of foundations needed. Bearing capacity of the foundation depends on bearing capacity factors, soil cohesion, vertical stress, weight of supporting soil, and footing width (Sørensen J. 2011, p. 35). Soil properties also affect the sliding resistance between soil and foundation footing. Foundation stiffness is used for estimating capacity to bear torsional forces. These would be smaller in LWPP as there the shared support structure reduces tower freedom of moment in horizontal directions.

Terrain at wind sites is rarely even which makes the bases of WPPs in a farm be at different elevations. The shared structure of LWPP would need foundations to be at same elevation to connect the towers together. Some leeway can be had with tolerances between structural elements or foundation heights could be altered with depressions or extensions to a point. Ensuring even elevation between foundation sites might require additional earthworks in the form of excavation or grading. But this requirement for elevation uniformity would pose an additional design criterion to account for in site feasibility studies and another task in project construction.

One of the goals of LWPP was to gain cost savings with reduction in needed foundation sizes. Summary of gravitational and bending moment loads showed that the total forces would be of similar magnitude to common V150-4.5 turbines, making the required foundation size of 300 m and 200 m LWPP towers similar to those. LWPP also needs foundations for the smaller 100 m towers. Forces on 100 m towers are only 12,7 and 15,4 % of reference gravitational and bending forces. Size of their foundations is assumed to be 25 % of the size of the reference ones, to have values be conservative. LWPP would need

foundations for guy-wiring. In example design they need to handle maximum of 700 kN of pulling force, which is around halve of gravitational load on 100 m tower foundation. Guy-wiring would use eight foundations and their size is assumed to be halve of 100 m turbine foundations making each of them be 12,5 % of reference foundation size. The number of LWPP tower and guy-wiring foundations would increase the total foundation material need compared to conventional WPPs.

5.2.3 Blades

Turbine blades used in LWPP are similar to conventional ones. Rotors made of composite of fibre glass, and carbon fibre or balsa wood are typically used. Smaller rotors used in LWPP have slower tip speeds due to shorter blade lengths than in typical conventional rotors. Largest difference is the loads that the blades need to endure. Wind speed increase from height increase increases the forces by up to third compared to speeds at 150 m reference height.

Blade fatigue from wake turbulence was estimated to be 5 times stronger in LWPP than in a conventional wind farm as discussed in chapter 5.1.1 . This fatigue increase shortens blade lifespan and increases their maintenance need. To counteract this, blades could be made of stronger materials, or turbine yaw could be limited to reduce wake overlap. These changes would increase material costs or reduce power production, making the design less economical.

The trend in wind turbine manufacturing has been to create ever larger turbines with larger blades. LWPP has little use for large blades as mass scaling of smaller blades is core part of the concept. Need for smaller turbines would create demand for turbine manufacturers to restart manufacturing them, but this would contradict current development trends, making it a tall order.

5.2.4 Structures summary

Tower masses are adjusted to 256 and 472 % of the reference tower mass based on Dykes et al. (2018) study, but by factoring in the side beam load modifiers of 1,08 and 0,42, these change to 276 and 198 % for 200m and 300 m towers, respectively. Used tower mass for V150-4.5 is 566 t based on constant tower mass increase with height. Side beams of 100 m towers are ignored in estimations as their effect is negligible.

Combining preliminary calculations with additional considerations we get following scaling for LWPP structure shown in Table 13. Scaling is done based on mass of equivalent reference V150-4.5 parts. Summing up the four 100 m towers, two 200 m towers, one 300 m tower, the four V80-1.8 turbines, three V112-3.3 turbines, and all side beams and guy-wiring results in total scaling for the structure. Tower and guy-wiring foundations are added together for each relevant tower into total for foundations.

Table 13. Resulting scaling of LWPP parts compared to V150-4.5 parts.

Scaling [%]	**Turbine tower**			**Based on**
	100 m	**200 m**	**300 m**	
RNA	26	54	54	RNA
Tower	49	276	198	Tower
Side beams	-	64	78	Tower
Guy-wiring	-	2	7	Tower
Foundations	25	125	150	Foundation
Total structure	12,1			Tower
Total foundations	4			Foundation

Table 13 shows that an LWPP unit would be proximately 12 times larger, and its foundations would be 4 times larger than in single V150-4.5 WPP. Better comparison would be a small equivalent capacity wind farm of 4 such WPPs which brings the LWPP unit to be 3 times larger than it and foundations to be of equal size.

5.3 Maintenance

One of the goals of LWPP concept is to be more maintainable than conventional WPPs. This is to be done using the side beams and the transport sleds on them for material and assembly transport to reduce the need for separate mobile crane lifting services during plant operation, and with better accessibility for service personnel. The concept includes cranes that can be fixed to the structure or be free moving along the side beams using rail or similar mountings. The increased ease of access to nacelles from access ways trough side beams, proximity of nacelles to each other, and the possibility for using hanging personnel carriages from side beams would reduce time needed to move equipment and personnel around the site.

The sled design and cranes were largely omitted from the example design to make it simpler for preliminary analysis. The chosen design of using towers for each turbine doesn't work well with the idea of having turbines be transportable using the side beams as the whole upper tower would need to be moved, or turbine would need to travel down the side of tower, which would be complicated and cause off axial loads on the tower.

Contrary to the aims, the taller towers would increase the distances needed to be climbed to reach nacelles for maintenance. The crawl spaces inside side beams would allow maintenance personnel to avoid climbing the whole way down a tower to move to the next one, but they would add moving through them, and even with laddering it would be difficult to move around.

Having small inbuilt cranes in wind turbines is already common practice (Gasch R. & Twele J. 2012, p. 75, 92). They can be used to move small loads such as equipment or small replacement parts. Replacement of larger parts like blades and drivetrains requires a mobile crane. Towers also include small lifts for getting up them and material transportation.

Scheduled maintenance is done regularly to turbines. Exact details depend on original manufacturer's instructions, but they generally include inspections, tightening connections, cleaning, checking filters, lubrications, and coolants. These can take from few hours to few days per turbine to be done. Travel time between turbines takes up a small amount of the tasks time, which makes the accessibility of LWPP only a minor benefit.

Larger number of smaller turbines adds more components to the system that need maintenance and provide chances for failure. Having to stop operation of smaller turbine

reduces total power production less than if the fault happened in a larger turbine. Over the lifetime of a wind farm the reduced power production loss from downtime of smaller turbines is expected to be compensated by the increased amount of downtime from increased turbine amount. This would make LWPP uptime be similar to WPP one but add to the times of needed maintenance. Maintenance time between larger and smaller turbines is expected to be negligible.

In the event of a catastrophic structural failure the shared structure of LWPP can be a liability. Falling of a LWPP tower would have a high risk of taking down other parts of the structure, while in WPP wind farm the falling of single tower doesn’t endanger nearby turbines as much due to distances between them.

In icy climates, icing would be riskier for LWPP as possible ice sheets breaking off from turbine blades would have higher change of hitting other structures due to their proximity. This would make anti-icing solutions more important for LWPP concepts.

6 Cost analysis

Major design parameters in wind farm design are the investment amount, project lifetime and profit from electricity sales. These need to be considered for the project to be profitable and hence worth building. Analysis of LWPP costs is done by using levelized cost of energy (LCOE), concept that assesses the revenue per unit of electricity that would be needed for project to break even over the wind power plant's entire lifecycle. Additional care needs to be paid for new technologies as there is a lot of uncertainty in their cost structure.

The key factor in success of new innovations is that, whether it will in mature production phase realise significant cost benefits. Prototyping may be more expensive by a factor of four compared to costs realised in established production. Therefore, the merit of an innovation needs to be compared to the potential benefit of when it is at similar stage of technology maturity to the standard solution. (Jamieson 2018, p. 213) This is why the cost analysis of LWPP doesn't account for additional costs from learning rate.

As component prices and other costs aren't readily available this analysis can be done only on approximate values. LWPP design also includes additional structures that are new to WPPs. Costs of these components are estimated based on scaling laws, volumetric material needs and referencing similar structures.

Cost structure of a wind energy project can be divided to investment, operational, financing costs and taxation. Investment, financing, and taxation make the capital expenditure (CAPEX) and operational costs are operational expenditures (OPEX). Revenue comes from sale of generated electricity which is heavily affected by price of electricity. Difference of these forms the monetary profits or losses of a project. Largest differences to conventional wind energy projects for LWPP projects are tower, internal cabling, land leasing and the cost of new structures of side beams and guy-wiring.

6.1 Cost structure of wind energy project

Jamieson (2018) has given typical cost fractions of a wind energy project (Jamieson 2018, p. 226). Stehly & Duffy (2022) have given typical CAPEX and OPEX structures (Stehly &

Duffy 2022, p. 26). Innwind project has example of project cost structure in European markets (Stoevesandt 2022, p. 22). These costs are based on foreign projects, so some alterations are made to better fit them to Finnish markets. Mainly Jamieson's costs are used with corrections and additions from Stehly & Duffy. Costs are redistributed to CAPEX and OPEX categories. Smaller costs are consolidated under main components. Electric costs are divided to internal cabling, substation & cabling, and grid connection fee.

Jamieson's cost structure doesn't include land leasing that would be typical for Finnish wind energy projects. Stehly & Duffy have given this for offshore projects at 4,6 % (Stehly & Duffy 2022, p. 35). Similar land leasing cost is added to the cost structure. Grid balancing cost is added in addition to costs mentioned by Jamieson. Financing and taxation costs are roughly doubled. Increased project costs fractions are normalized to 100 %. Resulting modified costs structure of wind energy project for Finnish markets is shown in Table 14.

Table 14. Cost structure of a typical wind energy project adjusted for Finnish markets. (Modified from Jamieson 2018, p. 226)

Cost category	Component	Sub component	Cost fraction [%]
CAPEX	Turbine		56,9
		Blades	10,4
		Drivetrain	23,2
		Nacelle	5,6
		Hub	5,6
		Tower	9,0
		Other	3,1
	Foundation		1,5
	Roads and buildings		2,2
	Electrics		10,0
		Internal cabling	2,5
		Substation & cabling	6
		Connection fee	1,5
OPEX	Maintenance		19,6
	Land leasing		4,5
	Legal and tax		2,1
	Financing		7,6
	Grid balance		16,3

6.2 CAPEX

Wind energy projects have larger investment costs than other types of energy projects, but the operational costs are lower due to lack of fuel costs. Investments are wind turbines, foundations, internal power grid, transmission or distribution grid connection, high voltage transformers, road infrastructure, lifting areas and other miscellaneous buildings. Out of these, wind turbines, grid connection and internal cabling make up the largest costs, taking up around 55, 25, and 5 % of investment costs, respectively (Jamieson 2018, p. 226). Typical

price per installed capacity for WPP investment is 1,2-1,5 mill.€/MW (Suomen Tuulivoimayhdistys 2022a).

Out of these LWPP has major changes to turbine and internal power grid costs. LWPP structural costs are divided to wind turbine and new structures cost; new structures being side beams and guy-wiring.

6.2.1 Wind turbine

The turbines themselves take up the largest fraction of costs in conventional wind farm investment. LWPP concept has larger structure which would increase this cost fraction even higher. Typical largest component costs in a wind turbine are tower, blades, and gearbox being 21,9; 17,7; and 14,3 % of the total turbine cost, respectively (Jamieson 2018, p. 215). Wind turbines themselves are around 55 % of wind energy project total lifetime costs (Jamieson 2018, p. 226).

Towers in LWPP are expected to be of multiple heights and sizes. Smaller turbines lessen the gravitational loads and shared support structure distributes these loads as was concluded in chapter 5.1.2 . Upscaling towers increases their size and material need considerably even with lessened loads and additional supporting elements. Combination of multiple tower sizes creates more complicated orders for turbine manufacturers, which could increase the tower costs. LWPP tower cost is dependent on the chosen design and can bring savings in some cases, but example design implies that the costs would usually increase.

The example LWPP uses three tower sizes that are dimensioned to support different loads. Preliminary structural analysis concluded that the sizes of these towers would be 49, 276, and 198 % compared to reference V150-4.5 tower. If we assume linearly relative cost increase to tower mass, we get cost changes from tower mass modifiers for the LWPP towers.

Blades in LWPP are expected to be as in conventional WPPs. Large increases in TI might require stronger blades which would increase costs, but this isn’t factored to the cost analysis.

Foundations are around 7 % of total cost of a wind turbine (Jamieson 2018, p. 226). LWPP structure foundation needs are 25, 125, and 150 % for 100, 200, and 300 m towers, respectively, compared to a conventional WPP. The total foundation need was calculated to be same when compared to an equivalent WPP wind farm, so no change to foundation costs is made.

6.2.2 New parts

Costs of the new parts used in the design are hard to estimate as there is no direct comparison or there is only little available data. Their costs are estimated based on material prices and project costs of similar structures like bridges, and mast towers.

Side beams were estimated to be similar in design to turbine towers. They were calculated to be around 64 and 78 % of reference WPP tower mass. Using the same cost scaling for side beams as per towers, we get their costs to be of same size from reference tower costs.

The example design uses 8 guy-wires, and they were estimated to be 250 and 130 m long. Total guy-wire masses were calculated to be 43,6 t for guy-wires connected to 300 m tower and 22,7 t for 200 m tower wires. Example price for 1,27 cm diameter guy-wire is 8,1 €/m (Mcmaster, 2023). Scaling this cost up to 5 cm diameter based on cross area increase, the price comes to 126,1 €/m. Using this price, the total rounded costs for guy-wiring would be 31 500 and 48 000 €. These represent 4,5 % of the cost of a single reference tower.

6.2.3 Power grids

LWPP has short distances between turbines due to its compactness. This means less need for inter turbine medium-voltage (MW) cabling. The example LWPP has only 400 m distance on the ground that needs to be cabled between towers. In an equivalent WPP wind farm of 4 V150-4.5 turbines with typical spacings of 5 D laterally, the need for cabling would be 3 000 m. This is 7,5 times longer distance. But this is only valid for a wind farm consisting of a single LWPP. In multi LWPP wind farm the cabling need would grow for each LWPP unit, as the units would need to be spaced like WPPs. This would add 560 m of cabling for

each additional LWPP unit. Distance of cabling for 2 LWPP wind farm would be 1 360 m while WPP would need 6 000 m, a 4,4 times difference.

In larger wind farms MV cabling is divided to strings with few turbines per string. Cabling is thickest between substation and first turbine in the string and reduces thereafter for each turbine. Each string has a connector at substation, and having fewer strings reduces the number of costly connectors needed. Having turbines spread throughout the site increases the amount of large diameter cabling needed for stringing turbines. LWPP would reduce this need by having shorter distance between subsequent turbines after the first one.

The internal power grid costs could decrease by around 75 % due to reduced distances of cabling. Internal cabling can be around 2 % of total investment, which would lead to 1,5 % savings from total investment.

High voltage transformer need would be same for LWPP and WPP wind farms, as would grid connection, typically. They depend on distance of power line route from substation to nearest grid connection point. Smaller project up to 60 MW can connect directly to 110 kV line with transmission line connection (Fingrid 2022). Larger projects need their own medium voltage to high voltage transformer, which are costly.

6.3 OPEX

Operational expenditure comes from transport and balancing of electricity distribution, maintenance, land leasing, taxes, and insurances. Costs are mainly divided to fixed and open costs. Fixed means that their rate isn’t expected to vary, and they can be predicted. Open costs vary and are harder to predict. Generally, O&M costs can account for 18 % of wind energy project lifetime costs (Jamieson 2018, p. 226).

6.3.1 Changing costs

Changing costs are expected to change and fluctuate during the operation of wind power park. In Finnish markets the largest changing costs are electricity transportation and balancing fees that are paid to Fingrid. Size of the fees depends on the amount of electricity

inputted into the electricity transmission grid. Balancing fee comes from the need to make up the difference between estimated and realised power production. Stabler wind speed distribution might reduce LWPP power production fluctuation, but winds at higher elevation might also be harder to predict. Due to these factors balancing fees aren't expected to differ from WPP projects for LWPP projects. Same is for transmission fees as there is no difference for them.

Another source for changing costs comes from unscheduled maintenance. Even tough turbines are regularly maintained, and their condition is monitored, something can still fail unexpectedly. Turbines in harsh environments are more likely to fail due to increased stresses on components. This would be the case too in LWPP as wake added turbulences were calculated to increase significantly. Maintenance data is usually proprietary, is gained slowly and doesn't remain relevant due to fast advances in turbine technology (Jamieson 2018, p. 225). Unscheduled and planned maintenance costs are usually covered together in project costs splits and will be so here too.

6.3.2 Fixed costs

These costs are expected to remain the same during operation of wind power park. Main ones are property tax to the municipality, land leasing costs, and maintenance costs.

Property tax

Property tax forms a large part of the fixed costs, around 12 % of the total fixed costs, but only 4 % of total lifetime expenditure. (Jamieson 2018, p. 226). Property tax is formulated differently for LWPP as it has different composition of taxable parts.

An instruction issued on 17.3.2022 defines the property tax formation for wind and solar power plants. Property tax is either based on power plant property tax for wind turbines in a wind farm or according to the municipality's general property tax for single turbines. Property tax is levied on a construction on owned or rented land. The Supreme Administrative Court of Finland made in their 11.11.2004 ruling a decision that only the foundation, tower, and shell of the nacelle of a wind power plant are taxable property.

Transmission, blades, and generator are considered as machines and movables equivalent and as such their capital costs aren't factored into property tax formation. (Vero, 2022)

Evaluation for tax is done by replacement value minus yearly age-discounts. Replacement value is set to be 75% of foundation, tower and empty nacelle building investment cost. According to evaluation law, yearly age-discount is 2,5%, but the minimum evaluation value is still 40% after discounts. (Vero, 2022)

Property tax percentage is determined by local municipality, and it can be 3,10 % maximally. If wind park is over 10 MVA, or there is more than one power plant connecting to distribution or transmission grid, it can use power plant tax percentage. Otherwise, common property tax is used. (Vero, 2022)

Share of property taxable turbine parts are usually 30 % of total investment. For conventional wind farms this can mean costs of 25 000 € per year per turbine. Age discounts bring this down overtime, usually to minimum within 24-25 years. (Suomen Tuulivoimayhdistys 2020)

This means that LWPP would have higher property tax due to increase in proportion of property taxable tower and support structures compared to rest of the components. Calculating from Table 14 values, non-taxable parts make up 70,5 % of WPP costs, and tower, nacelle, and foundations make up 29,5 %, the taxable portion of WPP costs. Total LWPP RNA scaling based on their combined mass is 66,5 % of an equivalent WPP wind farm's RNA masses. Similarly total tower scaling is 272 %. Scaling the WPP cost fractions by relevant modifiers to make the into LWPP cost fractions results in 47,3 % non-taxable and 52,7 % taxable portions. These bring the property tax of LWPP to be 52,7 % of the structure's cost while WPP property taxable portion is only 29,5 % of WPP cost.

Side beams and guy-wiring would likely fall into taxable category, under the property tax law. This would further increase the LWPP property taxes in comparison to reference WPP. Property tax is assumed to be double in LWPP based on these.

Land leasing

Land leasing costs can be around 9 % of OPEX costs, or 4,6 % of total costs (Gasch R. & Twele J. 2012, p. 496). Wind energy projects are usually wholly or partially built onto private land owned by landowners. The land needs to be rented or acquired for project building and

operating. Usually, the rent to the landowners starts when project clears permitting phase and building starts. Sometimes one-time milestone payments are paid to landowners during project development phase as incentives. Ways of determining rent amount differ between projects and project developers, but are usually fixed amount, or tied to profits from electricity sales as percentage. Size of the rented property, planned land use, and proximity to turbines are main factors on rent amount.

There could be saving here for LWPP as it has higher energy acreage and a wind farm producing same amount of energy would take less land area. Or a larger project could be built upon same area creating costs savings per produced energy. The calculated energy acreage increase of 2 times means that LWPP would need only halve the land area that WPP would need. This could up to halve the amount of land needed to lease, which would halve land leasing costs. This would be a saving of 4,5 %-p for typical total fixed costs.

Maintenance costs

Wind turbines require periodical maintenance, and the rate and type are specified turbine manufacturer. Most critical components for maintenance are rotor blades, pitch system, gearbox, generator, and control and electronics (Gasch R. & Twele J. 2012, p. 496).

LWPP concept is meant to be easier to maintain. Easier travel to and within LWPP would hasten maintenance tasks by a little which would decrease maintenance costs by a tad. It was also surmised that the amount of maintenance need would be greater due to increased number of turbines, meaning increased change of failures.

Increased TI also increases blade fatigue. This might shorten their lifetime and require more frequent replacement. Blades are normally expected to require significant maintenance between 6-year periods (Gasch R. & Twele J. 2012, p. 496). The TI increase would also increase torque on the drive train increasing gearbox and generator wear.

Due to some maintenance benefits and some risks, maintenance costs are kept the same.

6.4 Production

Wind energy project profits come from electricity sales from the produced energy. The power production of a LWPP was estimated in section 4.3 . AEP after wake loss and added TI was estimated to be between 58,9-81,3 GWh/a between the examined sites.

Wake losses were between 3,4-8,4 % of AEP between the sites. It needs to be noted that these losses are from within single LWPP unit. In a wind farm configuration, the losses would further increase by the typical 15 % WPP wind farm wake loss (Cao et al. 2022, p. 1).

Compared to equivalent capacity WPP wind farm the LWPP AEP was 17,1 % higher. Capacity factor also increased on average by 13,9 %.

6.5 LCOE

LCOE is the minimum price for electricity that needs to be set for project to recuperate the losses from the investment and operation. If realised energy sale price is larger, then project will turn profit. LCOE for LWPP is estimated by contrasting changes in LWPP project costs and energy production to an equivalent capacity WPP wind farm. Comparison farm energy production is from adjusted tuuliatlas data and cost structure from literature references and modifications to it. Cost changes from a typical WPP project are expected to be like in Table 15. These were calculated as percentage changes to WPP cost structure.

Table 15. LWPP changes to typical WPP project cost structure and power production.

Factor	**Component**	**Change of total expenditure [%-p]**
CAPEX	RNA	-16
	Tower	12,3
	Side beam	2,8
	Guy-wiring	0,2
	Foundations	0,4
	Internal grid	-1,9
OPEX	Property tax	0,5
	Land leasing	-2,3
		Change [%]
Production	Production	17,1

Table 15 shows the major changes that a LWPP would have in its cost structure. These were based on the discussed differences and modifiers. The complete new cost fractions table is shown in Table 16. These are normalised to the new cost structure making the sum of percentages 100 %.

Table 16. Cost fractions of a LWPP project.

Cost category	Component	Sub component	Cost fraction [%]
CAPEX	Turbine		45,8
		Blades	6,0
		Drivetrains	13,3
		Nacelles	3,2
		Hubs	3,2
		Towers	18,3
		Other	1,8
		Side beams	2,8
		Guy-wires	0,2
	Foundation		1,6
	Roads and buildings		0,9
	Electrics		7,0
		Internal cabling	0,5
		Substation & cabling	5,2
		Connection fee	1,3
OPEX	Maintenance		16,9
	Land leasing		1,9
	Legal and tax		2,3
	Financing		6,6
	Grid balance		14,1

Overall cost increase for LWPP project was 16 % over equivalent capacity 4 V150-4.5 WPP wind farm. Combining this with 17,1 % increase in energy production we get LCOE change of 0,9 %. This would result in practically no chance to the LCOE for LWPP when compared to conventional WPPs.

7 Environmental factors

One of the key factors in a successful wind farm project is assessing and limiting environmental impact. In Finland comprehensive analyses are required for projects that account for impact that the project would have on local landscape, wildlife, noise, and visuals. The environmental impact assessments are critical for a project to succeed.

Environmental impact assessment is required from wind farm projects that exceed 10 WPPs or 30 MW capacity (Ympäristöministeriö 2016a, p. 44). This would need to be adapted for LWPP as it is a multirotor system containing multiple turbines on a single structure. Single LWPP unit could be configured to exceed 30 MW mark by itself, or many used as wind farm.

LWPP concept would have different impact on these due to the size increase and arrangement of turbines. Most major differences are expected to be around avian, noise, and visuals. Extent of these impacts are analysed here.

7.1 Avian impact

Wind farms pose risks to birds through direct and indirect means. These can be collision to structures, blocking migratory paths, disturbance, and changes to habitat. These need to be considered in wind farm planning. (Ympäristöministeriö 2016b, p. 6)

Habitat changes come from physical changes to environment due to building, changes to feeding grounds, division of zones due to roads. LWPP has better energy acreage which reduces land usage, needed electrical and road infrastructure. This would reduce the overall land usage, but also concentrate the buildings to denser area, as opposed to conventional wind farms where structures and roads are spread throughout the site.

Bird movements were measured at a Dutch offshore wind farm. Bird flight heights and number of echo detections were divided to four seasons. Measurements showed that most bird flew below 50 m and there were more observations in autumn. On average 55,7 % of observed bird flights were below 101 m of altitude and 70,9 % flew below 201 m. (Fijn et

al. 2015, p. 563) This is for offshore conditions, but could mean that most avian flights would see small increase in collision probability for taller wind turbines, making LWPP height increase low risk.

Avian collision risk models are used to estimate the probability of collision, or the number of collisions. They can be based on known bird behaviour and vicinity to site, likelihood of bird entering turbine swept area, turbine characteristics like blade rotation frequency and size, and bird size and avoidance behaviour. From these a collision risk estimate can be formed. Some models assume birds to avoid inner radius at turbine hub as there blades move more slowly. (Masden 2016, p. 44) Blade tip speeds increase with turbine size which could mean that the blades of smaller turbines would be easier to avoid as they their tips speeds are lower.

LWPP has smaller overall turbine swept area and the swept areas are more concentrated within a wind farm. This reduces the likelihood of bird entering the turbine swept area. It could be surmised that the larger stationary structure would also act as a deterrent for flythroughs lessening the probability of collisions.

7.2 Noise emissions

LWPP has multiple turbines that act as noise sources in proximity and at higher elevation and that makes the noise it generates different to conventional wind turbines. The elevation of noise sources also affects noise propagation differently. Main concerns with noise emissions are the strength, or sound pressure level (SPL), and amplitude modulation, the periodic swishing sound from blade passings.

Rotation of the turbines generates noise by turbulent motions of approaching air colliding with leading edge, turbulence on wing surface leaving trailing edge and vortices formed on blade tips. Noise depends on atmospheric conditions and blade design. Other noises can come from hub, vibrations from gearbox, generator, or blade-tower interaction. Out of the noises, trailing edge noise is the dominant source. (Emeis 2018, p. 231) Larger turbines generally generate more noise, but blade design and atmospheric conditions are more important SPL factors. This would mean slightly lower noise level for LWPP with smaller turbines.

Wind turbine sources are typically 102-107 dB(A). (Suomen Tuulivoimayhdistys 2022c) Sound pressure decrease over distance is inversely proportional meaning that SPL decreases rapidly until evening out. SPL is typically below the guideline value of 40 dB at 700 m from turbines (Ympäristöministeriö 2016a, p. 78) (Gasch R. & Twele J. 2012, p. 488). Increase of 5 dB in emission SPL can increase the distance of reaching the target noise level by several hundred metres.

Sound waves from multiple turbines add up. Sound power levels without local interferences can be added up linearly. Turbines in wind farms are uncorrelated and most likely to be out of phase, during certain conditions turbines can sync up and this leads to increase in overall noise level of amplitude modulation. (Stoevesandt et al. 2022, p. 1388-1389) The amount, proximity, and size differences of turbines in LWPP makes phase syncing of multiple turbines less likely. Summation of source SPLs would roughly double it for each additional source. This would increase LWPP noise considerably if the turbines had same SPL as conventional farms, but smaller turbines might mitigate this compensating for the summation.

Sound propagation in the atmosphere is influenced by sound attenuation and refraction, and these are affected by wind speed, wind direction, air temperature, humidity, obstacles, and turbine wakes. Attenuation is energy of sound waves dissipating due to viscous friction between air molecules and short-term absorption. Higher frequencies attenuate more than lower frequencies. Refraction is sound waves changing direction due to air temperature distribution and/or wind shear. Vertical temperature gradient causes sound rays to refract upward as the sound speed increases with temperature increase. This usually happens during daytime. Inverse direction usually happens during night-time. Wind shear can modify these directions downwards as sound moves with the wind and wind speed typically increases with height. (Emeis 2018, p. 232-235)

Wakes affect sound refraction. Barlas et al. (2017) studied the effects of wind turbine wake on atmospheric sound propagation and found that acoustic energy is redistributed downwind from the wind turbine due to the wake induced flow field. The sound waves go through local upward and downward refraction regions due to wake deficit. Increase in inflow speed makes the sound pressure contours spread to wider area. Severe downward refraction is observed in far wake where wake breaks down. Far field noise, 700-3 000 m, is especially increased during stable atmospheric conditions and the amplification can be up to 7.5 dB at

wake centre. TI shortens the wake and simulations showed smaller relative sound pressure level increase for 10 % TI than for 0 %. (Barlas et al. 2017, p. 57-60)

This study indicates that the increased wake TI from LWPP at certain angles would shorten the wakes which would lead to stronger downward refraction than in a conventional wind farm, reducing SPL at distance. Height increase would on the other hand increase the reach of SPL refraction as it has more time to move downwards. So, the area of noise emissions in LWPP compared to conventional wind farm is indecisive.

7.3 Visual impact

Wind turbines are large structures that are visible far. They can change the look of the landscape and be an eyesore, but this is largely up to subjective experience. Size increase of a LWPP exasperates these visual impacts, which is why the visual impact is assessed and compared to conventional wind farm.

An illustrative comparison on the aesthetic differences between a small conventional wind farm and a LWPP unit in a landscape setting was modelled and rendered in Blender using the model introduced in chapter 2.4 . View modelling used 2 km distance from the vantage point to the installation and 1 km distance to the forest line that has a maximum height of 40 m. Example views of a LWPP and four WPPs are shown in Figure 22 and Figure 23, respectively.

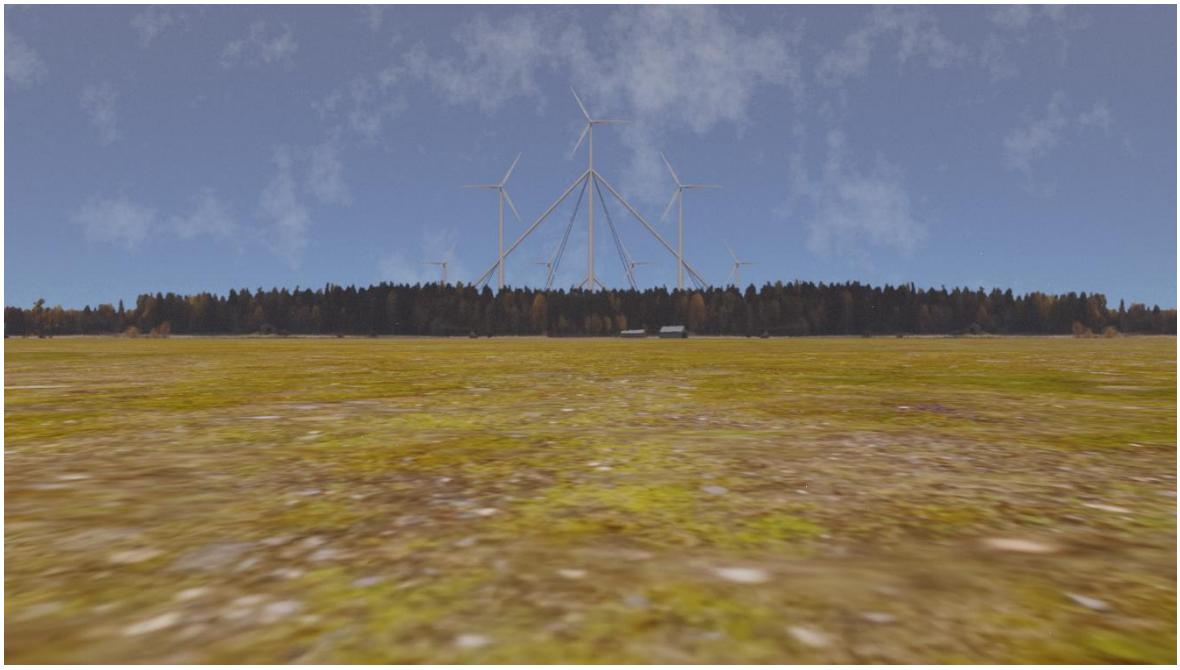

Figure 22. View of a LWPP from 3 km distance with 35 mm camera focal length.

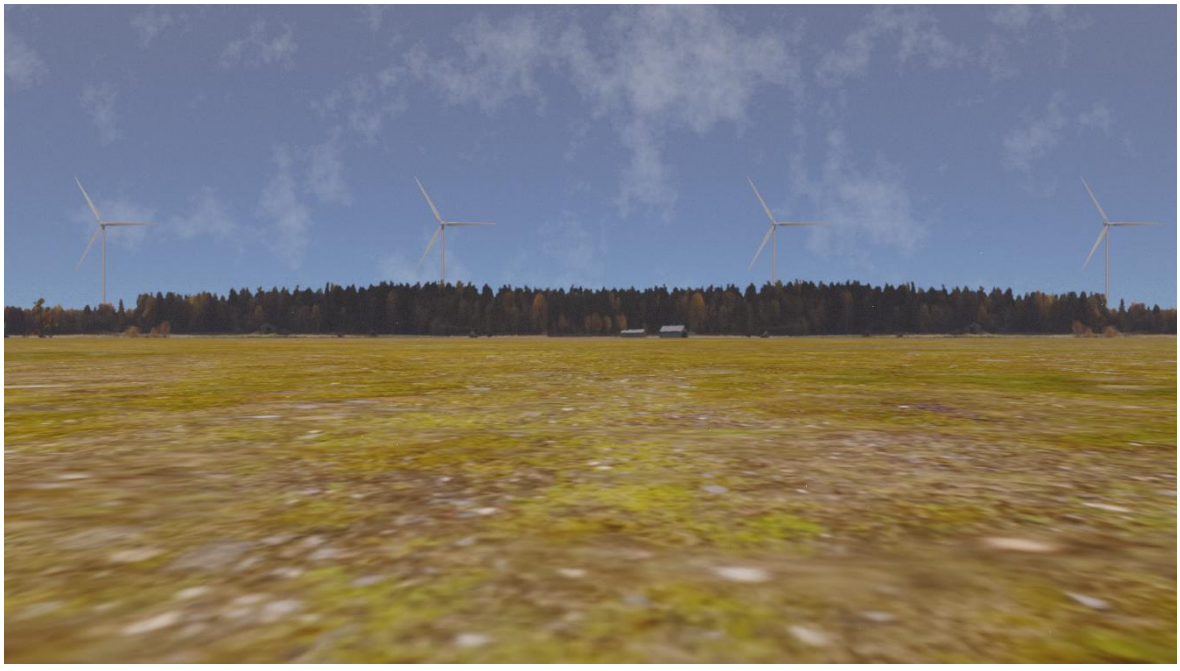

Figure 23. View of a conventional wind farm of four turbines from 3 km distance with 35 mm camera focal length.

The figure shows how the height increase of LWPP makes it stand out more in rural environment when compared to a conventional wind farm. Tree line is far from the observer

which makes turbines highly visible in this view. Both LWPP and traditional wind farm are facing the camera making this illustration show the largest scenic footprints of these systems. Due to the linear design of LWPP, the visual profile is starkly different when viewed from the side as the turbines and structures block out each other. This effect is less prominent in conventional wind farm as there turbines are spaced out more length wise.

Wind turbines will also have a visual impact during the night as they are equipped with flight obstruction lights that blink or emit a constant light. In Finland regulations on the type of night markings is given by Traficom and depend on blade tip of height of a turbine. LWPP would most likely fall to the last category, as do conventional turbines, where they need to use high power blinking white light during day and high-powered blinking white, medium-powered blinking red, or medium-powered constant red light on top of nacelle. (Traficom 2020) These lights would be grouped closer in LWPP due to turbine arrangement, and they would be visible further due to height increase. In a conventional wind farm the lights are spread more evenly through the park. This would create a more clustered light emission from LWPP park.

Moving rotor blades cause shadows that can be cast that is known as flickering. This can cause an annoyance to residents close to wind farms as the shadows can cause periodical illumination changes at residences. Wind farm planning takes this into account by calculating annual flicker zones near the farms and evaluating the severity of flickering by the number of hours per year that an area receives. (Gasch R. & Twele J. 2012, p. 489)

The flickering effect would be different for a LWPP as the high elevation turbines would cause longer shadows that reach further. On the other hand, it uses smaller rotors which reduces the flicker area. And as the energy acreage is greater the affected area could be reduced compared to conventional wind farms.

Wind turbines can cause disturbances to radio frequencies. These can affect military radars, radio communications or even tv signals. Especially important is the impact on military radars as it can impede territorial surveillance.

Due to height LWPP would block more in vertical direction, which increases radar cross section creating static clutter. Moving blades create Doppler ambiguities that confuse radar operators. (Sharma & Chintala 2022, p. 1) But due to power density have lower horizontal

footprint obscuring smaller sector from the radar. Affects need to be assessed especially on military radar coverage.

8 Conclusions

The aim of this thesis was to conduct a multi-faceted analysis on the LWPP concept to estimate its merits and their feasibility. Wide variety of variants can be created from the core LWPP concept. An example design consisting of 7 turbines with total nominal power of 17,1 MW was created to have concrete features to analyse. This design used some modernisations and as such doesn't represent the original LWPP concept fully but allowed for easier analysis of the main merits.

Wind resources literature review enforced the view that having turbines at higher hub height would increase their energy production and capacity factor. This was further strengthened by the wind data from examined sites. Wake losses and added TI hampered this increased productivity, especially at the lowest turbine row where wake losses resulted on average 11,5 % AEP reduction. Total wake losses were on average 6,7 %. Still the average AEP was 66 225 GWh/a, which was 17,1 % more than for an equivalent conventional wind farm that was used for comparisons. Capacity factor was also higher at 0,44 compared to 0,33. Increased energy production and more efficient land usage increased LWPP energy acreage to 82,3 GWh/km^2 which is double that of a conventional WPP wind farm.

The tuuliatlas data that was used for Excel tool wake loss and AEP calculations had some simplifications that limit the calculation accuracy. Having wind directions as sectors limited the wake loss calculations accuracy as did mismatch between Weibull distribution wind speed frequencies and directional frequencies. The used calculation tool also didn't give the same results for WPP AEP as was pregiven in the tuuliatlas data. This discrepancy was accounted for with adjustments to the comparison data. The need for adjustment means that the presented values aren't directly comparable to similar values in other literature. Despite these the calculations are accurate enough for preliminary considerations.

The structural feasibility of the concept was hard to estimate as it combined many features with little available literature references. The scaling of most structural elements was done using scaling laws with which they were proportionally down or upscaled. For some elements like towers this wasn't applicable, so they were scaled by extrapolating from example tower dimensions while preserving the other proportions. The smaller turbines reduced the gravitational loads acting on the towers as did the side beams. Guy-wiring was

found to provide support against thrust forces. These supporting elements with reduced RNA masses seemed to enable increased hub heights. Overall, the LWPP structure was 3 times larger than an equivalent conventional WPP wind farm, but the forces acting on the structure where on similar level, which lends credence to the structure's feasibility. The complicated structure and the new supporting elements on the example design didn't result in meaningful benefits for transportability, installation, or maintainability. Added TI from wakes was seen as risk for component lifetimes.

The up and downscaling of the components lead to cost increases and reductions. The component costs were calculated based on volumetric or mass change of the components compared to reference turbine cost structure. The LWPP had cheaper turbines, around 16 %-p, but the tower cost increase, around 12,3 %-p, mostly negated this saving. Overall costs were 16 % more than in an equivalent WPP wind farm. This cost increase combined with increased energy production resulted in no meaningful change for the example LWPP design's LCOE.

From an environmental viewpoint, the example design was estimated to have a greater visual impact. The larger structure is visible further and is more dominating in the landscape. Taller towers cause flickering to reach further and at night flight obstruction lights are more visible. Effects on avian and noise didn't present major risks.

Overall, the analyses conducted on the example LWPP design gave valuable insights to the degree of the concept's merits and flaws. Energy production saw clear improvements as did the energy acreage. Wake losses were major due to short distances between turbines. Designs with more turbines per row would exasperate these losses making the densest rows have poor performance. The concept's linear nature makes wake losses unavoidable. LWPP concept would be better suited for sites with wind directions focused on single axis. The examined shared support structure allowed for reduced loads and greater hub heights. Required tower elements were larger than in conventional WPPs and designs aiming for even greater sizes would face challenges. Better optimised designs could realise greater economic benefits, but the examined design was unable to lead to meaningful gains in the examined conditions. Therefore, some use cases and designs could prove opportune, but no general use adoption is predicted for the LWPP concept.

References

Baniotopoulos, C. C., Borri, C. and Stathopoulos, T. 2011. Environmental Wind Engineering and Design of Wind Energy Structures. Springer. Vienna. ISBN : 9783709109526

Barlas, E., Zhu, W., Shen, W., Kelly, M. and Andersen, S. 2017. Effects of wind turbine wake on atmospheric sound propagation. Applied acoustics, Vol.122, p.51-61. Elsevier Ltd. DOI: 10.1016/j.apacoust.2017.02.010

Bhattacharya, S. 2019. Design of foundations for offshore wind turbines. John Wiley & Sons Ltd. Hoboken. ISBN: 9781119128144

Cao, L., Ge, M., Gao, X., Du, B., Li, B., Huang, Z. and Liu Y. 2022. Wind farm layout optimization to minimize the wake induced turbulence effect on wind turbines. Applied Energy, Vol.323, p.119599. Elsevier Ltd. DOI: 10.1016/j.apenergy.2022.119599

Dykes, K., Damiani, R., Roberts, O. and Lantz, E. 2018. Analysis of Ideal Towers for Tall Wind Applications. National Renewable Energy Laboratory. NREL/CP-5000-70642.

Electrek. 2021. Vestas takes GE's 'world's largest offshore wind turbine' title. [website]. [Referenced: 20.9.2022]. Available: https://electrek.co/2021/02/10/vestas-gm-worlds-largest-offshore-wind-turbine/

Elforsk. 2010. Tall towers for large wind turbines. [Referenced: 20.9.2022]. Available https://www.osti.gov/etdeweb/servlets/purl/992745

Emeis S. 2018. Wind Energy Meteorology. 2nd ed. Springer International Publishing AG, Switzerland. ISBN 978-3-319-72859-9

FearnleySecurities. 2021. Wind Virtual Event. [Recording]. [Watched: 27.11.2022]. Available: https://research.fearnleysecurities.no/wind/

Fijn, R., Krijgsveld, K., Poot, M., Dirksen, S. and Fox, T. 2015. Bird movements at rotor heights measured continuously with vertical radar at a Dutch offshore wind farm. Ibis (London, England), Vol.157 (3), p.558-566. Academic Press. Oxford. DOI: 10.1111/ibi.12259

Fingrid. s.a. Kantaverkkoon liittyjän opas. [pdf]. [Referenced: 5.3.2023]. Available: https://www.fingrid.fi/globalassets/dokumentit/fi/palvelut/kulutuksen-ja-tuotannon-liittaminen-kantaverkkoon/kantaverkkoon-liittyjan-opas.pdf

Frandsen, S., Barthelmie, R., Pryor, S., Rathmann, O., Larsen, S., Højstrup, J. and Thøgersen, M. 2006. Analytical modelling of wind speed deficit in large offshore wind farms. Wind energy (Chichester, England), Vol.9 (1-2), p.39-53. John Wiley & Sons, Ltd. Chichester. DOI: 10.1002/we.189

Gasch, R. and Twele J. 2012. Wind Power Plants, Fundamentals, Design, Construction and Operation. Springer. Berlin. ISBN 978-3-642-22937-4

Hau, E. 2013. Wind Turbines Fundamentals, Technologies, Application, Economics. Springer. Berlin. ISBN : 9783642271519

Huang, X., Li, B., Zhou, X., Wang, Y. and Zhu, R. 2022. Geometric optimisation analysis of Steel–Concrete hybrid wind turbine towers. Structures (Oxford), Vol.35, p.1125-1137. Elsevier Ltd. DOI: 10.1016/j.istruc.2021.08.036

Iin kunta. 2020. Yli-Olhavan tuulivoimapuiston osayleiskaava kaavaehdotuksesta annetut lausunnot ja muistutukset sekä kaavan laatijan vastineet. [pdf]. [Referenced: 4.3.2023]. Available: https://www.ii.fi/sites/ii.fi/files/TIEDOSTOT/ASUMINEN_YMPARISTO/Kaavoitus/vastineet%20ehdotusvaiheessa%20saatuun%20palautteeseen%20Yli-Olhava.pdf

Ilmatieteen laitos. 2010. Suomen tuuliatlas yhteenvetoraportti. [pdf]. [Referenced: 16.9.2022]. Available: https://expo.fmi.fi/aqes/public/Tuuliatlas_yhteenvetoraportti.pdf

Intergovernmental panel on climate change. 2022. Climate Change 2022 Mitigation of Climate Change. [Web-document]. [Referenced: 6.4.2022]. Available: https://report.ipcc.ch/ar6wg3/pdf/IPCC_AR6_WGIII_FinalDraft_FullReport.pdf

Ishihara, T. and Qian, G. 2018. A new Gaussian-based analytical wake model for wind turbines considering ambient turbulence intensities and thrust coefficient effects. Journal of wind engineering and industrial aerodynamics, Vol.177, p.275-292. Elsevier Ltd. DOI: 10.1016/j.jweia.2018.04.010

Jamieson, P. 2018. Innovation in Wind Turbine Design. 2nd ed. John Wiley & Sons. Hoboken. ISBN: 9781119137900

Jamieson, P.; Branney, M. 2012. Multi-Rotors; A Solution to 20 MW and Beyond? Energy Procedia 24. Volume 24, Pages 52-59. Elsevier Ltd. https://doi.org/10.1016/j.egypro.2012.06.086

Jespersen, M. and Støttrup-Andersen, U. 2019. Guyed Wind Turbine Towers: Developments and outlook. ce/papers, Vol.3 (3-4), p.779-784. DOI: 10.1002/cepa.1133

Kaldellis, J., Triantafyllou, P. and Stinis, P. 2021. Critical evaluation of Wind Turbines' analytical wake models. Renewable & sustainable energy reviews, Vol.144, p.110991. Elsevier Ltd. DOI: 10.1016/j.rser.2021.110991

Laan, M. and Abkar, M. 2019b. Improved energy production of multi-rotor wind farms. Journal of physics. Conference series, 2019, Vol.1256 (1), p.12011. IOP Publishing. Ithaca. DOI: 10.1088/1742-6596/1256/1/01201

Laan, M., Andersen, S., García, N., Angeloul, N., Pirrung, G., Ott, S., Sjöholm, M., Sørensen, K., Neto, J., Kelly, M., Mikkelsen, T. and Larsen, G. 2019a. Power curve and wake analyses of the Vestas multi-rotor demonstrator. Wind Energ. Sci., 4, 251–271. https://doi.org/10.5194/wes-4-251-2019

Liu, Z., Li, Q., Ishihara, T. and Peng, J. 2020. Numerical simulations of fatigue loads on wind turbines operating in wakes. Wind energy (Chichester, England), Vol.23 (5), p.1301-1316. Wiley Subscription Services, Inc. DOI: 10.1002/we.2487

Masden, E. and Cook, A. 2016. Avian collision risk models for wind energy impact assessments. Environmental impact assessment review, 2016-01, Vol.56, p.43-49. Elsevier Inc. DOI: 10.1016/j.eiar.2015.09.001

McKenna, R., Ostman, P. and Fichtner, W. 2016. Key challenges and prospects for large wind turbines. Renewable and Sustainable Energy Reviews. Elsevier Ltd. DOI: 10.1016/j.rser.2015.09.080

Mcmaster. 2023. Difficult to bend wire rope for lifting. [Website]. [Referenced: 5.3.2023]. Available: https://www.mcmaster.com/guy-wire/difficult-to-bend-wire-rope-not-for-lifting/

Ng, C. and Ran, L. 2016. Offshore wind farms : technologies, design and operation. Woodhead Publishing. Amsterdam. ISBN : 0-08-100779-5

Pierella, F. and Sætran, L. 2017. Wind tunnel investigation on the effect of the turbine tower on wind turbines wake symmetry. Wind energy (Chichester, England), Vol.20 (10), p.1753-1769. Wiley Subscription Services, Inc. DOI: 10.1002/we.2120

Porté-Agel, F., Bastankhah, M. and Shamsoddin, S. 2020. Wind-Turbine and Wind-Farm Flows: A Review. Boundary-layer meteorology, Vol.174 (1), p.1-59. Springer Netherlands. Dordrecht. DOI: 10.1007/s10546-019-00473-0

PRH. 2009. Piirustukset. [Web-document]. [Referenced: 10.7.2022]. Available: https://patent.prh.fi/patdocs/public-doc.jsp?NroParam=X415713&HakemusParam=20070502&NID=&offset=0&Inx=1&P=T&PN=122078&LJ=&PD=20081226&lang=fi&dockey=FW1ULX2NPHOENIX&page=1

PRH. 2010a. Tiivistelmä (suomeksi). [Web-document]. [Referenced: 10.7.2022]. Available: https://patent.prh.fi/patdocs/public-doc.jsp?NroParam=X415713&HakemusParam=20070502&NID=&offset=0&Inx=1&P=T&PN=122078&LJ=&PD=20081226&lang=fi&dockey=GGW6ILDVPHOENIX&page=1

PRH. 2010b. Selitys (suomeksi). [Web-document]. [Referenced: 10.7.2022]. Available: https://patent.prh.fi/patdocs/public-doc.jsp?NroParam=X415713&HakemusParam=20070502&NID=&offset=0&Inx=1&P=T&PN=122078&LJ=&PD=20081226&lang=fi&dockey=GGW6ILD0PHOENIX&scale=75&page=1

PRH. 2010c. Vaatimukset (suomeksi). [Web-document]. [Referenced: 10.7.2022]. Available: https://patent.prh.fi/patdocs/public-doc.jsp?NroParam=X415713&HakemusParam=20070502&NID=&offset=0&Inx=1&P=T&PN=122078&LJ=&PD=20081226&lang=fi&dockey=GGW6ILDFPHOENIX&page=1

PRH. 2022. Application number 20070502. [Web-document]. [Referenced: 9.7.2022]. Available: https://patent.prh.fi/patinfo/tiedot.asp?NroParam=20070502&NID=&offset=&ID=X415713&Inx=1

Rao, K. 2019. Wind Energy for Power Generation Meeting the Challenge of Practical Implementation. Springer International Publishing. Cham. ISBN : 978-3-319-75134-4

Rebelo, C., Moura, A., Gervásio, H., Veljkovic, M. and Simões da Silva, L. 2014. Comparative life cycle assessment of tubular wind towers and foundations – Part 1: Structural design. Engineering structures, Vol.74, p.283-291. Elsevier Ltd. Kidlington. DOI: 10.1016/j.engstruct.2014.02.040

Reinwardt I., Gerke, N., Dalhoff, P., Steudel, D. and Moser, W. 2018. Validation of wind turbine wake models with focus on the dynamic wake meandering model. Journal of Physics: Conference Series, Volume 1037, Issue 7. IOP Publishing. Bristol. DOI 10.1088/1742-6596/1037/7/072028

Renkema, D. 2007. Validation of wind turbine wake models: Using wind farm data and wind tunnel measurements. Master of Science Thesis. Delf University of Technology.

Roga, S., Bardhan, S., Kumar, Y. and Dubey, S. 2022. Recent technology and challenges of wind energy generation: A review. Sustainable energy technologies and assessments, Vol.52, p.102239. Elsevier Ltd. DOI:10.1016/j.seta.2022.102239

Sedaghatizadeh, N., Arjomandi, M., Kelso, R., Cazzolato, B. and Ghayesh, M. 2018. Modelling of wind turbine wake using large eddy simulation. Renewable energy, Vol.115, p.1166-1176. Elsevier Ltd. DOI: 10.1016/j.renene.2017.09.017

Sharma, A. and Chintala, V. 2022. Augmenting the signal processing–based mitigation techniques for removing wind turbine and radar interference. Wind engineering, Vol.46 (2), p.670-680. SAGE Publications. London. DOI: 10.1177/0309524X20948543.

Sørensen, J. 2011. Wind energy systems : optimising design and construction for safe and reliable operation. Woodhead Publishing. Cambridge. ISBN : 1-84569-580-1.

Stehly, T. and Duffy, P. 2021 Cost of Wind Energy Review. National Renewable Energy Laboratory, 2022. [pdf]. [Referenced: 11.1.2023]. Available: https://www.nrel.gov/docs/fy23osti/84774.pdf

Stoevesandt, B., Shepers, G., Fuglsang, P. and Sun Y. 2022. Handbook of Wind Energy Aerodynamics. Springer. Cham. ISBN 978-3-030-31307-4

Störtenbecker, S., Anselm, R. and Dalhoff, P. 2020. Simplified approach for the optimal number of rotors and support structure design of a multi rotor wind turbine system. Journal of physics. Conference series, Vol.1618 (3), p.32009. IOP Publishing. DOI: 10.1088/1742-6596/1618/3/032009.

Suomen Tuulivoimayhdistys. 2020. Tuulivoimalan kiinteistöveron määräytyminen. [pdf]. [Referenced: 2.8.2022]. Available: https://www.tuulivoimayhdistys.fi/media/tuulivoimalan-kiinteistoveron-maaraytyminen_toukokuu20.pdf

Suomen Tuulivoimayhdistys. 2021. Tuulivoimatilastot 2021. [Web-document]. [Referenced: 12.3.2022]. Available: https://tuulivoimayhdistys.fi/ajankohtaista/tutkimukset-ja-julkaisut/tilastot/tuulivoimatilastot-2021

Suomen Tuulivoimayhdistys. 2022a. Investoinnit. [website]. [Referenced: 8.1.2023]. Available: https://tuulivoimayhdistys.fi/tietoa-tuulivoimasta-2/tietoa-tuulivoimasta/taloudellisuus/investoinnit

Suomen Tuulivoimayhdistys. 2022b. Tuulivoimaloiden rakenne. [website]. [Referenced: 24.1.2023]. Available: https://tuulivoimayhdistys.fi/tietoa-tuulivoimasta-2/tietoa-tuulivoimasta/tuulivoimatekniikka/tuulivoimaloiden-rakenne

Suomen Tuulivoimayhdistys. 2022c. Äänivaikutukset. [Website]. [Referenced: 5.3.2023]. Available: https://tuulivoimayhdistys.fi/tietoa-tuulivoimasta-2/tietoa-tuulivoimasta/tuulivoiman-vaikutukset/tuulivoiman-ymparistovaikutukset/aanivaikutukset

Suzuki, H., Shiohara, H., Schnepf, A., Houtani, H., Carmo, L., Hirabayashi, S., Haneda, K., Chujo, T., Nihei, Y., Malta, E. and Gonçalves, R. 2020. Wave and Wind Responses of a Very-Light FOWT with Guy-Wired-Supported Tower: Numerical and Experimental Studies. Journal of marine science and engineering, Vol.8 (11), p.841. MDPI AG. DOI: 10.3390/jmse8110841.

Traficom. 2020. Ohje tuulivoimaloiden päivämerkintään, lentoestevaloihin sekä valojen ryhmitykseen. [pdf]. [Referenced: 14.10.2022]. Available: https://www.traficom.fi/sites/default/files/media/file/Ohje%20tuulivoimaloiden%20p%C3

%A4iv%C3%A4merkint%C3%A4%C3%A4n%2C%20lentoestevaloihin%20sek%C3%A4%20valojen%20ryhmitykseen_07SEP2020.pdf

Vero. 2022. Tuulivoima- ja aurinkovoimalaitokset verotuksessa. [Website]. [Referenced: 2.8.2022]. Available: https://www.vero.fi/syventavat-vero-ohjeet/ohje-hakusivu/48501/tuulivoima--ja-aurinkovoimalaitokset-verotuksessa/

Vestas, 2022. AOM Active output management. [Website]. [Referenced: 4.3.2023]. Available: https://nozebra.ipapercms.dk/Vestas/Communication/Productbrochure/AOM/AOMconceptbrochure/?page=10

Weiwei, L. and Yoda, T. 2017. Bridge Engineering: Classifications, Design Loading, and Analysis Methods. Elsevier Science & Technology. Oxford. ISBN: 978-0-12-804433-9

WindEurope. 2020. Wind energy and economic recovery in Europe. [Web-document]. [Referenced: 7.4.2022]. Available: https://windeurope.org/intelligence-platform/product/wind-energy-and-economic-recovery-in-europe/

Wind-Turbine-Models. 2022. Compare power curves of wind turbines. [website]. [Referenced: 12.11.2022]. Available: https://en.wind-turbine-models.com/powercurves

Ympäristöministeriö. 2016a. Tuulivoimarakentamisen suunnittelu Päivitys 2016. [pdf]. [Referenced: 7.1.2023]. Available: http://urn.fi/URN:ISBN:978-952-11-4634-3

Ympäristöministeriö. 2016b. Linnustovaikutusten arviointi tuulivoimarakentamisessa. [pdf]. [Referenced: 7.1.2023]. Available: http://urn.fi/URN:ISBN:978-952-11-4624-4

Appendix 1. Ishihara & Qian 2018 wake loss model

Full description of equations governing the Ishihara & Qian (2018) analytical wake model are covered here.

Representative wake width is calculated with:

$$\frac{\sigma}{D} = k' \frac{x}{D} + \varepsilon = 0{,}11 C_T^{1{,}07} I_a^{0{,}2} \frac{x}{D} + 0{,}23 C_T^{0{,}25} I_a^{0{,}17} \quad (12)$$

Where *x* is distance downstream [m], D is rotor diameter [m^2], C_T is turbine thrust coefficient [-], and I_a is ambient turbulence intensity [-]. (Ishihara & Qian 2018, p. 284)

Velocity deficit

Velocity deficit is calculated by:

$$\frac{\Delta U(x,y,z)}{U_h} = \frac{1}{\left(a + \frac{bx}{D} + c(1 + x/D)^{-2} + p\right)^2} \exp\left(-\frac{r^2}{2\sigma^2}\right) \quad (13)$$

Where *x* is streamwise distance [m], *y* is spanwise distance [m], *z* is height wise distance [m], ΔU is velocity deficit [m/s], U_h is velocity of free flow at hub height [m/s], σ is wake width at distance x [m], variables *a*, *b* and *c* are by:

$$a = 0{,}93 C_T^{-0{,}75} I_a^{0.25} \quad (14)$$

$$b = 0{,}42 C_T^{0{,}6} I_a^{0{,}2} \quad (15)$$

$$c = 0{,}15 C_T^{-0{,}25} I_a^{-0{,}7} \tag{16}$$

Correction term *p* for speed deficit in near wake region is calculated with:

$$p = 0{,}15 C_T^{-0{,}25} I_a^{-0{,}7} (1 + x/D)^{-2} \tag{17}$$

Added turbulence intensity

Added turbulence intensity is calculated with:

$$\Delta I_1(x,y,z) = \frac{1}{d + e\frac{x}{D} + f(1 + x/D)^{-2} + q} \left(k_1 \exp\left(-\frac{\left(r - \frac{D}{2}\right)^2}{2\sigma^2} \right) + k_2 exp\left(-\frac{\left(r/\frac{D}{2}\right)^2}{2\sigma^2} \right) \right) - \delta(z) \tag{18}$$

Variables *d*, *e* and *f* are calculated by:

$$d = 2{,}3 C_T^{-1{,}2} \tag{19}$$

$$e = I_a^{0{,}1} \tag{20}$$

$$f = 0{,}7 C_T^{-3{,}2} I_a^{-0{,}45} \tag{21}$$

Correction term *q* for turbulence intensity in near wake region is calculated with:

$$q = 0{,}7C_T^{-3{,}2} I_a^{-0{,}45}(1 + x/D)^{-2} \tag{22}$$

Radial distance from the centre of the wake is calculated by:

$$r = \sqrt{y^2 + (z - H)^2} \tag{23}$$

Where *r* is radial distance from the centre [m], *y* is spanwise distance from wake centre [m], *z* is elevation from ground [m], *H* is hub height [m].

k_1 and k_2 are model parameters and are calculated by:

$$k_1 = f(x) = \begin{cases} \cos^2\left(\pi/2\left(\frac{r}{D} - 0{,}5\right)\right), & r/D \leq 0{,}5 \\ 1, & r/D > 0{,}5 \end{cases} \tag{24}$$

$$k_2 = f(x) = \begin{cases} \cos^2\left(\pi/2\left(\frac{r}{D} - 0{,}5\right)\right), & r/D \leq 0{,}5 \\ 0, & r/D > 0{,}5 \end{cases} \tag{25}$$

Correction term δ for weakened turbulence intensity in lower part of wake flow is calculated with:

$$\delta(z) = f(x) = \begin{cases} 0, & (z \geq H) \\ I_a \sin^2\left(\pi \frac{H - z}{H}\right), & (z < H) \end{cases} \tag{26}$$